Hydrometallurgical Process Design and Economics with SuperPro Designer

A White Paper by

Giuseppe Granata, PhD

KU Leuven

giuseppe.granata@kuleuven.be

and

Demetri Petrides, PhD

Intelligen, Inc.

dpetrides@intelligen.com

Contents

1. Hydrometallurgical Process Design and Economics 2
   1.1 Definitions and Background 2
   1.2 Hydrometallurgical Processes 3
      1.2.1 Synthesis of Hydrometallurgical Processes 3
      1.2.2 Feed Preparation 4
      1.2.3 Leaching and Bioleaching 6
      1.2.4 Solid-Liquid Separation 7
      1.2.5 Purification 8
      1.2.6 Recovery 10
   1.3 Process Analysis 11
      1.3.1 Spreadsheets 12
      1.3.2 Process Simulators and Their Benefits 12
      1.3.3 Process Simulators in Hydrometallurgy 15
   1.4 Process Economics 16
      1.4.1 Capital Cost Estimation 16
      1.4.2 Operating Cost Estimation 22
      1.4.3 Profitability Analysis 26
   1.5 Illustrative Examples 28
      1.5.1 Extraction of Lithium from Spodumene 28
      1.5.2 Bio-Hydrometallurgical Recovery of Copper and Gold 37
      1.5.3 Recycling of Solar Photovoltaic Panels 50
      1.5.4 Hydrometallurgical Recycling of Lithium-Ion Batteries 58
      1.5.5 Manufacturing of NMC 811 Cathode Material for Lithium-Ion Batteries 70
   1.6 Summary 81

References 83

1. Hydrometallurgical Process Design and Economics

The objective of this document is to provide students, researchers, and engineers with the fundamentals of hydrometallurgical process design and techno-economic assessment. The information contained in this document can be applied to hydrometallurgical processing of primary mineral resources and/or secondary resources such as industrial residues and end-of-life waste streams from urban mines.

One of the central goals of hydrometallurgical process design is to determine what resources are required to produce the desired annual amount of product. The resources in question include the process equipment, materials, utilities, and labor. Additional goals may include answering some of the following questions: Can the product be manufactured in an existing facility or is a new plant required? What is the total capital investment for a new facility? What is the manufacturing cost? Under what conditions does a process become economically feasible? Which design is the "best" (fastest or least expensive) among several plausible alternatives? If the process runs in batch mode, which process steps or resources constitute scheduling and throughput bottlenecks? How long does a single batch take? What is the minimum time between consecutive batches? Which process steps or resources are the likely production bottlenecks? What process and equipment changes can increase throughput? What is the environmental impact of the process?

1.1 Definitions and Background

According to the general principles of process design and independently of the specific chemical process, process design consists of two main activities, namely process synthesis and process analysis. The first is the selection and arrangement of processing steps (unit operations) that enable the manufacture of a desired product or the treatment of a specific waste stream at an acceptable cost and quality. Process analysis focuses on evaluating and comparing different solutions obtained through process synthesis. Process design is typically composed of an alternation of synthesis and analysis steps and contains elements of project economic evaluation.

The accuracy of process design and cost analysis clearly depends on the source of the data used, which in turn depends on the specific project stage [1]. Preliminary evaluations based solely on information from previous related projects (Stage I) are associated with high margins of error while evaluations prior to plant commissioning (Stage V) must be very accurate. The relationship between project stage and the accuracy of capital cost estimate is provided in Table 1.

Table 1. Types of design estimates, their cost and accuracy for a $50M project [2].

Level	Type of Estimate	Error (%)
I	Order of magnitude	-50% to +100%
II	Screening or feasibility	-30% to +50%
III	Budget authorization	-20% to +30%
IV	Contractor/bid tender	-15% to 20%
V	Construction management	-10% to +15%

1.2 Hydrometallurgical Processes

1.2.1 Synthesis of Hydrometallurgical Processes

The development of a flowsheet for the extraction and recovery of metal values from primary or secondary resources is a creative process that depends on the experience and imagination of the engineer. Experienced engineers rely heavily on certain *rules of thumb,* also called *heuristics,* for putting together the skeleton of an extraction, purification, and recovery process. A few such heuristics follow:

1. Remove the most abundant impurities first.
2. Remove the easiest-to-remove impurities first.
3. Make the most difficult and expensive separations last.
4. Select separation technologies that make use of the greatest differences in the properties of the product and its impurities.
5. Select recovery operations that minimize waste generation.

Figure 1 provides a generalized structure of a hydrometallurgical process for the extraction and recovery of metal values from primary or secondary resources. The structure of Figure 1 along with the above heuristics and information available in the scientific and patent literature can be of great value to new engineers for conceptualizing and inventing new hydrometallurgical processes. However, it is important that all key performance assumptions made during the conceptual process design stage of a project are verified by experimental work.

Hydrometallurgical processes for commodity metals and processes with large throughputs in general tend to operate in continuous mode while processes of small scale, such as those handling recycling of precious metals, typically operate in batch-mode.

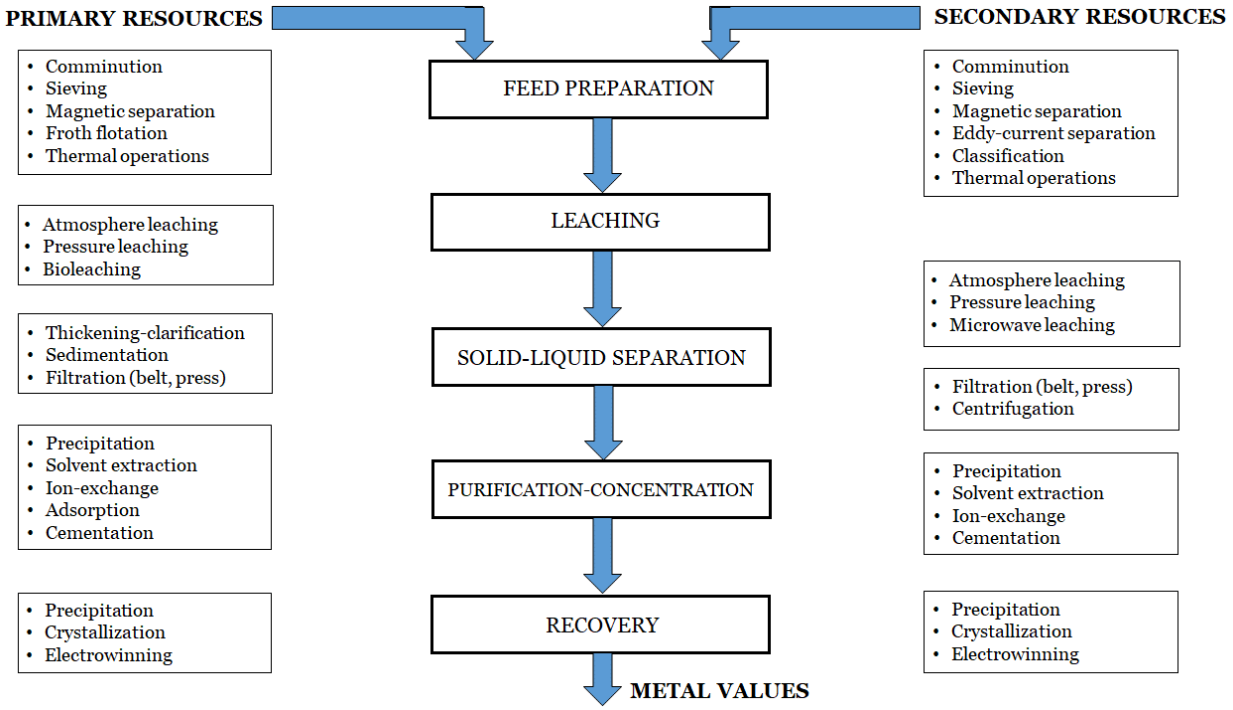

Figure 1. Generalized structure of a hydrometallurgical process.

1.2.2 Feed Preparation

Feed preparation represents the upstream processing in the recovery of metal values from primary and/or secondary resources. It encompasses mostly physical operations that take advantage of the differences in the properties between target materials and impurities. The feed preparation is referred to as *mineral processing* when the feed is ore or a concentrate. Instead, it is typically referred to as *pre-treatment* when the feed consists of secondary resources such as end-of-life streams.

Typical processing steps in feed preparation include **comminution** and **classification**. Comminution is typically carried out to separate the target materials from the bulk of the feed and maximize their liberation so that the performance of surface area-dependent downstream physical and/or chemical operations (e.g., flotation, leaching) can be improved. In comminution the particle size of the ore is progressively reduced so that the target mineral particles can be later separated. This typically takes place in multiple steps that are generally divided in crushing and grinding. Crushing is a dry operation that is performed on run-of-mine ore by exploiting mostly compression forces to reduce the particle size of the feed down to 10-200 mm. The most common types of crushers are the jaw crushers, gyratory crushers and roll crushers. Grinding typically follows crushing to reduce further the particle size of the ore down to the micron range. Unlike crushing, grinding is often a wet operation that takes place in tumbler media mills, where a combination of impact, attrition and abrasive forces

induced by the grinding media (e.g., balls, rods) is responsible for the comminution. Recent advances in comminution include high pressure grinding rolls (HPGR) as crushers and stirred media mills as grinders to reduce the overall energy consumption. In the last three decades, autogenous grinding (AG) and semi-autogenous grinding (SAG) mills enabling the combination of crushing and grinding in one operation have also become popular [3]. Detailed information on comminution in the minerals industry can be found in the dedicated literature [4–6]. Comminution in the recycling industry is somewhat similar although the presence of plastics along with the possibility to recover precious metals and lower throughputs create opportunities for new operations such as cryogenic and hammer milling [7,8]. Comminution operations followed by sieving are required to make best use of the difference in size-dependent physical properties between target materials and impurities (i.e., magnetic properties, wettability) in both primary and secondary resources.

Thermal operations find application in the treatment of both primary [9] and secondary [10,11] resources to induce chemical modifications in the treated materials. These modifications are sometimes simple temperature-induced crystal structure rearrangements [12] while, more often, are actual chemical reactions such as roasting, calcination, reduction, etc. [13]. For this reason, thermal operations are often viewed as actual pyrometallurgical processes rather than preliminary operations, especially when they precede hydrometallurgical processing. The fundamentals and applications of pyrometallurgy are extensively described elsewhere [14,15].

Froth flotation is widely used in the minerals processing industry to separate sulfide, carbonates, phosphates and oxides minerals [16–18] by exploiting their differences in hydrophobicity-hydrophilicity, thus wettability in a mineral/water slurry. In froth flotation, particles are separated based on the ability of air bubbles to selectively adhere to the surfaces of specific minerals. The hydrophobic particles attached to air bubble can in fact rise to the surface of the slurry and be separated from the hydrophilic ones that remain in the bulk of the liquid phase [19]. This requires the aid of additives such as collectors, frothing agents, and modifiers to enhance or suppress the wettability, thus enhancing the separation. Given the clear dependence of wettability on surface area, froth flotation is often performed upon comminution-classification to level out any difference in behavior due to particle size. The fundamentals and application of froth flotation are extensively described in the literature [20,21].

One of the most important operations in recycling is the **eddy-current separation,** which enables the separation of non-ferrous metals from non-metals based on the different electrical response of these materials to a magnetic field that changes over time [22]. This operation is mostly used in the recycling of waste of electric and electronic equipment and other residues (e.g., automobile shredding residues) [23] since these scraps are typically very heterogeneous in composition. When coupled with magnetic separation, the same operation also enables the separation of ferrous metals.

1.2.3 Leaching and Bioleaching

Leaching is the solid-liquid extraction of metal values from a solid matrix into the leaching media called leachant [24]. Since the extraction is the decisive step to achieve the recovery of the target metals, this operation represents the core of hydrometallurgical processes. Therefore, it should extract the target values quantitatively and as selectively as possible.

Leaching is typically carried out using aqueous solutions of acidic agents such as mineral acids and organic acids or under alkaline conditions with sodium hydroxide, ammonia, and cyanide. Specific thermodynamic parameters, namely pH and redox potential, play a crucial role in determining whether the metals can be dissolved in aqueous solutions or not. Normally, aqueous solutions of acids or bases can only be used if the dissolution potential lies within the water stability range, whereas above and below this range water decomposes into oxygen and hydrogen gas. In this region of water stability, the extent and rate of the heterogeneous (leaching) reactions can be modulated by manipulating operating parameters such as pH, redox potential, temperature, time, concentration of reagents, solid-liquid interfacial area, rate of mixing, and pressure [25]. Pressure can be modulated to directly affect the equilibria of the gaseous species or to control them indirectly by simply allowing operating temperatures above 100°C.

Bioleaching encompasses the use of bacteria to enhance the extraction of metals from ore/concentrate under ambient conditions. It is typically carried out using autotrophic bacteria in sulfate media and in the presence of ferric ions to oxidize the metal-bearing sulfide minerals. Under these conditions, the ferric ion initially acts as the final electron acceptor in the oxidation of the sulfide minerals and is then re-oxidized by the autotrophic bacteria that carry out their catabolic cycles.

Leaching operations can be performed using different type of technologies such as *in situ*, dump, heap, and tank atmospheric or pressure leaching [26]. *In situ* leaching involves the dissolution of metals from their source without removing it from its natural deposit. This is only possible if the entire system that undergoes leaching has a suitable porosity and the metals to be extracted are present in soluble form. Dump leaching consists of dumping the ore over the edges of mining terrain (or on leaching pads) and irrigating it from above with leaching solutions. Letting the leaching solutions percolate through the dump determines the extraction of the metal values into aqueous solutions. This technology is typically applied on low-grade ore without performing any comminution that would otherwise not allow percolation. Heap leaching is like dump leaching but is typically performed on higher grade ores prior to partial comminution. This along with ore height of less than 10 meters and a proper aeration from the bottom determines faster operations but higher operating costs. Heap leaching technologies [27] are widely used in the sulfate leaching of low grade copper sulfide minerals that would otherwise be uneconomical to process in conventional chemical reactors. If the specific value of the material to be leached is higher due to a higher concentration of target minerals/metals

(i.e. concentrates) or due to the presence of precious metals, stirred tanks are instead the preferred reactor technology for leaching or bioleaching [28].

Tank leaching is typically applied to high grade ore upon comminution and concentration via froth flotation, magnetic separation, and other typical mineral processing operations, either to leach the target metals or to remove impurities. For example, gold ores and/or concentrates are leached in stirred and aerated tanks, typically in cyanide-based media [29]. In the zinc industry, zinc is often leached from sulfide minerals after calcination [30] while iron is also removed from zinc sulfides by leaching upon roasting. Secondary resources, such as residues and end-of-life streams, also undergo tank leaching due to their higher concentrations in target metals and typically lower processing volumes.

If the raw material is particularly refractory to leaching in the temperature range from 25 to 100°C, high pressure leaching, i.e. autoclave leaching, may be the technology of choice, especially when the cost is justified by the economic value of the product [24]. The increase in pressure requires pressure-resistant vessels as well as higher operating costs for compression and flashing. However, increasing the pressure is sometimes the only way to efficiently leach metal values, as the pressure can directly or indirectly influence the chemical equilibria by allowing temperatures above 100°C [31]. A typical case of this type is the pressure acidic leaching for the efficient extraction of nickel and cobalt from laterites [32]. Another relevant industrial application of pressure leaching is in the aluminum industry, where high pressure alkaline leaching (HPAL) with caustic soda is applied to dissolve from the bauxite matrices the aluminum values as aluminate while leaving the desilication product in the residue [33]. Detailed information on leaching and bioleaching fundamentals, engineering, and applications can be found in the dedicated literature [26,31].

1.2.4 Solid-Liquid Separation

Separation of solids from liquids (S-L separation) is widely used in the mining and metals industries from minerals processing to extractive metallurgy and product recovery. The solid-liquid separation in the treatment stage aims to separate valuable concentrated solids from the treatment water, although tailings are sometimes also dewatered. Since the difference in density between mineral particles and water is typically large, separation takes place by gravity sedimentation or thickening [22]. This operation can remove up to 80% of the water, producing pulps that contain 55-65% solids. Further dewatering of up to 80-90% solids can be achieved by filtration or centrifugation which is conducted when the concentrates have to be transported over long distances [34]. This is also the case with continuous and large-throughput hydrometallurgical processes, in which the separated solids tend to retain portions of valuable pregnant leach solutions or soluble impurities must be removed from precipitated products [35].

Filtration can be performed using various automated technologies. **Pressure filters** are typically preferred over vacuum filters due to their higher flux rates and better washing and drying performances. In addition, the higher-pressure differential that drives the S-L separation enables the efficient separation of finer particles. Pressure filters can work up to 100 bar [36] with alternating cycles of "feeding" - to pressurize and squeeze a first portion of water out – followed by "air dewatering" with pressurized air [37]. The intrinsic cyclical nature of this type of filtration requires multiple filter presses operating in stagger mode (i.e., alternating among cycles) or storage tanks before and after the operation.

Vacuum filters are also widely utilized in the mining and metals industries in both batch and continuous modes. Among them, **rotary vacuum** filters allow the continuous separation of coarse, freely draining, quick-settling materials from concentrated slurries (i.e. separation of crystallized salts) [38]. **Belt** filters can instead ensure higher capacity throughputs and lower operating costs. However, due to the lower operating pressure differences they are less efficient in the separation of fine particles and produce cakes with a higher residual moisture content [39].

1.2.5 Purification

Hydrometallurgical processes for both primary and secondary resources include the purification of the pregnant leach solution to separate the target metal values from impurities. This is typically done by taking advantage of the difference in their chemical and electrochemical properties *through* precipitation, cementation, solvent-extraction, and ion exchange.

The selective **precipitation** of dissolved metal ions in water takes place by adding specific precipitating agents, which leads to the formation of sparingly soluble compounds of the species to be separated. This is often done by using alkaline agents (e.g., soda, lime) to precipitate metallic hydroxides, soluble sulfides to precipitate metal sulfides and/or carbonates to precipitate metal carbonates. Clearly, the choice of the precipitating agents and their sequence depends strictly on the species to be separated. Accordingly, the precipitation performance can be controlled by not only proper selection of the precipitating agent but also by manipulating process variables such as pH, temperature and time [24]. Time and temperature-related considerations are particularly important when it comes to controlling the type and quality (e.g., particle size) of the precipitated products. In this case, the theory to be considered includes not only thermodynamic considerations through precipitation equilibria but also the kinetic aspects of crystallization [40]. In this regard, the purification of pregnant leach solutions can be treated as chemical precipitation reactions in one or multiple stirred tank reactors or as crystallizations in evaporators-crystallizers. Due to the relative simplicity of scaling-up and operating such processes, the scientific literature highlights many investigations on the selective precipitation of metals in both primary [41] and secondary resources processing [42]. The precipitation properties of the metal ions to be separated, however, do not always differ significantly

enough to enable selective separations by precipitation. This is the typical case of light rare earth elements such as cerium, lanthanum, neodymium and praseodymium, among which only cerium can be separated selectively *via* oxidizing precipitation [43,44]. This also applies to cobalt and nickel, the separation of which by selective precipitation always leads to impure mixed precipitates [45,46]. In such cases, solvent extraction is often the preferred method to achieve the separation.

During **solvent extraction**, a target metal ion is transferred from the pregnant leach solution to an immiscible organic liquid via reaction with a complexing/chelating agent dissolved in the organic phase [24]. The reaction between the chelating agent and metal ions is typically represented as a pseudo-chemical equilibrium with a certain distribution coefficient that describes quantitatively the concentration of metals that transfer into the organic phase. The most commonly used organic phases are represented by organophosphorus agents dissolved in highly hydrophobic media such as kerosene [47], although phase modifiers are sometimes used to improve extraction. Solvent extraction is typically followed by scrubbing to remove some specific impurities from the organic phase and stripping to bring the target metals back into the aqueous phase. Both extraction and stripping typically take place in mixer-settlers. The mixer allows the aqueous and organic phases to come into contact, while the settlers allow them to separate. The organic solution from the extraction stage feeds the stripping mixer-settler, where the contact with the stripping agent reverses the extraction and brings the target metal ion(s) back into the aqueous phase. Depending on the specific repartition properties of the metal ions between the organic and aqueous phase, one or multiple stages are required to achieve satisfactory separations. Apart from rare earth production [48] and nickel-cobalt separation [49–51], the most well-known use of solvent extraction in hydrometallurgy is perhaps the one adopted in the copper industry to purify the copper pregnant liquor prior to electrowinning [52].

Cementation is also used in hydrometallurgical processes to separate metal ions based on their electrochemical properties. During cementation, dissolved metal ions can be reduced and thus separated by adding a more electropositive metal in its zerovalent form. Therefore, the applicability of cementation depends on the electrode potentials of the displacing and displaced metals. In particular, the redox potential of the metal added in its zero-valent form must be more negative than that the one of the metal ion to be removed from solution [31].

Ion exchange is another method to purify the pregnant leach solutions in hydrometallurgical processes. The product solution is passed through a column containing a functionalized polymeric resin that exchanges the cation(s) on the functionalized group with the metal ion(s) to be removed from the solution. Typical ion exchange resins used to separate metal ions in hydrometallurgical processes are of the strong or weak acidic type although weak and strong basic resins are also utilized to exchange anions [24]. In strong acidic resins, the polymer backbone is typically functionalized with the sulfonic group while in weak resins with carboxylic groups. In both types, the metal ion is exchanged with the hydronium ion or the ammonium ion of the functionalizing anionic group, which

determines a decrease in the pH of the solution. While weak acidic resins are active across a narrower pH range (4-14) than strong acidic resins, they are more advantageous for the recovery of the adsorbed metals *via* elution. Due to the relatively low selectivity and high cost of the resins, the need to regenerate and replace them as well as the intrinsic batch nature of the ion-exchange operation, the purification by ion-exchange finds application only in relatively low-throughput processes and/or in those processes addressing the recovery of high value materials such as precious and platinum group metals [53]. The largest application of ion-exchange in hydrometallurgy is based on the use of basic resins for the recovery of uranium from the pregnant leach solutions of primary uranium ore [54].

1.2.6 Recovery

The recovery of metal values from (purified) pregnant leach solution can be accomplished via chemical and electrochemical methods.

Electrochemical recovery of metals is typically done by **electrowinning**. In electrowinning, one of several metal ions are reduced to the metal state onto a cathode while other species contained in the electrolyte are oxidized on the anode. This requires the application of an external potential or current between the electrodes immersed in the electrolyte solution. According to general thermodynamic principles, the electrode potential or the current provides the electrochemical work so that the otherwise non-spontaneous electrochemical reaction to become spontaneous. This work determines the preferential reduction of the most electronegative species in solution and the oxidation of the most electropositive ones. This implies that the recovery of electropositive metals cannot take place in the presence of more electronegative ones as the latter would be preferentially reduced onto the cathode. Accordingly, the solutions undergoing electrowinning require a preliminary purification to reduce and/or eliminate those metal ions that are more electronegative than the target one. This also poses a peculiar limitation to the application of electrowinning to recover metals from aqueous solutions. From a thermodynamic point of view, metal ions that are more electropositive than the hydronium ion could not be reduced, or at least not preferentially. However, overpotentials up to-1.5 V associated with the evolution of hydrogen at the cathode extend the applicability of electrowinning from aqueous solutions to metals as electropositive as zinc. In some cases, adding ammonia or ammonium salts can increase even further the difference in reducing potentials between target metal reduction and hydrogen evolution. A typical case of this kind is the production of electrolytic manganese via reduction as ammonia complex, which would otherwise not be possible to the very low reducing potential of the couple Mn^{2+}/Mn (-1.18 V). More electropositive metal ions are instead reduced from molten salt media or alternative non-aqueous media.

Electrowinning is widely applied in the hydrometallurgy of primary resources to recover from purified aqueous solutions non-ferrous metals such copper [55], zinc [56], cobalt and nickel [57] upon leaching and solvent extraction. The same technology is also widely utilized in hydrometallurgical

processes for the recovery of metal values from secondary resources, as in the case of zinc from alkaline batteries [58] and precious metals from printed circuit boards [59]. Besides, electrowinning is the common industrial practice in the metallurgy of aluminum, where alumina is electro-reduced to aluminum metal onto carbon electrodes in molten salt media [60]. Detailed information on electrowinning fundamentals, engineering and applications can be found in the dedicated literature [61,62].

Precipitation is an alternative method to recover metals from aqueous solutions as oxides/hydroxides, sulfides and/or other insoluble salts according to their solubility products. Although the behavior of specific metal ions in precipitation is well known and the operation is relatively easy to conduct and scale-up, the use of precipitation for the recovery of metals is limited to only a few specific applications. The reason behind this technological choice typically arises from the high consumption of neutralizing agents required to neutralize the pregnant leach solutions along with the large production of sludge and the possible presence of neutralization salts in the precipitated products. From this point of view, precipitation can be a valid alternative to electrowinning when the metal to be recovered cannot be efficiently electrodeposited from an aqueous medium, as in the case of uranium [63] or when the product finds main applications as an oxide, sulfide and/or specific inorganic salt. This is, for instance, the case of rare earth elements, which are typically recovered and marketed as oxides [64] and which would otherwise require electrowinning from molten salt [65]. This is also the case with hydrometallurgical recycling processes, in which the recovered product does not enter the metal supply chain from the top but is processed straight away as it is. A typical example of this kind is the hydrometallurgical recycling of lithium-ion batteries in which the recovered nickel, cobalt and manganese are precipitated as hydroxides and later roasted in the presence of lithium to regenerate the cathode material.

A similar consideration applies to **crystallization**, which is also used in hydrometallurgical processes to recover metal values from solution. In contrast to precipitation, crystallization requires a preliminary evaporation to oversaturate solutions of otherwise (typically) soluble metal salts such as sulfates and chlorides. At the same time, it does not involve any neutralization, which is particularly convenient as it enables the recirculation of the residual solutions upstream to leaching without major pH adjustments and concerns associated with the unwanted generation of sludge. Overall, crystallization can only be preferred to electrowinning in particular situations, such as in remote hydrometallurgical operations [66] and processes for the production of metal salts/precursors.

1.3 Process Analysis

The flowsheets created during process synthesis must be analyzed and compared based on capital investment, manufacturing cost, environmental impact, and other criteria to decide which ideas to

consider further. Methodologies for estimating capital investment and manufacturing cost are presented in the next section of this document. In both cases, estimation is based on the results of material and energy balances and equipment sizing. These calculations are typically done using spreadsheets or process simulators. Use of computer tools enables the process design team to redo the entire series of calculations quickly and accurately for a different set of assumptions and other input data.

1.3.1 Spreadsheets

Spreadsheet applications like Microsoft Excel are now as easy to use as word processors and graphics packages. In its simplest form, a spreadsheet is an electronic piece of paper with empty boxes, known as cells. The user can enter data into these cells, perform calculations, and generate results. Results from spreadsheets can be easily plotted in a variety of graphs.

1.3.2 Process Simulators and their Benefits

Process simulators are software applications that enable the user to readily represent and analyze integrated processes. They have been used in the petrochemical industries since the early 1960's. Established simulators for the petrochemical industries include: Aspen Plus and HYSYS from Aspen Technology, Inc. (Burlington, MA), ChemCAD from Chemstations, Inc. (Houston, TX), and PRO/II from SimSci-Esscor, Inc. (Lake Forest, CA). Popular simulators in the field of hydrometallurgical engineering include HSC (Metso Outotec), Metsim (MetSim Interational), and Fact Sage (CRCT & GTT Technologies). These simulators were developed to model mainly continuous processes and their transient behavior. Small-scale hydrometallurgical processes for end-of-life streams, however, typically operate in batch and semi-continuous mode. Such processes are best modeled with batch process simulators that consider the time-dependency and sequencing of events. The first simulator specifically developed for batch processes was called Batches (from Batch Process Technologies in West Lafayette, IN). It was commercialized in the mid-1980s. All its operation models are dynamic, and simulation always involves integration of differential equations over a period of time. In the mid-1990s, Aspen Technology (Burlington, MA) introduced Batch Plus (now called Aspen Batch Process Developer), a recipe-driven simulator that targeted batch pharmaceutical processes. Around the same time, Intelligen, Inc. (Scotch Plains, NJ) introduced SuperPro Designer [27, 28].

SuperPro Designer is a flowsheet-driven simulator that handles material and energy balances, equipment sizing and costing, economic evaluation, environmental impact assessment, process scheduling, and debottlenecking of batch and continuous processes.

The benefits from the use of process simulators depend on the type of product, the stage of development and the size of the investment. In the production of commodity metals from primary

resources process simulators are particularly useful for optimizing well-established processes, thereby leading to a reduction in capital and operating costs. In the case of higher-value metals (e.g., PGMs) or innovative recycling processes for end-of-life streams (batteries, WEEE, etc.,), systematic process development coupled with process simulation is particularly useful to assess the economic feasibility and shorten the time for commercialization. Figure 2 shows a pictorial representation of the benefits of using such tools at the various stages of the development and commercialization process.

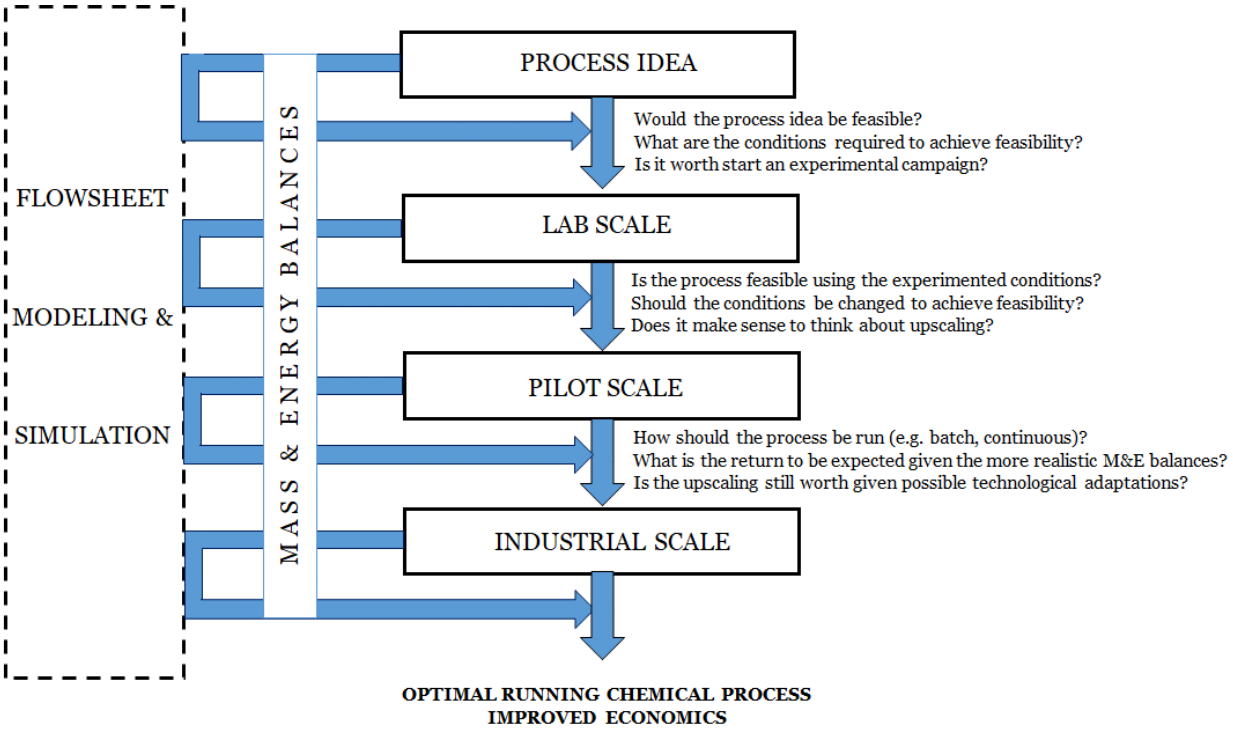

Figure 2. Use of process simulators at different stages of the process development activity.

Flowsheet modeling and simulation tools are used in the early stages of process development to analyze process ideas and evaluate whether it is worth proceeding with an experimental campaign. The rough mass and energy balances produced at this stage based on literature data or user assumptions represent the basis for a preliminary economic evaluation. These results enable decision makers not only to determine whether a process idea is worth further investigation, but also allow to identify the conditions for which an idea could be economically viable, which is of crucial importance for project screening and the strategic planning of R&D actions.

Lab Scale. At this stage, the unit processes and unit operations contained in the process idea are investigated experimentally. This enables to (i) verify the possibility of generating a specific product with a certain yield and purity starting from a specific raw material, (ii) identify the optimal operating conditions for reactions and separation operations, and (iii) generate a more realistic process

flowsheet with related mass and energy balances. The use of process simulators at this stage represents a systematic approach to obtain mass and energy balances and to estimate the process economics. The model built at this stage enables the team to assess how mass and energy balances as well as process economics react to qualitative and quantitative changes in the process inputs (e.g., change in raw materials composition, change in reaction kinetics, etc.), which in turn enables the identification of cost-sensitive points of the process that lead to further lab and pilot plant studies. Process simulators are in this way useful in guiding and refining the experimental campaign. For instance, as hydrometallurgical processes typically work under high-recirculation regimes to minimize the costs for waste/wastewater treatment, impurities tend to build up through the recirculation cycles. This typically results in liquid streams with higher concentrations than those observed in single batch experiments. From this point of view, simulation tools enable the prediction of the impurity build-up in the loops and estimation of the required purging of recycled materials. Reliable mass balances are also important to assess all inputs and outputs of the process, which is crucial for identifying the required storage space for raw materials, products, and waste during the process upscaling.

Process Development and Commercialization. The experimental campaign at pilot scale aims to identify the technological solutions that allow to obtain the process performance (e.g., product yield and purity) observed at lab-scale. However, the yields obtained at pilot scale may sometimes be lower than those observed at lab-scale, requiring some corrections to the mass and energy balances, while possibly seeking better technological solutions. Having simulation tools and already built models is clearly crucial at this stage. For instance, the impact of a decrease in reaction yield on the amount of generated product (and expected revenues) can be easily assessed with a few clicks. In addition, the actual investment costs and thus a more accurate cost-analysis can be obtained only after having a clear idea of the type of equipment to be used. In addition, process simulation tools greatly facilitate the transfer of a new process from the pilot plant to the large-scale facility. When a new facility needs to be built, process simulators can size the process equipment and supporting utilities and estimate the capital investment required. In transferring production to existing manufacturing sites (technology transfer), process simulators can be used to evaluate the various sites from a capacity and cost point of view and select the most appropriate one.

Large Scale Manufacturing. In large scale production, simulation tools are particularly useful for optimizing the process on an on-going basis and performing debottlenecking studies in the case of batch processes. Tools equipped with production planning and scheduling capabilities can be used to generate production schedules on an on-going basis in a way that does not violate constraints related to the limited availability of equipment, labor resources, utilities, inventories of materials, etc.

1.3.3 Process Simulators in Hydrometallurgy

The minimum requirements for a hydrometallurgical process simulator are the ability to handle both batch and continuous processes and the ability to model the unit operations that are specific to hydrometallurgy. Because SuperPro Designer (from Intelligen, Inc.) satisfies these requirements and enables quick and accurate cost-analysis, we will use it to demonstrate the role of such tools in hydrometallurgical process design. A functional evaluation version of SuperPro Designer can be downloaded from Intelligen's website (www.intelligen.com). Videos on the use of SuperPro Designer are available at https://www.intelligen.com/training/videos/.

To model an integrated process through a simulator, the user starts by developing a flowsheet that represents the overall process. For instance, Figure 3 displays the flowsheet of a hypothetical process on the main window of SuperPro Designer. The flowsheet is developed by putting together the required process tasks (referred to as "unit procedures," as explained later in this section) and connecting them with material flow streams. Next, the user initializes the flowsheet by registering the various materials to be used in the process (by selecting them from the component database or creating them as new materials) and specifying the operating conditions and performance parameters for the various operations.

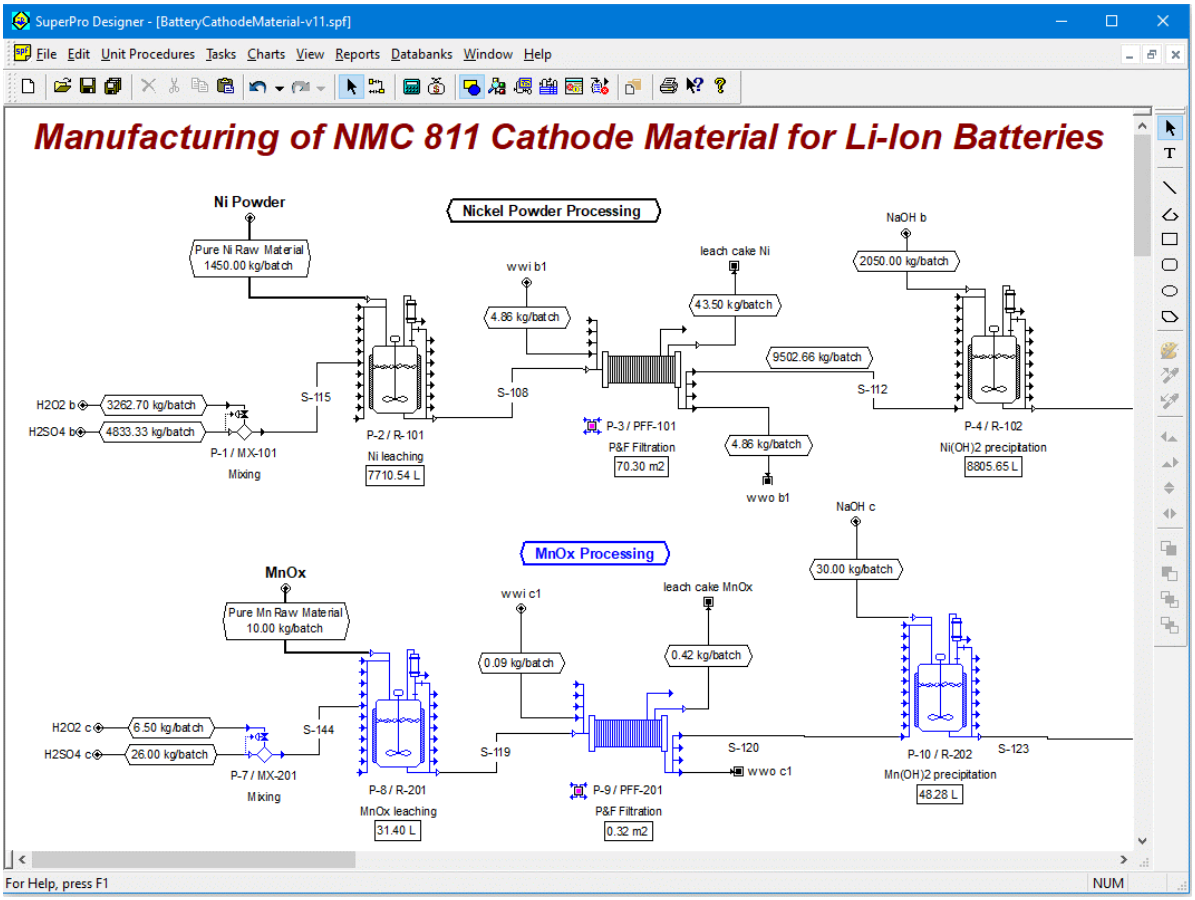

Figure 3. A flowsheet on the main window of SuperPro Designer.

Hydrometallurgical processes are operated in batch or continuous mode. The well-established processes of commodity metals typically operate in continuous mode while hydrometallurgical recycling processes for secondary resources (e.g., end-of-life streams) or precious metals are typically operated in batch or semi-continuous mode because of the lower throughputs involved. In continuous operation, a piece of equipment performs the same task all the time which is consistent with the notion of a "unit operation". In batch processing, on the other hand, a piece of equipment goes through a cycle of operations. For instance, the cycle of an ion-exchange resin used to purify leach liquors includes loading, washing, elution, and regeneration. In SuperPro Designer, the set of operations that comprise a processing step is called a “unit procedure” (as opposed to a “unit operation”). Each unit procedure contains individual tasks (e.g., equilibration, loading) that in SuperPro Designer are referred to as “operations”. A unit procedure is represented on the screen with a single equipment-looking icon (e.g., P-2 / R-101 in Figure 3 represents a leaching reaction step). In other words, a unit procedure consists of a sequence of actions that are required to complete a certain processing step. For each operation within a unit procedure, SuperPro has a mathematical model that performs material and energy balance calculations. Based on material and energy balances, SuperPro performs equipment-sizing calculations. If multiple operations within a unit procedure dictate different sizes for a certain piece of equipment, the software reconciles the different demands and selects an equipment size that is appropriate for all operations. In other words, the equipment is sized to ensure that it can execute all assigned tasks but is no larger than necessary (to minimize capital costs). In addition, for vessel-type procedures, the software checks to ensure that the vessel contents will not fall below a user-specified minimum volume (e.g., a minimum impeller volume) for applicable operations.

1.4 Process Economics

The preliminary economic evaluation of a project for the hydrometallurgical production of metals and/or metal-based materials usually involves the estimation of capital investment, operating costs, and revenues, thus enabling the analysis of profitability.

1.4.1 Capital Cost Estimation

The capital investment for a new plant includes three main items: direct fixed capital (DFC), working capital, and start-up and validation cost.

Equipment Purchase Cost (PC)

The equipment purchase cost represents the cost of the processing equipment required to implement the process. These costs can be estimated using vendor quotations, published data, company data compiled from earlier projects, and by using process simulators that are equipped with appropriate costing capabilities. Vendor quotations are time-consuming to obtain and are, therefore, usually avoided for preliminary cost estimates. Instead, engineers tend to rely on the other three sources. It should be noted that equipment purchase cost is a strong function of the industrial application and plant location. The data of Figures 4 to 7 are applicable to hydrometallurgical facilities in developed countries.

The default equipment cost models in SuperPro Designer are better suited to industries that manufacture high-value products, such as fine chemicals and pharmaceuticals. For other industries, users have the option to specify their own cost models to improve the accuracy of equipment cost estimates.

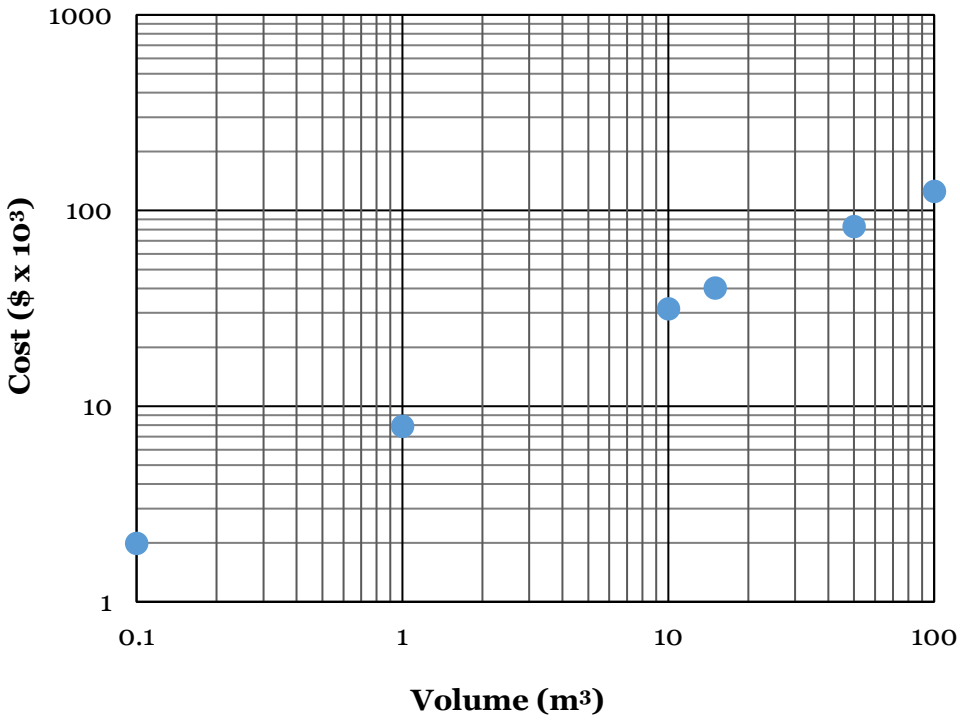

Figure 4. Purchase cost of stirred open plastic tanks (2021 prices).

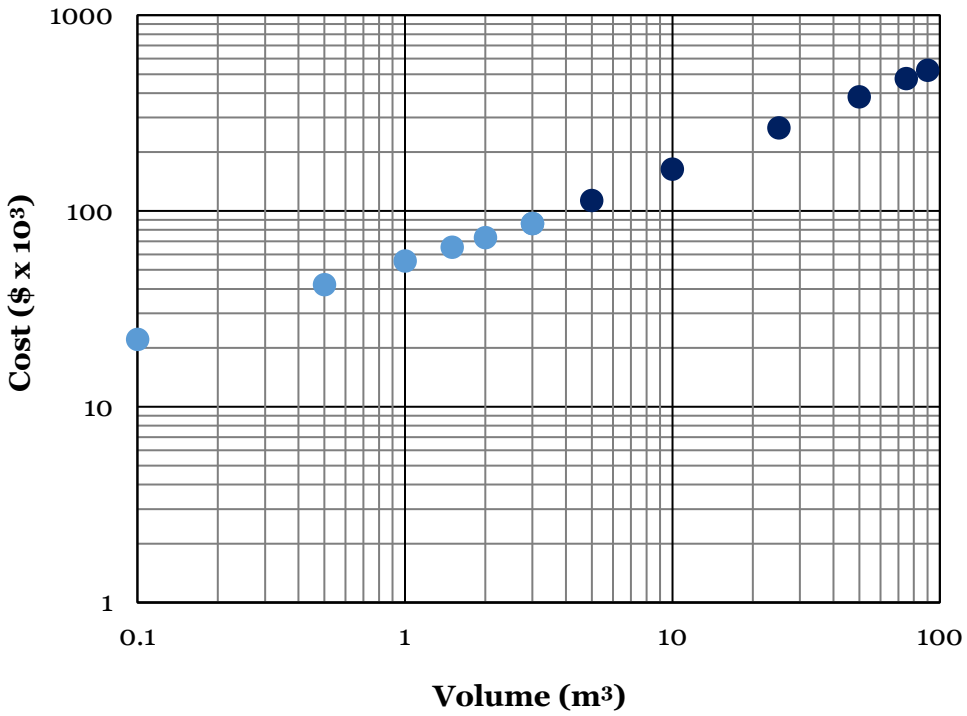

Figure 5. Purchase cost of stainless-steel pressure tanks (P_{max} = 3 bar) (2021 prices). Two different cost-models are used in the volume range 0.1-5 m³ and 5-100 m³.

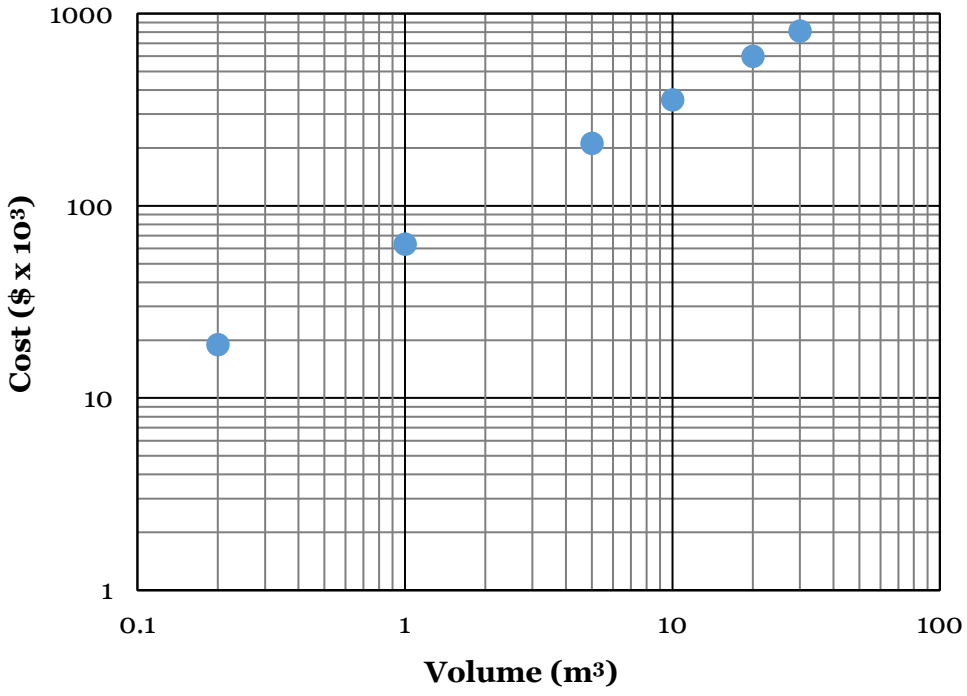

Figure 6. Purchase costs of batch evaporative crystallizers (2021 prices).

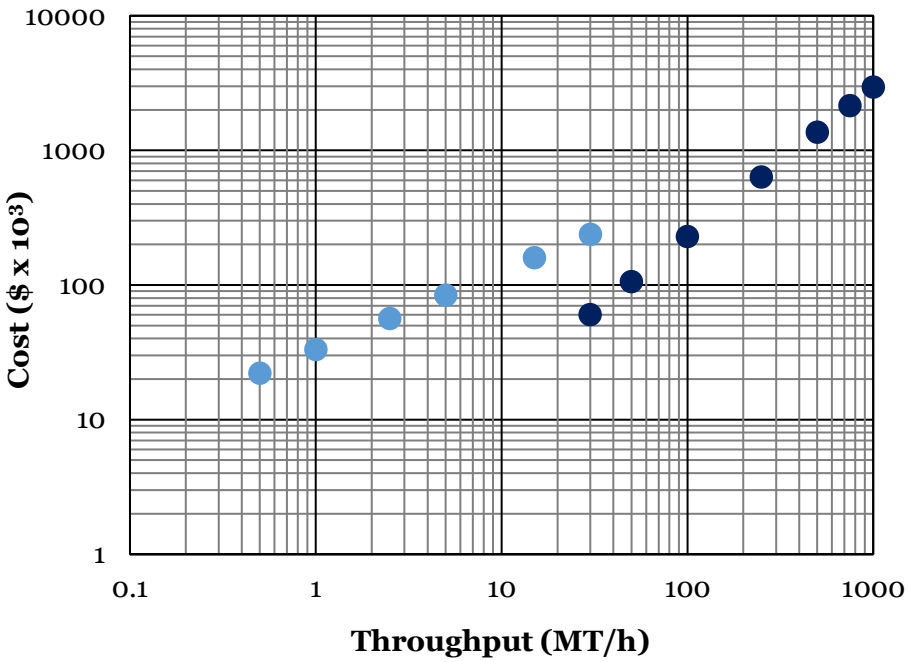

Figure 7. Purchase cost of jaw crushers (2021 prices). Two different cost-models are used in the throughput range 0.1-30 m³ and 30-1000 MT/h.

Often times, cost data for one or two discrete equipment sizes are available, but the cost for a different size piece of equipment must be estimated. In such cases, the following (power) scaling law can be used:

$$cost_2 = cost_1 \left(\frac{size_2}{size_1}\right)^{\alpha} \quad (1)$$

The mathematical form of the scaling law explains why cost-versus-size data graphed on logarithmic coordinates tend to fall on a straight line. The value of the exponent α in equation (1) ranges between 0.5 and 1.0, with an average value for vessels of around 0.6 (this explains why the scaling law is also known as the "0.6 rule"). According to this rule, when the size of a vessel doubles, its cost increases by a factor of (2/1)^0.6, or approximately 52%. This result is often referred to as the economy of scale. In using the scaling law, it is important to make sure that the piece of equipment whose cost is being estimated has a size that does not exceed the maximum available size for that type of equipment.

The price of equipment changes over time due to inflation and other market conditions. This price change is captured by the Chemical Engineering Plant Cost Index (CE Index), which is published monthly by the Chemical Engineering magazine. The index I is used to update equipment cost data according to the following equation:

$$cost_2 = cost_1 \frac{I_2}{I_1} \quad (2)$$

Another factor that affects equipment purchase cost is the material of construction. In this regard, a material factor (MF) can be defined as in (3) taking as a reference material carbon steel (CS):

$$\text{MF} = \frac{purchase\ cost\ of\ an\ item}{purchase\ cost\ of\ the\ same\ item\ made\ of\ CS} \quad (3)$$

For instance, a tank made of stainless-steel costs approximately 2.5 to 3 times the cost a carbon steel tank of the same size (MF=2.5-3). A tank made of titanium costs around 15 times the cost of a carbon steel tank of the same size (MF=15).

Direct Fixed Capital (DFC)

The direct fixed capital (DFC) of a chemical plant includes many components in addition to the cost of the processing equipment. Processing equipment must be installed, structurally supported, and interconnected by piping and/or conveyors. Electrical lines and instrumentation are also needed to ensure the proper functioning and control of the plant. The costs of auxiliary facilities such as boilers, generators, and other utility and support systems cannot be neglected. All these capital cost items make up the total plant direct cost (TPDC). Engineering and construction costs are also very important in calculating the DFC; they are part of the total plant indirect cost (TPIC). The total plant cost (TPC) includes both the direct and indirect costs whereas the DFC also includes the costs for contractor's fee and contingency (CFC) [67]. Accordingly, the DFC is calculated as in (4):

$$DFC = TPC + CFC \quad (4)$$

Where:

$$TPC = TPDC + TPIC \quad (5)$$

All costs that contribute to TPDC, TPIC, TPC, CFC and thus DFC are considered as fractions of the total equipment purchase cost (PC) and estimated by multiplying the PC by several multipliers. These multipliers are sometimes referred to as "Lang Factors" (if a composite factor is used for all capital cost components) or "Hand Factors" (C_e) and vary significantly depending on the type of processing plant. These factors are particularly important when estimating the TPDC as this is the largest portion of the DFC (building, instrumentation, piping, etc. represent a large portion of the capital investment). The TPDC is calculated from the PC and factors as in (6):

$$TPDC = PC + \sum PC \times C_e \quad (6)$$

Table 2. Multipliers (expressed as fraction of PC) in the estimation of DFC.

Group	Component	Liquid processing	Solid-liquid processing	Solid processing
PC	Equipment purchase cost	1.0	1.0	1.0
TPDC	Equipment installation	0.3	0.5	0.6
	Piping	0.8	0.6	0.2
	Instrumentation and control	0.3	0.3	0.2
	Electrical	0.2	0.2	0.15
	Civil	0.3	0.3	0.2
	Structures and buildings	0.2	0.2	0.1
	Lagging and paint	0.1	0.1	0.05
TPIC	Engineering	0.3	0.25	0.2
	Construction	0.4	0.35	0.3
CFC	Contingency	0.1	0.1	0.1
	Contractor's fee	0.05	0.05	0.05
DFC	Total	3.05	2.95	2.15

Table 2 provides common values of the multipliers to be considered for estimating TDPC, TPIC and CFC from PC. Detailed definitions of the various cost items and additional information can be found in traditional process design textbooks and the technical literature [4]. Table 2 also highlights the fact that some multipliers play a more significant role in liquid processing chemical plants (e.g., piping) while others are more important in solid processing (e.g., equipment installation). Based on Table 2, the DFC for a hydrometallurgical plant (solid-liquid processing) could be as a first approach estimated as:

$$\mathrm{DFC} = \mathrm{TPC} + \mathrm{CFC} = \mathrm{TPDC} + \mathrm{TPIC} + \mathrm{CFC} = \mathrm{PC} + 2.2\mathrm{PC} + 0.6\mathrm{PC} + 0.15\mathrm{PC} = 3.95\mathrm{PC}$$

It must be noted, however, that the differences between specific process scenarios could contribute significantly to the variation in the overall multiplier(s) between different hydrometallurgical processes.

Working Capital

Working capital (WC) accounts for the cash that must be available to cover on-going operating expenses. These expenses may include the cost of raw materials for 1 to 2 months, labor for 2 to 3 months, utilities for a month, waste treatment/disposal for a month, and other miscellaneous expenses. The required amount of working capital for a process is usually 10 to 20% of the DFC.

Start-up and Validation

Start-up and validation costs (SVC) can also represent a significant capital investment. A value of 5 to 10% of DFC is common for hydrometallurgical plants.

Total Capital Investment

The Total Capital Investment (TCI) refers to all capital expenditures that are associated with a process. This is calculated as the sum of the previous cost items plus possibly up-front R&D costs and royalties as in:

$$TCI = DFC + WC + SVC + R\&D + Royalties \quad (7)$$

This cost item is typically very large in high-throughput hydrometallurgical facilities that produce metal commodities but significantly smaller in the recycling of end-of-life streams. For instance, the TCI of a plant producing Cu cathodes with annual capacity in the range of 40,000-200,000 metric tons (MT) per year is in the range of 4,000-5,000 $/year per MT of copper, which is cut by half if the cost of mining operations is excluded [68].

1.4.2 Operating Cost Estimation

The operating cost is the sum of all annual expenses that are necessary for the operation of the manufacturing facility. Typical items that contribute to the operating costs are the raw materials, labor, consumables, utilities, waste disposal and facility overhead. While the operating costs are clearly dependent on the plant capacity, the unit production costs, which is obtained from dividing the annual operating cost by the annual production rate represents a more useful quantity for comparing different production scenarios.

The unit costs and selling prices of metal-based materials mainly depend on the amount of metal contained in the material itself, the prices of which are determined by the exchange market (e.g., London Metal Exchange - LME). The operations of extraction, purification, and metal recovery from ore, concentrates and/or end-of-life streams add progressive value to the materials being produced. However, establishing the actual price of a metal resource in the Mining & Metals can be quite a challenging task as this often depends on specific agreements/contracts. For this reason, cost analysis is often accompanied by sensitivity analysis to determine the purchase price of a specific raw material that yields a suitable profit margin considering the unit processing cost.

The margins associated with hydrometallurgical processes are generally closer to those for commodities than specialty chemicals, thus requiring extensive process optimization to minimize the operating costs and increase the profit margins. For instance, Mokmeli (2020) identified a margin of

$1-2 per kg of Cu cathode (Cu price: $6423/MT) for a new extraction and hydrometallurgical operation to be economically feasible [69]. In contrast, higher margins - closer to specialties - must be expected in the production of high-grade metals (e.g., >99.99%) and/or metal-based materials with special applications (e.g., battery grade metal oxides). In these cases, additional *premiums* are added on top of the metal value to determine the selling price of the product.

Table 3 displays various types of operating cost associated with the Mt. Gordon hydrometallurgical process to produce 50,000 MT/year of copper. This process treats 8% chalcocite via comminution, leaching, solvent extraction and electrowinning, for a total unit processing cost of $0.507/kg of copper. The breakdown of the operating costs is shown in Table 3. Clearly, these costs represent only an example, but it is reasonable to assume that they are representative of a wider range of possible values.

Table 3. Contribution (%) to the total operating costs in the Mt. Gordon operation [68].

Reagent cost	Labor	Utilities	Maintenance	Other
25.1	8.0	32.3	19.0	15.6

It should be noted that in SuperPro Designer the total operating cost is analyzed in greater detail and includes the following items: raw materials, labor, consumables, lab/QC/QA, waste disposal, utilities, facility overhead and miscellaneous. These operating cost items are described in greater detail in the examples of this document.

Raw Materials

The raw materials cost includes the cost of the metal resource to be processed as well as the cost of all reagents. The metal resource typically represents the most significant item of the raw materials cost. This is especially true in the hydrometallurgical production of commodity metals. For high value products that require solvent extraction and/or extensive processing with acids and bases, the cost of solvents and reagents can be a significant portion of the raw materials cost. Extensive solvent recycling can reduce these costs and minimize the environmental impact of such processes.

Labor

Labor is estimated based on the total number of operators, which in turn is calculated by summing up the operator requirements of the various operations as a function of time. Typically, batch hydrometallurgical processes that produce at small scale specialty metals and/or treat end-of-life streams require a larger number of operators per processing step due to the low level of automation. For instance, in a small batch hydrometallurgical plant, a simple leaching reactor may require two to

three operators for equipment cleaning and setup, loading and unloading of materials, etc., whereas a large, highly automated continuous leaching reactor might work well with a single operator that operates it remotely from the control room. The annual cost of an operator (including salary and benefits) varies widely depending on the specific geographic location. It is in the range of $10,000 to $20,000 in developing countries and can exceed $50,000 in developed countries.

Consumables

Consumables are items that may be used up, fouled, or otherwise damaged during processing, such as membranes, chromatography resins, activated carbon, etc. These items must be replaced periodically, which affects the costs and possibly the scheduling of batch processes. An example later in this document will illustrate the inclusion of these costs for the replacement of two typical consumable items in hydrometallurgical processes, namely electrowinning cathodes and ion-exchange resins. These items have very different replacement frequencies, with cathodes lasting for years and resins requiring one or more replacements per year. The unit cost of typical ion exchange resins used in the separation of specific metal ions from aqueous solutions ranges from $1.4-$7/L for the acidic type to $4.5-$7/L for the base ones. The unit cost of the metal cathode is directly proportional to its weight, since it represents the price of the metal fixed at the exchange market level. Regarding membrane filtration operations, the unit cost of MF/UF membranes used (in the form of hollow-fiber cartridges or cassettes) is in the range of $100 to $200/$m^2$, which explains why this kind of separation method is very rare in low-margin hydrometallurgical processes.

Laboratory/QC/QA

Laboratory, QC, and QA activities include off-line analysis, quality control (QC), and quality assurance (QA) costs. In contrast to fine chemical and biochemical operations where analysis and physical property characterization are crucial from raw materials to final product, in hydrometallurgical processes this cost item contributes relatively less to the overall operating cost. For comparison, Laboratory/QC/QA cost is usually 10 to 20% of the labor cost in the biopharma industry but less than 5% in the hydrometallurgical industry.

Waste Treatment and Disposal

The treatment of wastewater and the disposal of solid waste is another important contributor to the operating cost. The amount and composition of the various waste streams is derived from material balances. Multiplying the amount of each waste stream by the appropriate unit cost yields the cost of treatment and disposal. Treatment of low biological oxygen demand (BOD) wastewater (<1000 mg/L) by a municipal wastewater treatment facility usually costs from $0.2 to $0.5/$m^3$. The treatment of

industrial wastewater contaminated by acidic agents and metal ions can instead cost up to $10/m^3, which is one of the main reasons why hydrometallurgical processes tend to work under high recirculation regimes. This is particularly true for hydrometallurgical processes used in the production of base metals (e.g., Zn, Cu), which are characterized by very high throughputs and low profit margins. In these processes, even a 3-5% reduction in the extent of recycling can result in increased wastewater treatment costs of millions of US dollars. The same consideration applies to the treatment of organic liquid stream such as those produced during solvent extraction. The disposal/treatment cost for organic solvent waste can exceed $1/kg, which along with the high cost of the solvents ($7.5-$15/kg) are the reasons for adopting closed-loop processes with nearly 100% solvent recirculation.

The cost of solid waste disposal can become a problem in cases where solid by-products from mineral processing, leaching or precipitation cannot be returned to mines and/or disposed *via* cost-effective disposal methods such as tailing ponds. Solid waste disposal has limited impact in near-mine operations but can be significant in the hydrometallurgical recycling of end-of-life streams.

Utilities

Utility costs include the cost of heating and cooling agents (steam, high pressure steam, water, chilled water, etc.) as well as electricity. The amounts are calculated as part of the material and energy balances. In hydrometallurgical processes, electrowinning units for the electrodeposition of metals are clearly the main consumers of electricity. These units typically consume from 1.5 to 5 kWh of electricity per kg of recovered metals, which translates into $10-50M per year in plants producing 20,000-50,000 metric tons of metals. Autoclave leaching reactors are also associated with a large consumption of utilities due to compression and heating. For instance, the pressure leaching of sulfide ores and concentrates can require temperatures as high as 200-220°C and pressures around 3000 kPa [70]. Intermediate cooling is also required when using series of autoclaves, which can consume significant amounts of energy. For instance, cooling down 40 m^3 of leachate between two autoclaves requires 7-8 MWh ($6 \cdot 10^6$-$7 \cdot 10^6$ kcal) of energy. Given the cost of heat removal by cooling water of $0.002 to $0.02/1000 kcal of heat removed, this translates into $0.1-0.4M per year.

Cooling down to lower temperatures using chilled water and refrigerants is of course associated with higher costs, typically in the range of $0.05 to $0.1/1000 kcal of heat removed. The cost of steam as a heating agent ranges from $20 to 40 per MT depending on the pressure (low, medium, high), the type of fuel used for its generation and the scale of production.

Facility Overhead

Facility overhead costs account for the depreciation of the fixed capital investment, maintenance costs for equipment, insurance, local (property) taxes, and possibly other overhead-type expenses. In the case of preliminary cost estimates, the entire fixed capital investment is usually depreciated

linearly over a 10-year period. In the real world, the U.S. government allows corporations to depreciate equipment in 5 to 7 years and buildings in 25 to 30 years. The value of land cannot be depreciated. Annual maintenance costs can be estimated as a percentage of the equipment's purchase cost (usually 10%) or as a percentage of the overall fixed capital investment (usually 3-5%). The insurance rate depends to a considerable extent upon the maintenance of a safe plant in good repair condition. An insurance value in the range of 0.5 to 1% of DFC is typical for most hydrometallurgical facilities. The processing of flammable, explosive, or highly toxic materials usually leads to higher insurance rates. The local (property) tax is usually 1 to 5% of DFC. The factory expense represents overhead cost incurred by the operation of non-process-oriented facilities and organizations, such as accounting, payroll, fire protection, security, and cafeteria. A value of 5 to 10% of DFC is appropriate for these costs.

Miscellaneous

Included in miscellaneous costs are ongoing R&D, process validation, and other overhead-type expenses that can be ignored in preliminary cost estimates. Other general expenses of a corporation include royalties, advertising, and sales. If any part of the process or any equipment used in the process is protected by a patent that has not been assigned to the corporation undertaking the new project, permission to use the technology covered by the patent must be negotiated, and some form of royalty or license fee is usually required. Advertising and selling covers expenses associated with the activities of the marketing and sales departments.

1.4.3 Profitability Analysis

After estimating capital investment, operating costs, and revenues, a project can be analyzed to find out whether it is economically feasible or not and possibly find the conditions that make it feasible. This implies taking various metrics of economic profitability into account. The most appropriate economic indices to consider at design and development stage are the gross margin, return on investment (ROI), and payback time.

Gross margin is a measure of profitability that indicates the portion of revenues that become gross profit. It is calculated as the ratio between gross profit and revenues as in (8):

$$\text{Gross Margin}(\%) = \frac{Gross\ profit}{Revenues} \times 100 \tag{8}$$

Since gross profit is equal to revenues minus annual operating costs (AOC), equation (8) becomes:

$$Gross\ Margin(\%) = \frac{Revenues - AOC}{Revenues} \times 100 \tag{9}$$

Return on investment (ROI) is a measure of the profitability related to the required investment. It is calculated as the ratio of net profit per year divided by total investment:

$$ROI(\%) = \frac{Net\ Profit\ per\ Year}{Total\ Investment} \times 100 \quad (10)$$

ROI represents the portion of the total investment that is paid back annually. The payback time is a measure of the time needed for the total capital investment to be exactly balanced by the cumulative net profits. It is calculated by dividing the total capital investment by the annual net profit:

$$Payback\ Time = \frac{Total\ Investment}{Net\ Profit\ per\ Year} \quad (11)$$

Clearly, the shorter the payback time, the more attractive the project appears to be. Other useful metrics to assess the profitability of a project are the net present value (NPV) and internal rate of return (IRR). Both measures consider the cash flows of a project over its evaluation life and the time-value of money, thus also enabling profitability comparisons between different investments. The NPV represents the total value of the future net cash flows (spread over the lifetime of a project), discounted as values at the time corresponding to the beginning of the project. Essentially, the NPV indicates whether a particular investment is worthwhile by looking at all the money expected from an investment over a certain period and by translating that money into the value it would have at present day. It is calculated as in (12):

$$NPV = \sum_{t=0}^{T} \frac{Cf_t}{(1+DR)^t} \quad (12)$$

Where:

t is a specific year within a project lifetime

DR is the discount rate

Cf_t is the cash flow at year t

T is the entire project lifetime

Determining the NPV requires performing a cash flow analysis year by year over the project lifetime, which in turn requires knowing not only operating costs and revenues but also information such as income tax, depreciation rate, construction, and start-up time. The negative cash flows related to capital expenditures while the plant construction lasts should also be included in the corresponding years.

The internal rate of return (IRR) indicates the discount rate that makes the NPV of all cash flows equal to zero in a discounted cash flow basis.

More detailed information on discount rates, cash flow and other economics can be found in the relevant literature (e.g. [71]). The examples presented next demonstrate how these economic evaluation metrics facilitate the decision-making process.

1.5 Illustrative Examples

In this section, SuperPro Designer is used to illustrate the analysis and evaluation of five hydrometallurgical processes that produce metal values from primary resources and via recycling of end-of-life streams. The first example analyzes the production of battery-grade lithium carbonate from spodumene. The second example deals with the bio-hydrometallurgical production of copper and gold from a copper-gold concentrate. The third example addresses the recycling of solar photovoltaic panels. The fourth example analyzes the recycling of lithium-ion batteries while the fifth and last example focuses on the production of nickel-rich cathode materials for lithium-ion batteries. The generation of these flowsheets was based on information available in the patent and scientific literature combined with our engineering judgment and experience in the hydrometallurgical field.

The detailed computer models and ReadMe files for these examples are available as part of the free trial edition of SuperPro Designer that can be downloaded from www.intelligen.com. SuperPro Designer includes additional examples related to metallurgical processes. A description of all metallurgical examples is available at www.intelligen.com/industries/metallurgy.

1.5.1 Example 1 - Extraction of Lithium from Spodumene

Due to its high electrochemical activity, highest specific heat capacity among solid elements, low atomic mass, and low coefficient of thermal expansion, lithium (Li) is today one the most interesting commodities [72]. It is in fact the key element in lithium-ion batteries (LiBs), whose global market demand is expected to reach $700 billion by 2025 following the shift to electric mobility and the new possibility to accumulate in LiBs wind/solar energy [73]. In spite of the 25% demand increase per year in this specific sector, Li is widely used also in ceramics and glass (35%), lubricating greases (8%), continuous casting mold flux powders (6%) and other uses, for a total demand that in 2013 accounted for about 130,000 MT/year [74]. Accordingly, the British and US geological survey as well as the EU, have placed Li on the list of critical materials in terms of supply risk and economic importance.

Natural raw materials for lithium are brines and high-grade lithium ores, which contain about 59% and 25% of the total world lithium, respectively. Among hard rocks, spodumene ($LiAlO_6Si_2$) represents the most important source of lithium, with a world production of lithium of around 80,000 MT/year. Spodumene is a pyroxene mineral consisting of lithium aluminum inosilicate. It occurs as colorless to yellowish, purplish, or lilac kunzite, yellowish-green or emerald-green hiddenite, prismatic crystals, often of great size. Concentrates suitable for lithium carbonate (Li2CO3) production contain 75-87% spodumene. Their raw materials are primarily obtained from the Greenbushes pegmatite of Western Australia and from some Chinese and Chilean sources though the Talison mine in Greenbushes, Western Australia, is reported to be the largest and to have the highest ore grade.

This example analyzes the production of battery-grade Li2CO3 from a spodumene concentrate. In the process, a decrepitation reaction at 1070°C converts the non-reactive α-spodumene to β-spodumene, prior to sulfatation-roasting of the β-spodumene. The sulfate intermediate undergoes then neutralization with lime, carbonation, and evaporation-crystallization, which yields battery-grade Li2CO3. The composition of the concentrate considered in the example is listed in Table 4.

Table 4. Composition of the spodumene concentrate

Material	Formula	(%)
Spodumene	$LiAlO_6Si_2$	80
Quartz	SiO_2	10
Alumina	Al_2O_3	5
Annite	$KFe_3AlSi_3O_{10}(OH)_2$	2.5
Phlogopite	$KMg_3AlSi_3O_{10}(OH)_2$	2.5

The process runs in continuous mode and produces 1.3 MT/h of battery-grade Li2CO3 crystals by processing 10 MT/h of spodumene concentrate, which corresponds to 79,200 MT/year of raw material processed. A simplified version of the flowsheet is illustrated in Figure 8. The detailed flowsheet and the actual SuperPro Designer computer file of this example is available as part of the evaluation edition of SuperPro Designer which can be downloaded from www.intelligen.com.

Process Description

The process is divided in three sections. In the first section, Decrepitation & Sulfation, the concentrate is fed to a grinder (P-3) for size reduction through a hopper (P-2) and then to a kiln (P-4) where it is heated to over 1070 °C for decrepitation by burning natural gas. This step is needed to convert the monoclinic α-Spodumene (which is refractory to any chemical or thermal treatment) to tetragonal β-Spodumene. The molar stoichiometry, conversion, and reaction heat of the decrepitation reaction are given in Table 5.

Table 5. Chemical reactions involved in the decrepitation step (P-4/KLN-101).

Reaction Stoichiometry	Yield	Heat
$LiAlO_6Si_2 \rightarrow LiAlSi_2O_6$	96 %	150 $kJ/kg_{LiAlO6Si2}$

Figure 8. Lithium Extraction from Spodumene

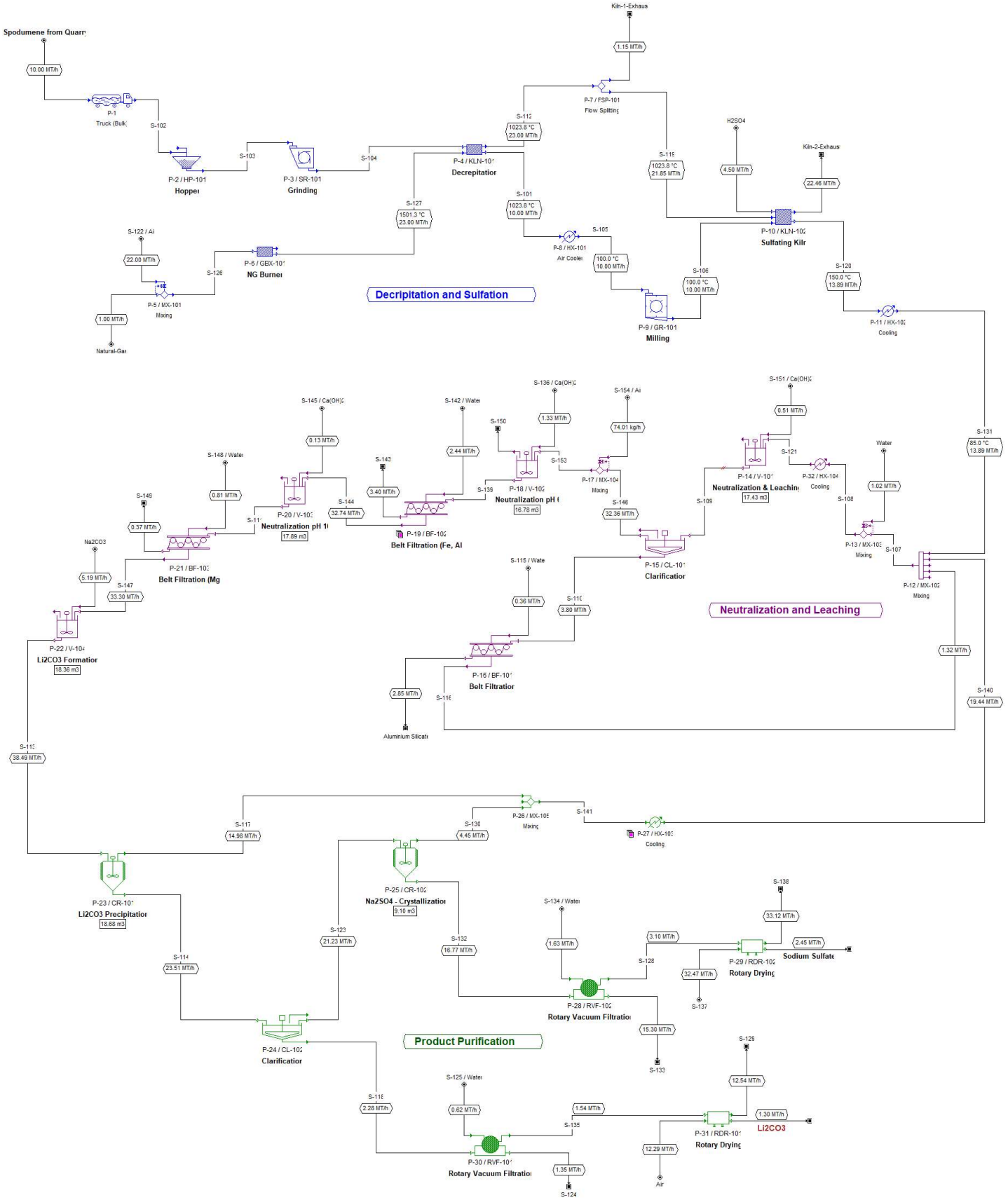

The decrepitated material is cooled to around 100 °C using an air cooler (P-8) and directed to a milling unit (P-9) for additional size reduction. The milled material is then fed to another kiln (P-10) for sulfation with sulfuric acid at 250 °C. This kiln is heated by transferring a fraction of the exhaust gases from the decrepitation kiln (stream S-119). In sulfation-roasting, β-spodumene, alumina, and the solid biotite mixture are converted into their respective sulfates [75,76]. The molar stoichiometry, conversion, and reaction heat of the sulfation reactions in procedure P-10 are listed in Table 6.

Table 6. Chemical reactions in sulfatation-roasting (P-10/KLN-102).

Reaction Stoichiometry	Yield	Heat
$LiAlSi_2O_6 + H_2SO_4 \rightarrow Li_2SO_4 + H_2O{\cdot}Al_2O_3{\cdot}4SiO_2$	97 %	4847 $kJ/kg_{LiAlSi2O6}$
$Al_2O_3 + 3H_2SO_4 \rightarrow Al_2(SO_4)_3 + 3H_2O$	96 %	-1771 kJ/kg_{Al2O3}
$2KFe_3AlSi_3O_{10}(OH)_2 + H_2SO_4 \rightarrow K_2SO_4 + 6FeSO_4 + Al_2(SO_4)_3 + 6H_4SiO_4$	96 %	-795 $kJ/kg_{KFe3AlSi3O10(OH)2}$
$2KMg_3AlSi_3O_{10}(OH)_2 + H_2SO_4 \rightarrow K_2SO_4 + 6MgSO_4 + Al_2(SO_4)_3 + 6H_4SiO_4$	96 %	-803 $kJ/kg_{KMg3AlSi3O10(OH)2}$

The material from the sulfation kiln is cooled down to 95 °C using a cooler (P-11) and then mixed in P-12 with recycled water from the crystallizers (P-23 and P-25) as well as recycled material from a downstream belt filtration unit (P-16). Following this operation, extra water is added using a custom mixer (P-13) to ensure that the final water content is no lower than 50% w/w. The addition of water results in the dissolution of the converted sulfates while the sulfuric acid in the mixture is neutralized with calcium hydroxide (P-14/V-101) according to the reactions given in Table 7.

Table 7. Chemical reactions involved in the neutralization-leaching step (P-14/V-101).

Reaction Stoichiometry	Yield	Heat
$H_2SO_4 \rightarrow H_2SO_4(aq)$	100 %	-973 kJ/kg_{H2SO4}
$Al_2(SO_4)_3 \rightarrow Al_2(SO_4)_3(aq)$	100%	-1025 $kJ/kg_{Al2(SO4)3}$
$Mg_2SO_4 \rightarrow Mg_2SO_4(aq)$	100%	-783 kJ/kg_{MgSO4}
$FeSO_4 \rightarrow FeSO_4(aq)$	100%	-458 kJ/kg_{FeSO4}
$Li_2SO_4 \rightarrow Li_2SO_4(aq)$	100%	-272 kJ/kg_{Li2SO4}
$K_2SO_4 \rightarrow K_2SO_4(aq)$	100%	-135 kJ/kg_{K2SO4}
$H_2SO_4(aq) + Ca(OH)_2 \rightarrow CaSO_4 + 2H_2O$	100%	-1125 kJ/kg_{H2SO4}
$H_4SiO_4 \rightarrow SiO_2 + 2H_2O$	100%	-143 kJ/kg_{H4SiO4}

The neutralization vessel also acts as a leaching unit for lithium sulfate (Li_2SO_4). At this point in

the process, almost all lithium sulfate remains in solution because of its high solubility in water. A clarifier (P-15) is then used to remove the suspended and precipitated materials (unreacted spodumene, aluminum silicate and the generated $CaSO_4$ which has low solubility in water). The solids stream of the clarifier (S-110) is fed to a belt filter (P-16) for dewatering and washing. The filtrate stream (S-116) from the belt filter, which contains considerable amounts of Li_2SO_4, is recycled to the process by connecting the stream to mixing procedure P-12, as mentioned earlier. This increases the product recovery yield and minimizes consumption of fresh water.

The supernatant of the clarifier (stream S-146) contains most of the dissolved Li_2SO_4 along with iron, aluminum, and magnesium impurities. Therefore, two additional neutralization steps are needed to precipitate iron, aluminum and magnesium as hydroxides: one step conducted at pH 5.5-6 removes iron and aluminum (P-18/V-102) whereas a subsequent one at pH 10-11 (P-20/V-103) removes magnesium [77]. The precipitation of iron can be enhanced by blowing air into the precipitation vessel (S-154), thereby inducing its oxidation to goethite/hematite. The molar stoichiometry of the neutralization reactions at pH 6 and 10 are given in Table 8 and Table 9, respectively.

Table 8. Chemical reactions involved in the neutralization at pH 6 (P-18/V-102).

Reaction Stoichiometry	Yield	Heat
$4FeSO_4(aq) + 4Ca(OH)_2 + O_2 \rightarrow 4FeOOH + 4CaSO_4 + 2H_2O$	100 %	-251 kJ/kg_{FeSO4}
$Al_2(SO_4)_3(aq) + 3Ca(OH)_2 \rightarrow Al_2O_3 + 3CaSO_4 + 3H_2O$	100 %	-1008 $kJ/kg_{Al2(SO4)3}$

Table 9. Chemical reactions involved in the neutralization at pH 10 (P-20/V-103).

Reaction Stoichiometry	Yield	Heat
$MgSO_4(aq) + Ca(OH)_2 \rightarrow Mg(OH)_2 + CaSO_4$	100 %	-137 kJ/kg_{MgSO4}

Each neutralization step is followed by belt filtration to remove the precipitates. The filtrate from the second belt filtration (stream S-147), which contains most of the dissolved Li_2SO_4, is then fed to another neutralization procedure (P-22/V-104) where Li_2SO_4 reacts with sodium carbonate (Na_2CO_3) to form Li_2CO_3 according to the reactions given in Table 10.

Table 10. Chemical reaction in Li2CO3 formation (P-22/V-104).

Reaction Stoichiometry	Yield	Heat
$Li_2SO_4(aq) + Na_2CO_3 \rightarrow Li_2CO_3(aq) + Na_2SO_4(aq)$	98 %	-11 kJ/kg_{Li2SO4}

The carbonated solution (stream S-113) is fed to an evaporator / crystallizer (P-23/CR-101) where 55% of the water is evaporated to concentrate Li_2CO_3 from 55 to 80 g/L. Cooling down the concentrate

to 35 °C determines the crystallization of about 90% of the Li_2CO_3. Next, a clarifier (P-24/CL-102) is used to separate the crystallized Li_2CO_3 from the mother liquor. The solids stream from the clarifier (S-118) is further concentrated using a rotary vacuum filter (P-30/RVF-101), in which the cake is washed with water to remove the dissolved impurities. The moisture of the purified cake is finally removed using a rotary dryer (P-31/RDR-101); the dried product is sold for battery applications.

The supernatant of the clarifier (stream S-123) is sent to another evaporator / crystallizer (P-25/CR-102) where 50% of the remaining water is evaporated to concentrate the accumulated sodium sulfate (Na_2SO_4) up to 250 g/L. Cooling down the concentrate to 35 °C facilitates the crystallization and precipitation of Na_2SO_4, which is recovered using another rotary vacuum filter (P-28/RVF-102), and dried using a second rotary drier (P-29). This dried material is sold as a co-product in the process. The water vapor generated by the two crystallizers is condensed using a cooling procedure (P-27/HX-103) and, as mentioned earlier, the condensate is recycled back to the neutralization and leaching section to minimize the requirements for fresh water.

Material Balances

The material requirements for this process are shown in Table 11. Clearly, the major material requirements in the process are the spodumene ore and water, accounting for about 80,000 and 65,000 MT/year, respectively. Other materials required in the process are the sulfuric acid used for sulfatation-roasting and the alkaline agents $Ca(OH)_2$ and Na_2CO_3 utilized in neutralization-precipitation, whose consumption accounts for 35,640, 15,665, and 40,932 MT/year, respectively.

Table 11. Material requirements for the entire Process.

Bulk Material	Unit Cost ($)	Annual Amount		Annual Cost ($)	%
Air	0.00	525,799	MT	0	0.00
Ca(OH)2	50.00	15,477	MT	773,838	1.77
H2SO4	70.00	35,640	MT	2,494,800	5.70
Na2CO3(aq)	0.05	16,266	MT	813,290	1.86
Natural Gas	500.00	7,920	MT	3,960,000	9.05
Spodumene Ore	450.00	79,200	MT	35,640,000	81.43
Water	1.10	80,275	m3(STP)	88,302	0.20
TOTAL				43,770,230	100.00

Cost Analysis

The list of equipment units required to implement this process to produce battery-grade Li_2CO_3 from spodumene is listed in Table 12. Table 12 provides information about the number of units of each type, their size and purchase cost. The total equipment purchase cost for a facility of this scale is between $12M and $13M. Table 13 displays the items of the fixed capital investment (DFC) which is approximately $60M.

Table 12. Equipment specification and fob cost (2020 prices).

Quantity/ Standby/ Staggered	Name	Description	Unit Cost ($)	Cost ($)
1 / 0 / 0	KLN-101	Generic Box	1,500,000	1,500,000
		Rated Throughput = 32999.95 kg/h		
1 / 0 / 0	KLN-102	Generic Box	1,500,000	1,500,000
		Rated Throughput = 36349.95 kg/h		
1 / 0 / 0	SR-101	Shredder	1,000,000	1,000,000
		Rated Throughput = 10000.00 kg/h		
1 / 0 / 0	GR-101	Grinder	1,000,000	1,000,000
		Rated Throughput = 10000.00 kg/h		
1 / 0 / 0	CR-101	Crystallizer	782,000	782,000
		Vessel Volume = 18537.65 L		
1 / 0 / 0	CR-102	Crystallizer	717,000	717,000
		Vessel Volume = 9028.18 L		
1 / 0 / 0	CL-101	Clarifier	690,000	690,000
		Surface Area = 1214.88 m2		
1 / 0 / 0	RDR-102	Rotary Dryer	394,000	394,000
		Drying Area = 63.80 m2		
1 / 0 / 0	BF-101	Belt Filter	268,000	268,000
		Belt Width = 1.22 m		
3 / 0 / 0	BF-102	Belt Filter	259,000	777,000
		Belt Width = 3.37 m		
1 / 0 / 0	BF-103	Belt Filter	251,000	251,000
		Belt Width = 1.12 m		
1 / 0 / 0	RDR-101	Rotary Dryer	217,000	217,000
		Drying Area = 33.38 m2		

1 / 0 / 0	RVF-102	Rotary Vaccum Filter	165,000	165,000
		Filter Area = 47.15 m2		
1 / 0 / 0	V-104	Neutralizer	109,000	109,000
		Vessel Volume = 18288.11 L		
1 / 0 / 0	V-103	Neutralizer	107,000	107,000
		Vessel Volume = 17827.18 L		
1 / 0 / 0	V-101	Neutralizer	106,000	106,000
		Vessel Volume = 17596.03 L		
1 / 0 / 0	V-102	Neutralizer	101,000	101,000
		Vessel Volume = 15847.20 L		
1 / 0 / 0	GBX-101	Generic Box	100,000	100,000
		Rated Throughput = 23000.00 kg/h		
2 / 0 / 0	HX-103	Heat Exchanger	87,000	174,000
		Heat Exchange Area = 57.00 m2		
1 / 0 / 0	RVF-101	Rotary Vaccum Filter	64,000	64,000
		Filter Area = 4.47 m2		
1 / 0 / 0	CL-102	Clarifier	54,000	54,000
		Surface Area = 17.37 m2		
1 / 0 / 0	HX-101	Heat Exchanger	23,000	23,000
		Heat Exchange Area = 6.19 m2		
1 / 0 / 0	HX-102	Heat Exchanger	8,000	8,000
		Heat Exchange Area = 0.86 m2		
		Unlisted Equipment		2,527,000
			TOTAL	12,633,000

The total operating cost for this process is about $76M per year (Table 14). As shown in Figure 9, raw materials contribute 58% of the operating cost. Among the raw materials, the spodumene concentrate alone accounts for approximately 81-82% of the total (Table 11). The remaining 18-19% of the total materials cost is associated with natural gas (9.1%), sulfuric acid (5.7%) and hydrated lime (1.8%). The second and third highest operating cost items are the facility-dependent and labor-dependent costs, respectively. Facility-dependent costs accounts for 15% and include the depreciation and maintenance of the facility, as well as some overhead costs.

Table 13. Fixed capital estimate summary (2020 prices in $).

3A. Total Plant Direct Cost (TPDC) (physical cost)	
1. Equipment Purchase Cost	12,633,000
2. Installation	5,667,000
3. Process Piping	2,992,000
4. Instrumentation	3,149,000
5. Insulation	379,000
6. Electrical	1,263,000
7. Buildings	1,812,000
8. Yard Improvement	1,895,000
9. Auxiliary Facilities	3,323,000
TPDC	33,113,000
3B. Total Plant Indirect Cost (TPIC)	
10. Engineering	8,278,000
11. Construction	11,589,000
TPIC	19,868,000
3C. Total Plant Cost (TPC = TPDC+TPIC)	
TPC	52,980,000
3D. Contractor's Fee & Contingency (CFC)	
12. Contractor's Fee	2,649,000
13. Contingency	5,298,000
CFC = 12+13	7,947,000
3E. Direct Fixed Capital Cost (DFC = TPC+CFC)	
DFC	60,927,000

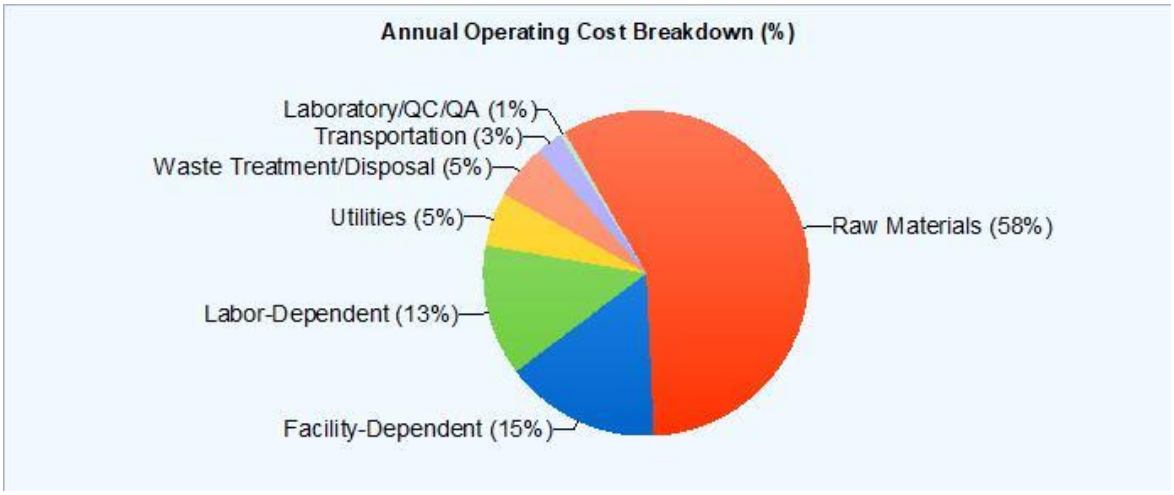

Figure 9. Operating cost breakdown.

Table 14: Executive summary extracted from the economic evaluation report.

EXECUTIVE SUMMARY (2020 prices)	
Total Capital Investment	69,594,000 $
Capital Investment Charged to This Project	69,594,000 $
Operating Cost	75,996,000 $/year
Revenues	91,545,000 $/year
Cost Basis Annual Rate	10,177 MT MP/year
Unit Production Cost	7,467.58 $/MT MP
Unit Production Revenue	8,995.50 $/MT MP
Gross Margin	16.99 %
Return On Investment	26.19 %
Payback Time	3.82 years
IRR (After Taxes)	18.07 %
NPV (at 7.0% Interest)	58,013,000 $

Assuming a selling price of $13,500/MT for Li_2CO_3, the process produces revenues for about $92M per year. This results in a gross margin of 17% and a return on investment (ROI) of approximately 26%, which leads to a payback time slightly less than 4 years (Table 14). These metrics indicate that this process would be economically viable, obviously subjected to the validity of all assumptions.

1.5.2 Example #2

Bio-Hydrometallurgical Recovery of Copper and Gold

Copper (Cu) and gold (Au) represent two important metal commodities that are of vital importance in many industrial sectors. Around 18 million metric tons (MT) of Cu and 3,500 MT of Au are produced every year using pyrometallurgical and hydrometallurgical technologies. Copper is produced on a large scale using pyrometallurgical smelting technologies or hydrometallurgical methods based on leaching, solvent extraction and electrowinning [57]. Gold is typically produced using hydrometallurgical cyanidation technologies prior to purification based on carbon adsorption and electrowinning [65].

Due to the decreasing availability of gold deposits with a simple mineralogy, a large proportion of gold is expected to be produced from complex gold ores containing significant amounts of copper minerals [78]. Clearly, any economically sustainable process should involve the recovery of both metal values from the ore. However, more complex mineralogy adds extra complexity to the processing

method, especially when the native gold is trapped within the grains of copper and/or iron sulfide minerals. This particular kind of resource, also known as refractory copper-gold ore, cannot be processed using conventional cyanidation methods due to the excessive cyanide consumption and the low extraction yields [79]. A more effective and economical strategy to recover gold from refractory ores involves the preliminary bacterial leaching of the refractory ore/concentrate to oxidize the sulfide minerals and dissolve copper, thereby enhancing the accessibility to the trapped gold [80].

Bio-hydrometallurgical technologies have been widely utilized in the copper industry [81,82], especially for the processing of chalcopyrite, which is well-known for being refractory to conventional leaching methods [83]. Gold has been mainly produced using hydrometallurgical methods based on cyanide leaching [29]. However, environmental concern associated with the use of cyanide agents as well as the increasing presence of gold in polymetallic refractory minerals requires the adoption of alternative and greener extraction methods. Among them, the copper sulfate-catalyzed thiosulfate-ammonia leaching seems to be the most promising [84].

This example analyzes a bio-hydrometallurgical process producing Cu and Au. The mineral composition of the concentrate considered as a raw material in this example is listed in Table 15 [85]. The main metal resource in the concentrate is copper, mainly as chalcopyrite. Despite the approximately 10,000x higher intrinsic value ($7.1/kg *vs* $60,000/kg), gold represents a secondary resource in the concentrate, accounting for only 0.0018% (18 ppm) of its weight.

In the process, copper is extracted from the sulfide ore by bioleaching and recovered by electrowinning upon solvent extraction. Gold is extracted from the bioleaching residue via thiosulfate leaching and recovered by electrowinning after purification-concentration *via* ion-exchange. The process runs in continuous mode although the two-step ion-exchange purification runs in batch mode. The process treats approximately 328,000 MT/year of Cu-Au concentrate (40 MT/h) and generates 87,000 MT of copper and 3.65 MT of gold per year.

Table 15. Composition of the Cu-Au concentrate.

Material	Formula	(%)
Chalcopyrite	CuFeS2	32
Pyrite	FeS2	18
Bornite	Cu5FeS4	6
Arseniopyrite	FeAsS	5-10
Covellite	CuS	6
Chalcocite	Cu2S	2.8
Tenorite	CuO	1.6
Gold	Au	0.0018
Silica	SiO2	To balance (23.9982)

A simplified version of the analyzed flowsheet is shown in Figure 10. The detailed flowsheet and the actual SuperPro Designer computer file of this example is available as part of the evaluation edition of SuperPro Designer which can be downloaded from www.intelligen.com.

Process Description

The analyzed process is divided into three sections: Feed Preparation and Bioleaching, Copper Purification & Recovery, and Gold Processing. In the Feed Preparation and Bioleaching section, the Cu-Au concentrate is transported via a conveyor belt from the receiving site to a grinding unit that reduces the particle size of the feed below 10 μm. The ground material is then fed to a bioleaching reactor (P-7/FR-101) where, in the presence of sulfur-oxidizing bacteria, the copper minerals are oxidized by the bacteria-produced ferric ions and the oxygen dissolved in the leaching medium [86,87]. The presence of oxygen in the bioleaching reactor is ensured by a centrifugal compressor that compresses the atmospheric air up to 3 atm, followed by a heat exchanger that cools it down to 40°C. The reactions taking place during bioleaching are listed in Table 16 along with their extent and enthalpy.

The slurry from bioleaching is fed to a second reactor (P-8/FR-102), in which sulfur-oxidizing bacteria grow using a mix of carbon dioxide from the air and sodium bicarbonate as the carbon source and ammonium salts as the nitrogen source [88,89] and from the ferrous ion resulting from the oxidation of copper minerals as an energy source [90]. Accordingly, the biomass growth results in the regeneration of ferric ions, which are later recirculated in the bioleach reactor. In the same reactor, the iron oxidation is accompanied by the bacterial oxidation of sulfur, which mitigate the overall consumption of sulfuric acid [91]. The reactions taking place during the biological oxidation are listed in table 17 along with their enthalpies and kinetic rate laws.

Figure 10. Bio-Hydrometallurgical Production of Copper and Gold

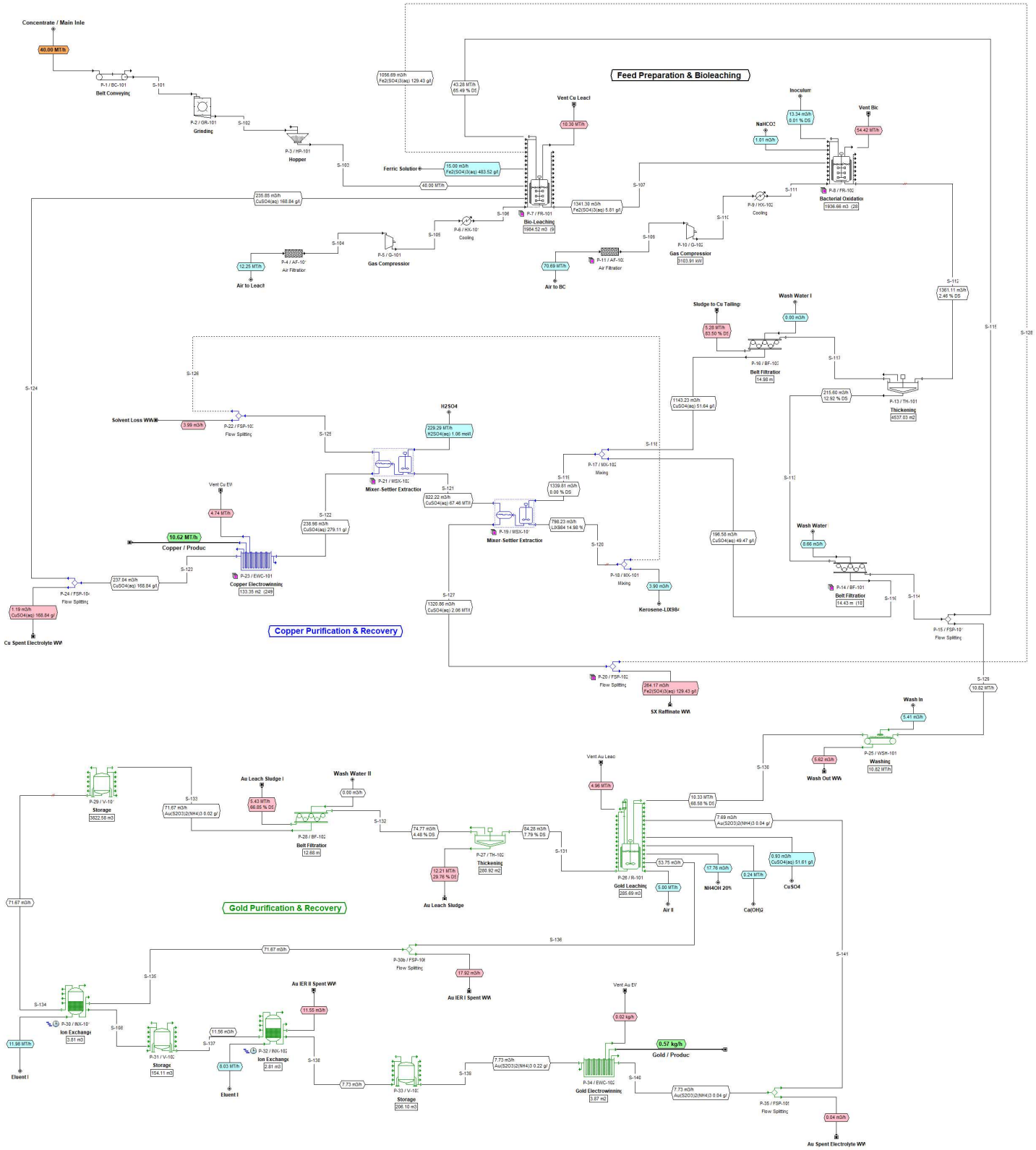

Table 16. Reactions and their extent in bioleaching (procedure P-7).

Reaction Stoichiometry	Yield	Heat
$CuO + H_2SO_4(aq) \rightarrow CuSO_4(aq) + H_2O$	100%	-820 kJ/kg_{CuO}
$FeS_2 + 7Fe_2(SO_4)3(aq) + 8H_2O \rightarrow 15FeSO_4(aq) + 8H_2SO_4(aq)$	40%	13 kJ/kg_{FeS2}
$2FeS_2 + 3H_2SO_4(aq) + 1.5O_2 \rightarrow Fe_2(SO_4)_3(aq) + 3H_2O + 4S$	85%	-2549 kJ/kg_{FeS2}
$FeAsS + 4Fe_2(SO_4)_3(aq) + 4H_2O \rightarrow FeAsO_4 + 8FeSO_4(aq) + S + 4H_2SO_4(aq)$	85%	-23 kJ/kg_{FeAsS}
$4FeAsS + 6H_2O + 11O_2 \rightarrow 4H_3AsO_3(aq) + 4FeSO_4(aq)$	35%	-7779 kJ/kg_{FeAsS}
$Cu_5FeS_4 + 6Fe_2(SO_4)_3(aq) \rightarrow 5CuSO_4(aq) + 13FeSO_4(aq) + 4S$	80%	259 $kJ/kg_{Cu5FeS4}$
$Cu_5FeS_4 + 6H_2SO_4(aq) + 3O_2 \rightarrow 5CuSO_4(aq) + FeSO_4(aq) + 6H_2O + 4S$	80%	-2191 $kJ/kg_{Cu5FeS4}$
$CuFeS_2 + 2Fe_2(SO_4)_3(aq) \rightarrow CuSO_4(aq) + 5FeSO_4(aq) + 2S$	80%	24 kJ/kg_{CuFeS2}
$CuFeS_2 + 2H_2SO_4(aq) + O_2 \rightarrow CuSO_4(aq) + FeSO_4(aq) + 2H_2O + 2S$	70%	-2210 kJ/kg_{CuFeS2}
$Cu_2S + 2Fe_2(SO_4)_3(aq) \rightarrow 2CuSO4(aq) + 4FeSO_4(aq) + S$	80%	297 kJ/kg_{Cu2S}
$Cu_2S + 2H_2SO_4(aq) + 2O_2 \rightarrow 2CuSO_4(aq) + 2H_2O + 2S$	90%	-2278 kJ/kg_{Cu2S}
$CuS + Fe_2(SO_4)_3(aq) \rightarrow CuSO_4(aq) + 2FeSO_4(aq) + S$	75%	413 kJ/kg_{CuS}
$CuS + H_2SO_4(aq) + 0.5O_2 \rightarrow CuSO_4(aq) + H_2O + S$	90%	-1730 kJ/kg_{CuS}

Table 17. Reactions and their rate laws in biological oxidation (procedure P-8).

Reaction Stoichiometry	Rate Law	Heat
$2NaHCO_3 + H_2SO_4(aq) \rightarrow 2CO_2 + 2H_2O + Na_2SO_4(aq)$	$r = 10[NaHCO_3]$	31 kJ/kg_{NaHCO3}
$0.0028(NH_4)_2SO_4(aq) + 0.0278CO_2 + FeSO_4(aq) + 0.4972H_2SO_4(aq) + 0.2223O_2 \rightarrow 0.0056C_5H_7O_2N + 0.5Fe_2(SO_4)_3(aq) + 0.4889H_2O$	$r = 1.5[FeSO_4]/(75 + [FeSO_4])$	-88 kJ/kg_{FeSO4}
$2S + 3O_2 + 2H_2O \rightarrow 2H_2SO_4(aq)$	$r = 0.15[S]/(200 + [S])$	-624 kJ/kg_S

After bioleaching and bio-oxidation, the leach slurry undergoes thickening (P-13/TH-101), from where the Cu-rich overflow proceeds to the Copper Purification & Recovery section upon secondary filtration (P-16/BF-103) while the Au-containing underflow (S-113) is filtered in a belt filter (P-14/BF-101) and sent to the Gold Processing section. The filtered Cu-rich leach solution (stream S-119) is sent to a mixer settler unit (P-19/MSX-101) which separates copper from the other dissolved impurities by adding a 15% LIX984 solution in kerosene in A/O ratio of 2:1 with the Cu-rich aqueous solution [92,93]. Under these conditions, 98% of copper is extracted into the organic phase in one stage, while the dissolved ferric ion remains in the aqueous raffinate [94]. The raffinate solution (S-127) is partially recirculated back to the bioleaching reactor, where the ferric ion will oxidize again the copper minerals.

The Cu-loaded organic phase is sent to a second mixer-settler (P-21/MSX-102) where a 1 M H_2SO_4 solution in O/A ratio of 3:1 strips 99% of copper out of the organic phase [95]. Following solvent extraction, the Cu-rich aqueous solution is sent to an electrowinning unit in a tank-house (P-23/EWC-101), where copper is reduced to the metal state onto stainless steel cathodes. The active cathode area in the electrowinning unit is sized to achieve 40% copper reduction. The electrowinning of copper was modeled according to the stoichiometry and parameters shown in Table 18.

Table 18. Chemical reactions in copper electrowinning (procedure P-23).

Reaction Stoichiometry	Yield	Current Efficiency	Current Density
$CuSO_4 + H_2O \rightarrow Cu + 0.5O_2 + H_2SO_4(aq)$	40%	90%	300 A/m²

In the Gold Processing section, the solid material from bioleaching-thickening-filtration is sent to a washing unit (P-25/WSH-101) to remove the impurities dissolved in the retained liquid and then fed to a leaching reactor (P-26/R-101) where it undergoes leaching in ammonia-thiosulfate medium at 60 °C [84,96]. The thiosulfate required in this reactor to oxidize and dissolve gold is generated in-situ by oxidizing with an ammonia solution the elemental sulfur generated in bioleaching [97]. The reactions considered in the leaching of gold are as listed in Table 19.

Table 19. Reactions and their conversion in gold leaching procedure (procedure P-26).

Reaction Stoichiometry	Yield	Heat
$H_2SO_4(aq) + Ca(OH)_2 \rightarrow CaSO_4 + 2H_2O$	100%	-1127 kJ/kg_{H2SO4}
$4S + 6NH_4OH \rightarrow NH_4S(aq) + (NH_4)_2S_2O_3(aq) + 3H_2O$	80%	-
$4FeS_2 + 8NH_4OH + 7O_2 \rightarrow 4(NH_4)2S_2O_3(aq) + 2Fe_2O_3 + 4H_2O$	95%	-6828 kJ/kg_{Fe2O3}
$CuSO_4(aq) + 4NH_4OH(aq) \rightarrow Cu(NH_3)_4SO_4(aq) + 4H_2O$	90%	-
$4Au + O_2 + 8(NH_4)2S_2O_3(aq) \rightarrow 4Au(S_2O_3)2(NH_4)_3(aq) + 4NH_3 + 2H_2O$	99%	-
$2Cu(NH_3)4SO_4(aq) + 6(NH_4)2S_2O_3(aq) \rightarrow (NH_4)_2S_4O_6(aq) + 2(NH_4)_2SO_4(aq) + 2Cu(S_2O_3)_2(NH_4)_3(aq) + 8NH_3$	80%	-

The leach slurry (stream S-131) is fed to a thickener which concentrates the solids to a thickened sludge from the initial 10% to about 30% while generating a partially clarified stream containing about 6% of solids. The clarified stream (S-132) from thickening undergoes filtration (P-28/BF-102) and purification-concentration by ion-exchange [98] as an alternative to the common industrial practice on the basis of carbon-in-pulp (CIP) and carbon-in-leach (CIL) [78]. The filtered solution containing the dissolved gold and copper is fed into a bed ion-exchange column (P-30/INX-101) packed with a strong basic anion exchange resin having a total binding capacity of 10 g/L. Under sufficiently alkaline

conditions (pH 11), gold is preferentially exchanged for copper, thereby realizing a first separation [99]. The metals loaded onto the resin are then eluted with 2 bed volumes (BV) per hour of a composite eluant solution of sodium sulfite coupled with ammonia over a period of 5 hours [100]. To enhance the separation and concentration of gold, the eluted Au-containing solution (S-137) is fed into a second ion-exchange column (P-32/INX-102) that operates under the same conditions as the first one, whereas the residual solution (stream S-135) is partially recirculated back to the leaching reactor to minimize gold losses and wastewater treatment costs. Overall, the two-step ion-exchange processing step produces a solution containing around 170 ppm of gold and 100 ppm of copper that is sent to an electrowinning unit (P-34/EWC-102) where gold is electrowon and recovered onto stainless steel cathodes [101]. The cathode surface area of the electrowinning unit is sized to enable the 80% discharge of gold with a current density of 150 A/m² and a current efficiency of 20%. The electrowinning of gold was modeled as in Table 20.

Table 20. Chemical reactions in gold electrowinning (procedure P-34)

Reaction Stoichiometry	Yield	Current Efficiency	Current Density
$4Au(S_2O_3)_2(NH_4)_3(aq) + 4NH_4OH \rightarrow 4Au + 8(NH_4)_2S_2O_3(aq) + O_2 + 2H_2O$	80%	20%	150 A/m²

Scheduling of the Ion Exchange Columns

Overall, this bio-hydrometallurgical process runs in continuous mode with an Annual Operating Time of 8,200 h (341 days). Although the overall process is set to continuous mode, specific unit procedures within the flowsheet are individually set to batch mode. In particular, the gold leach liquor purification via ion-exchange columns (P-30/INX-101 and P-32/INX-102) run in batch mode due to the intrinsic batch nature of this operation, which requires cycles of loading and elution. To handle a continuous inlet flow, each ion exchange step utilizes a total of four columns operating in staggered model and rotating every 2 hours which is equal to the duration of the load operation. The cycle duration of each column is 7 hours (2 hours of loading and 5 hours of elution). Figure 11 displays the occupancy of the ion exchange columns over a period of 3 days. The top four lines correspond to the four columns of the first ion exchange step (P-30/INX-101). The bottom four lines correspond to the four columns of the second ion exchange step (P-31/INX-102). In this chart, each colored bar represents the execution of a unit procedure hosted by a certain equipment item; moreover, each bar has vertical borders inside that distinguish the operations and idle times within each procedure.

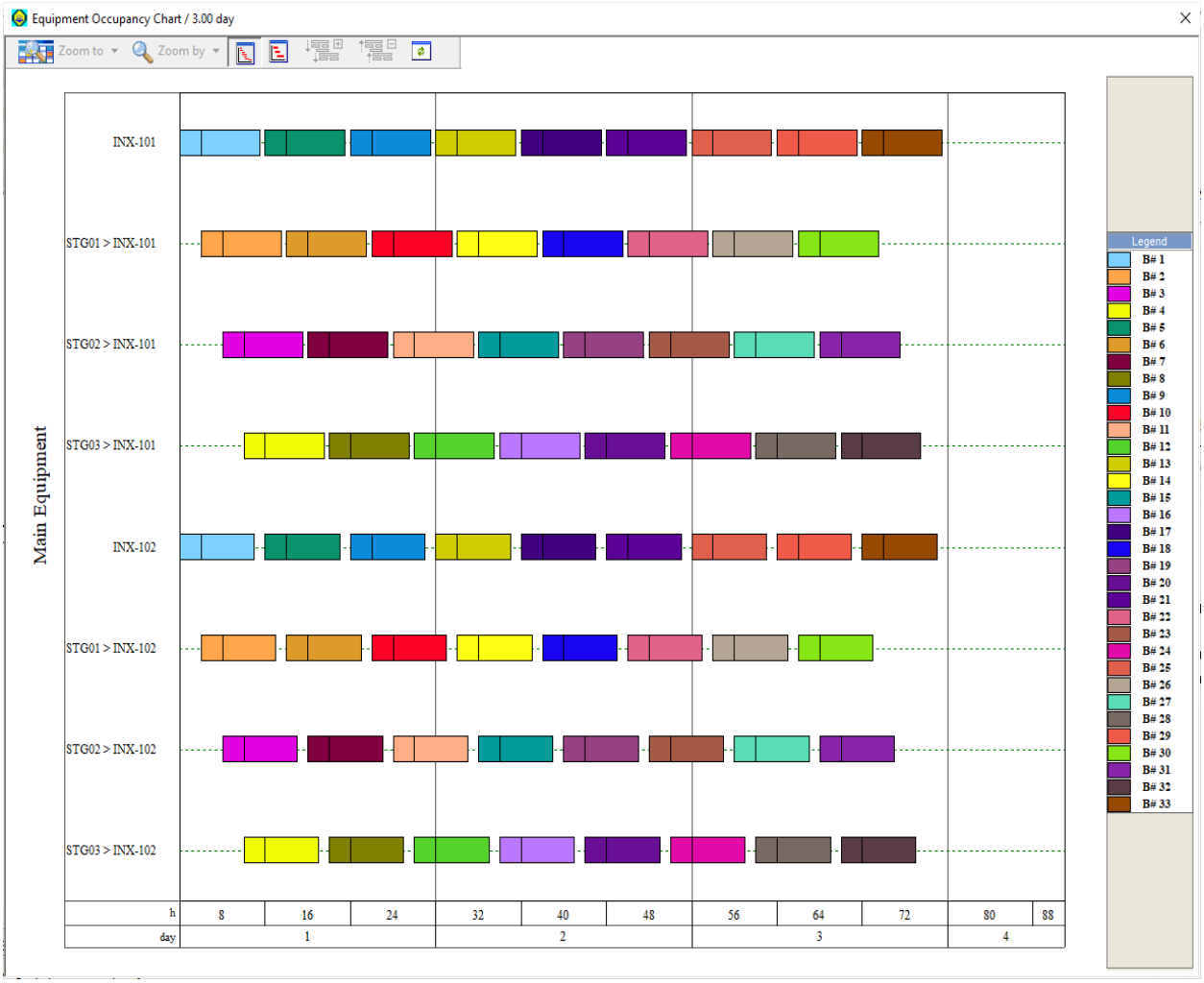

Figure 11. Equipment occupancy chart over 3 days of operation of the ion exchange columns.

Material Balances

The raw material requirements and cost for the analyzed bio-hydrometallurgical process is displayed in Table 21. Table 21 clearly indicates that the main materials are the metal concentrate (328,000 MT/year), the ion exchange elution solution (325,000 MT/year) and water. Despite their importance in the process, sulfuric acid, and ferric sulfate together account for less than 250,000 MT/year. This is possible due to their regeneration within the process through bacterial oxidation and electrowinning operations. The highest intrinsic material cost is associated with the LIX984, which is used to extract copper from the pregnant leach liquor. However, due to the almost complete recirculation within the process, the material costs make up less than 4% of the total material costs.

Table 21. Material Requirements and costs for the bio-hydrometallurgical flowsheet.

Bulk Material	Unit Cost ($)	Annual Amount	Annual Cost ($)	%
Air	0.00	721,224MT	0	0.00
Biomass	0.10	175MT	18	0.00
Ca(OH)2	150.00	1,963MT	294,391	0.05
Concentrate	1,600.00	328,000MT	524,800,000	83.37
Eluant	120.00	324,980MT	38,997,589	6.20
Fe2(SO4)3(aq)	50.00	59,473MT	2,973,672	0.47
H2SO4(aq)	70.00	188,345MT	13,184,122	2.09
Inoculum	100.00	119,298MT	11,929,770	1.90
Kerosene	100.00	17,076MT	1,707,601	0.27
LIX984	8,000.00	3,013MT	24,107,307	3.83
NaHCO3	175.00	18,450MT	3,228,750	0.51
NH4OH	150.00	27,880MT	4,182,000	0.66
Water	2.00	2,032,279MT	4,064,559	0.65
TOTAL			629,469,777	100.00

Cost Analysis

The list of equipment units required for this facility is listed in Table 22. Information is provided about the number of units of each type, their sizes, and the cost of purchase. The total equipment purchase cost for a facility of this scale is around $209M. Table 23 displays the items of the fixed capital investment (DFC) which is approximately $780M.

Table 22. Equipment specification and fob cost (2020 prices)

Quantity/Standby/ Staggered	Name	Description	Unit Cost ($)	Cost ($)
1 / 0 / 0	G-102	Centrifugal Compressor	3,308,000	3,308,000
		Compressor Power = 3103.90 kW		
1 / 0 / 0	TH-101	Thickener	1,477,000	1,477,000
		Surface Area = 4537.05 m2		
9 / 0 / 0	FR-101	Fermentor	750,000	6,750,000
		Vessel Volume = 1984.51 m3		
28 / 0 / 0	FR-102	Fermentor	750,000	21,000,000

		Vessel Volume = 1936.66 m3		
1 / 0 / 0	V-101	Vertical-On-Legs Tank	680,000	680,000
		Vessel Volume = 3823.56 m3		
1 / 0 / 0	G-101	Centrifugal Compressor	638,000	638,000
		Compressor Power = 538.08 kW		
249 / 0 / 0	EWC-101	Electrowinning Cell	588,000	146,412,000
		Area = 133.35 m2		
1 / 0 / 0	TH-102	Thickener	278,000	278,000
		Surface Area = 280.99 m2		
10 / 0 / 0	BF-101	Belt Filter	261,000	2,610,000
		Belt Width = 14.43 m		
1 / 0 / 0	BC-101	Belt Conveyor	260,000	260,000
		Belt Length = 100.00 m		
1 / 0 / 0	BF-102	Belt Filter	259,000	259,000
		Belt Width = 12.68 m		
2 / 0 / 0	BF-103	Belt Filter	256,000	512,000
		Belt Width = 7.53 m		
6 / 0 / 0	MSX-102	Mixer-Settler Extractor	192,000	1,152,000
		Rated Throughput = 173.84 m3/h		
1 / 0 / 3	INX-101	Ion Exchanger	148,000	592,000
		Column Volume = 3.81 m3		
1 / 0 / 0	R-101	Stirred Reactor	135,000	135,000
		Vessel Volume = 285.75 m3		
1 / 0 / 3	INX-102	Ion Exchanger	127,000	508,000
		Column Volume = 2.81 m3		
1 / 0 / 0	V-103	Vertical-On-Legs Tank	108,000	108,000
		Vessel Volume = 206.11 m3		
1 / 0 / 0	WSH-101	Washer	100,000	100,000
		Rated Throughput = 10.82 MT/h		
1 / 0 / 0	V-102	Vertical-On-Legs Tank	90,000	90,000
		Vessel Volume = 154.11 m3		
1 / 0 / 0	GR-101	Grinder	84,000	84,000
		Rated Throughput = 40.00 MT/h		
11 / 0 / 0	MSX-101	Mixer-Settler Extractor	68,000	748,000

		Rated Throughput = 194.45 m3/h		
1 / 0 / 0	HX-102	Heat Exchanger	54,000	54,000
		Heat Exchange Area = 27.21 m2		
5 / 0 / 0	AF-102	Air Filter	45,000	225,000
		Rated Throughput = 11986.85 m3/h		
1 / 0 / 0	AF-101	Air Filter	39,000	39,000
		Rated Throughput = 10389.81 m3/h		
1 / 0 / 0	HX-101	Heat Exchanger	19,000	19,000
		Heat Exchange Area = 4.72 m2		
1 / 0 / 0	EWC-102	Electrowinning Cell	3,000	3,000
		Area = 3.87 m2		
		Unlisted Equipment		20,886,000
				Auxiliary Equipment
1	AUX-Group101	Rectifier+Stripping+Crane	1,000,000	1,000,000
		Power = 300.00 kW		
1	AUX-101	Rectifier	100,000	100,000
		Power = 100.00 kW		
			TOTAL	208,861,000

The annual operating cost for a facility of this scale is around 864 million dollars. Figure 12 displays a breakdown of the annual operating cost. Raw materials account for 72% of the total operating cost. As previously listed in Table 21, the metal concentrate contributes 83% to the overall raw materials cost whereas the second highest cost is associated with the sulfite-ammonia solution used to elute gold from the ion-exchange resins. Although this solution does not have a particularly high unit cost, the volumes used are relatively large due to a recirculation rate of only 75%. Around 3% of the raw materials cost is associated with the extractant LIX984.

Facility-dependent expenses contribute 18% to the total operating costs. This expense item primarily accounts for the amortization and maintenance of the facility.

Table 23. Fixed capital estimate summary (2020 prices in $).

3A. Total Plant Direct Cost (TPDC) (physical cost)	
1. Equipment Purchase Cost	208,861,000
2. Installation	67,708,000
3. Process Piping	37,654,000
4. Instrumentation	37,654,000
5. Insulation	6,266,000
6. Electrical	27,063,000
7. Buildings	25,711,000
8. Yard Improvement	29,270,000
9. Auxiliary Facilities	17,591,000
TPDC	457,778,000
3B. Total Plant Indirect Cost (TPIC)	
10. Engineering	114,445,000
11. Construction	137,334,000
TPIC	251,778,000
3C. Total Plant Cost (TPC = TPDC+TPIC)	
TPC	709,557,000
3D. Contractor's Fee & Contingency (CFC)	
12. Contractor's Fee	35,478,000
13. Contingency	35,478,000
CFC = 12+13	70,956,000
3E. Direct Fixed Capital Cost (DFC = TPC+CFC)	
DFC	780,512,000

Wastewater treatment and waste disposal costs account for 4% of the total. This cost is kept low by employing extensive recycling in the process. Finally, utilities account for about 3% of the total operating costs. As expected, the electricity required for electrowinning contributes around 90% to this cost item.

Table 24 displays the Executive Summary of the Economic Evaluation Report. Despite the high capital investment for such a facility (approximately $830M) and the high annual operating cost (approximately $864M), the process is profitable thanks to its more than $900M annual revenues. About 67% of this revenue is associated with copper whereas the remaining 33% with gold. The gross margin is only 6%, which is typical for commodity manufacturing facilities in which economic

feasibility is ensured by the large production volumes. The analyzed bio-hydrometallurgical process exhibits a return on investment of 16.17%, which in turn results in a payback time of 6.2 years. For a discount interest rate of 3%, the NPV of the project is around $1 billion.

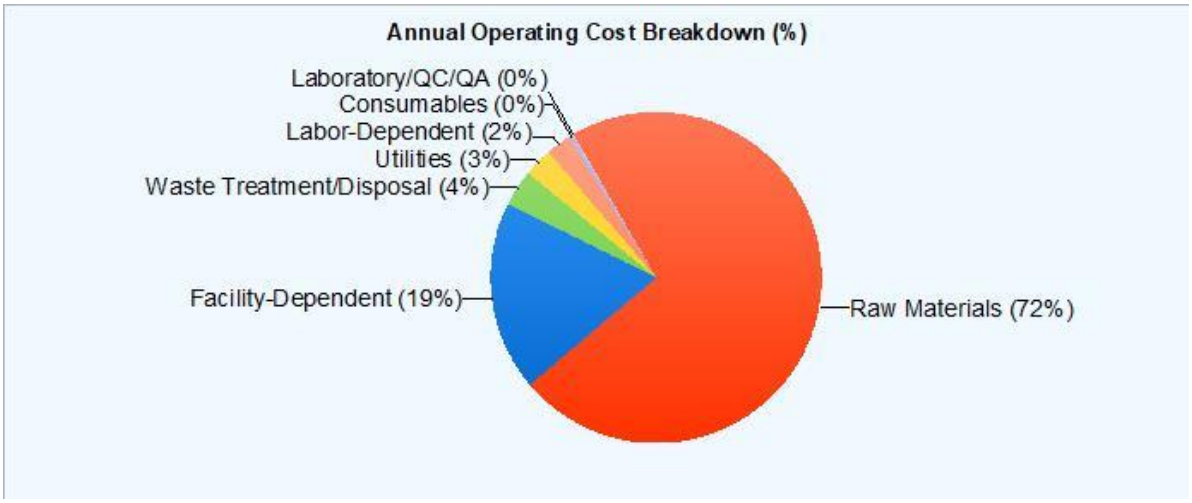

Figure 12. Operating cost breakdown.

Table 24. Executive Summary for the analyzed bio-hydrometallurgical process.

EXECUTIVE SUMMARY (2020 prices)	
Total Capital Investment	829,744,000 $
Capital Investment Charged to This Project	829,744,000 $
Operating Cost	864,304,000 $/year
Main Revenue	618,584,000 $/year
Other Revenues	300,443,125 $/year
Total Revenues	919,027,000 $/year
Cost Basis Annual Rate	87,125 MT UPRF/year
Unit Production Cost	9,920.33 $/MT UPRF
Net Unit Production Cost	9,916.01 $/MT UPRF
Unit Production Revenue	10,548.43 $/MT UPRF
Gross Margin	6.00 %
Return On Investment	16.17 %
Payback Time	6.19 years
IRR (After Taxes)	12.33 %
NPV (at 3.0% Interest)	1,013,021,000 $

UPRF = Total Flow of Stream 'Copper'

1.5.3 Example #3 - Recycling of Solar Photovoltaic Panels

Solar photovoltaic (PV) panels represent one of the most sustainable solutions for generating electricity from renewable energy sources, in particular solar energy [102]. The installed PV power has been constantly increasing in the last decades and is forecasted to reach 4,500 GW by 2050 [103]. Accordingly, PV waste is also expected to increase from an annual amount of 43,500-250,000 metric tons (MT) in 2016 to 8 million MT by 2030 and 80 million MT by 2050 [104]. The composition of this waste stream will clearly depend on the PV technologies that will be commercialized in the future. Currently, the crystalline silicon (Si-crystalline) PV technology predominates over the Cd-Te and CIGS, covering over 90% of the global market [105]. And this is forecasted to remain the market scenario for at least the next decade.

Given this expected amount of PV waste, the European Union has set minimum targets for the collection, recycling, and recovery of end-of-life (EoL) PV panels. As of August 2018, collection, recycling and recovery must be at least 65%, 80%, and 85%, respectively [106]. Therefore, having a suitable recycling technology for EoL PV panels has become crucial.

This example analyzes a physical-chemical process for recycling of EoL Crystalline-Si PV panels. These devices are realized by encapsulating silicon-made PV cells between layers of ethylene vinyl acetate (EVA) and by covering the module with glass on the front and Tedlar sheet on the back. Crystalline-Si PV panels also contain non-negligible amounts of silver as electrical connectors between the cells [107]. Glass accounts for 65-75% of photovoltaic panel weight while EVA and the cell account for 7-15% and 1-2%, respectively. An aluminum frame, which accounts for around 10% of the panel weight mechanically supports the entire module. The composition of the EoL-PV waste, which is considered as input material in the analyzed process is listed in Table 25.

Table 25. Composition of EoL-PV panels.

Material	(%)
Glass	69.5
EVA	11.25
Aluminum frame	10
Tedlar	4.3
Silicon	3.7
Coppper	1.08
Aluminum	0.12
Silver	0.05

The process analyzed in this example is based on the flowsheet proposed by Rubino et al. [108], which enables glass, silver and silicon recovery. This is accomplished by performing an initial dry

pre-treatment of the PV waste stream followed by a wet treatment with cyclohexane, which determines the chemical conditioning of the EVA polymer. This in turn facilitates the separation and recovery of the liberated components by other physical and hydrometallurgical means.

In the process, the EoL-PV panels are first subjected to manual dismantling, crushing, and sieving to separate the Al frames and enable an initial partial recovery of clean glass. The pre-treated material is then suspended in cyclohexane, which induces chemical modification of the encapsulating EVA polymer and determines the detachment of the cell from the glass. Silver and silicon are recovered from the EVA sheets by hydrometallurgical means upon thermal decomposition of the polymer. Glass and metal wires are recovered by screening and air classification. The process includes extensive recycling of cyclohexane and water to minimize raw material consumption and wastewater treatment costs. A simplified version of the analyzed flowsheet is shown in Figure 13. The detailed flowsheet and the actual SuperPro Designer computer file of this example is available as part of the evaluation edition of SuperPro Designer which can be downloaded from www.intelligen.com.

The main product of the process is glass as this material represents from a quantitative point of view the main component of the EoL-PV waste stream. The main revenue of the process is represented by the EoL-PVP panels themselves, assuming the recyclers will receive from the collectors and PV panel producers a certain fee to sustain the economy of the recycling process. This fee is usually paid by PV panel consumers through an overprice of about $5-10/PV on the purchase and installation of PV panels. Given the average weight of 20 kg/PV panel, such fee translates into $0.25-0.50/kg. Additional revenues are generated from the recovered amounts of silver, silicon, and the mixed Cu-Al material from the metal contacts.

The recycling process runs in continuous mode for a total annual operating time of 7,920 hours (330 days). The throughput of the process as well as the recycling fee associated with the PV waste stream have been investigated simultaneously through a multi-parametric analysis to identify the conditions that determine the economic feasibility of the process.

Process Description

The waste material is received into the recycling facility and stored in mobile totes (P-1/BCL-101) before being subjected to manual dismantling for the removal of the aluminum frames from the panels (P-2/GBX-101). The manually separated aluminum frames represent a revenue source of the process. The residual cell material is fed to a grinding operation (P-4/GR-101) for size reduction and liberation of 35% of the glass contained in the waste as well as some silver and silicon. The ground cell material is sent to a sieve (P-5/CSP-101) that produces three fractions, a coarse fraction, an intermediate fraction, and a fine fraction. The coarse fraction is represented by the ground cell itself, whose components are kept together thanks to the gluing action of the EVA polymer.

Figure 13. Recycling of End-of-Life Solar Photovoltaic Panels

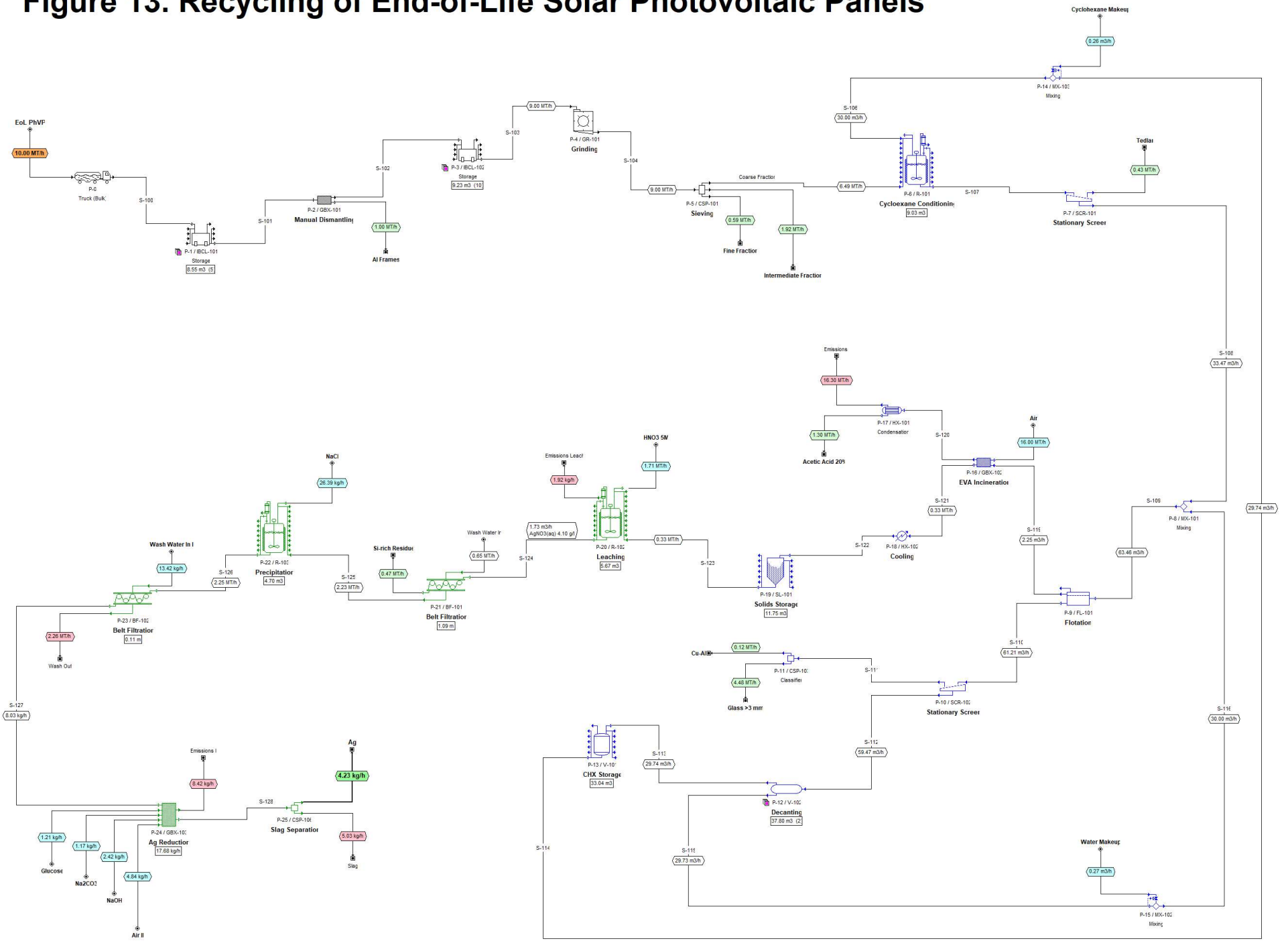

The intermediate and fine fractions are composed of the materials liberated during grinding. In particular, the intermediate fraction contains 76% of the liberated glass (27% of the total glass) and all the liberated silicon (11% of the total silicon), whereas the fine fraction contains the remaining 24% of the liberated glass and all liberated silver (10% of the total silver). The intermediate and fine fractions constitute revenue streams while the coarse fraction enters the physical-chemical classification section. Here this coarse fraction enters a chemical reactor (P-6/R-101) where it is mixed with cyclohexane in a solid-liquid ratio of 1:2 at 35 °C. This operation determines the chemical modifications in the EVA polymer that loses its gluing power and liberates all remaining PV components.

The suspension leaving the chemical reactor (stream S-107) passes through a stationary screen (P-7/SCR-101) employing a wide mesh sieve (7 mm) that retains the Tedlar® while allowing through the cyclohexane and the remaining solids therein suspended. The under-sieve suspension is then mixed with water (P-8/MX-101) in a volume ratio 1:1 and fed to a flotation cell (P-9/FL-101) while the Tedlar represents an outlet stream of the process.

In the flotation cell, water and cyclohexane stratify, thus allowing the EVA sheets to float on the cyclohexane and the heavier glass and metal filaments to sediment in the water. This enables the removal of the EVA sheets through the top of the flotation and the separation of the heavy solids from the bottom.

The water-cyclohexane mixture bearing the heavy suspended solids (S-110) is passed through a stationary screen (P-10/SCR-102) that retains the solids while allowing the liquid to flow through. The liquid mixture undergoes decanting (P-12/V-102) for the separation of cyclohexane from water, which is recirculated to the conditioning reactor (P-6/R-101) and the flotation cell (P-9/FL-101), respectively. The solid mixture of glass and metal filaments retained by the stationary screen is sent to an air classifier, which separates the heavier glass from the lighter metal filaments. Both separated streams represent sources of revenue for the process.

Since the function of the EVA layers in the PV panels is to encapsulate the PV cell, the EVA sheets separated by flotation bear valuable materials such as silver and silicon. These materials are recovered in the hydrometallurgical section of the flowsheet upon thermal decomposition of the EVA polymer. The thermal decomposition is conducted in a kiln (P-16/GBX-102) that operates at 400°C in the presence of air. The reactions taking place in the kiln are as listed in Table 25.

Table 25. Chemical reactions in the thermal decomposition of EVA (P-16/GBX-102).

Reaction Stoichiometry	Yield	Heat
$EVA + 2042.5O_2 \rightarrow 175CH_3COOH + 1420CO_2 + 1245H_2O$	100%	-45,000 kJ/kg_{EVA}
$Cyclohexane + 9O_2 \rightarrow 6CO_2 + 6H_2O$	100%	-46,577 $kJ/ kg_{Cyclohexane}$

The gas stream leaving the kiln is sent to a condenser (P-17/HX-101) that condenses acetic acid and water, thus resulting in a 20% acetic acid solution while liberating carbon dioxide and air in the atmosphere. The residual solid from the thermal decomposition is cooled (P-18/HX-102) and stored (P-19/SL-101) prior to hydrometallurgical processing for recovery of silver and silicon.

Silver and silicon are recovered from the ashes produced in the thermal decomposition of the EVA sheets. The ashes are fed to a leaching reactor (P-20/R-102) with a 5M HNO3 solution that oxidizes and dissolves silver as nitrate while leaving silicon as the solid residue. The leaching reactor operates at 60°C with a residence time of 3 hours. Table 26 displays the reaction taking place in the leaching reactor.

Table 26. Chemical reactions in leaching (P-20/R-102).

Reaction Stoichiometry	Yield	Heat
$Ag + 2HNO_3(aq) \rightarrow AgNO_3(aq) + NO_2(g) + H_2O$	100%	276 kJ/kg_{Ag}

The leach slurry leaving the reactor is fed to a belt filter (P-21/BF-101) that generates a filtrate solution rich in silver and a solid residue containing the undissolved silicon. The solid residue retained by the filter represents an output (and revenue) of the process. The filtrate (S-125) enters a precipitation reactor (P-22/R-103) where the dissolved silver is precipitated as chloride through the addition of NaCl. The precipitation reactor operates adiabatically with a residence time of 2 hours. The chemical reactions taking place during precipitation are listed in Table 27.

Table 27. Chemical reactions in the precipitation of silver (P-22/R-103).

Reaction Stoichiometry	Yield	Heat
$NaCl \rightarrow NaCl(aq)$	100%	150 kJ/kg_{NaCl}
$AgNO_3(aq) + NaCl(aq) \rightarrow AgCl + HNO_3(aq)$	100%	-440 kJ/kg_{AgNO3}

Following precipitation, another solid-liquid separation is conducted by filtration in a belt filter (P-23/BF-102), which also washes the cake using 2 L/min of water per meter of belt. The washed cake is sent to a reducing furnace for recovery of silver while the liquid stream made of filtrate and wash water is assigned to a receiving storage unit that collects wastewater. The washed cake (S-127) containing 70% AgCl is then fed to a furnace (P-24/GBX-103) where silver is reduced to the metal state by glucose at 600°C. The furnace also receives caustic soda to assist the reduction and sodium carbonate as a flux. The set of reactions considered in this operation are listed in Table 28. Silver represents a revenue source while the slag is considered a solid waste.

Table 28. Chemical reaction in the reduction of silver (P-24/GBX-103).

Reaction Stoichiometry	Yield	Heat
$24AgCl + C_6H_{12}O_6 + 30NaOH \rightarrow 24Ag + 24NaCl + 6NaHCO_3 + 18H_2O$	75%	597 kJ/kg_{AgCl}
$2AgCl + Na2CO_3 \rightarrow 2Ag + 2NaCl + CO_2 + 0.5O_2$	100%	590 kJ/kg_{AgCl}
$NaCl(aq) \rightarrow NaCl$	100%	-150 kJ/kg_{NaCl}
$NaNO_3(aq) \rightarrow NaNO_3$	100%	-239 kJ/kg_{NaNO3}
$C_6H_{12}O_6 + 6O_2 \rightarrow 6CO_2 + 6H_2O$	100%	-15,557 $kJ/kg_{C6H12O6}$

Material Requirements

Table 29 shows the raw material requirements in MT/year for a facility that processes 30,000 MT/year of PV panels. Although cyclohexane is used in a liquid-to-solid ratio of 5:1, its annual consumption is only 551 MT/year thanks to its extensive recycling in the process. The same consideration applies to water. The main chemical agent used in the process is the 5M HNO3 solution for the leaching of silver. Five volumes of acidic solution are required per unit weight of solid Ag-containing powder.

Table 29. Material requirements in the recycling of PV panels.

Bulk Material	Unit Cost ($/kg)	Annual Amount		Annual Cost ($)	%
Air	0.00	21,752,7	MT	0	0.00
Cyclohexane	1.00	551,0	MT	551,035	70.87
Glucose	0.00	4.1	MT	0	0.00
HNO3 5 M	0.14	1,502,8	MT	216,390	27.83
Na2CO3	0.20	4.0	MT	807	0.10
NaCl	0.02	29.8	MT	596	0.08
NaOH	0.25	17.0	MT	4,257	0.55
Water	1.50	2,928	m3(STP)	4,405	0.57
TOTAL				777,491	100.00

Cost Analysis

Table 30 displays the Executive Summary of the economic evaluation for a facility that treats 30,000 metric tons (MT) of EoL PV panels per year. The total capital investment for such a facility is around $26M. Total annual revenues of around $60M against $34M operating costs produce a ROI of 73% and a payback time of 1.36 years. The gross margin is also relatively high, accounting for 43%. It must be noted, however, that approximately 33% of the revenues are associated with the fee ($0.25/kgEoL-PVP) the community/collectors would pay to recyclers to treat the PV waste.

Table 30. Executive Summary for the analyzed PV recycling process.

EXECUTIVE SUMMARY (2020 prices)	
Total Capital Investment	25,849,000 $
Capital Investment Charged to This Project	25,849,000 $
Operating Cost	34,225,000 $/year
Main Revenue	19,800,000 $/year
Other Revenues	40,365,000 $/year
Total Revenues	60,165,000 $/year
Cost Basis Annual Rate	79,200 MT UPRF/year
Unit Processing Cost	432.13 $/MT UPRF
Unit Processing Revenue	759.66 $/MT UPRF
Gross Margin	43.12 %
Return On Investment	73.40 %
Payback Time	1.36 years
IRR (After Taxes)	40.53 %
NPV (at 3.0% Interest)	144,372,000 $

A better understanding of the origins of operating costs can be obtained by looking at the annual operating cost breakdown chart in Figure 14.

As can be seen in the chart, the main operating cost of the process is the labor-dependent cost, which accounts for 50% of the total operating expenses. This cost is largely due to the large number of operators required in the upstream process to separate the Al frames from the PV panels. As a matter of fact, as one person can disassemble one frame in 5 minutes, over 40 labor hours are required to process 10 MT of EoL-PVPs entering the process every hour. Clearly, replacing the manual labor with automated operations is expected to significantly reduce the operating costs. Raw materials account for 17% of the total operating costs. The third highest operating cost (12%) is the facility-dependent expenses which account for the depreciation of the fixed capital investment and the maintenance of the facility.

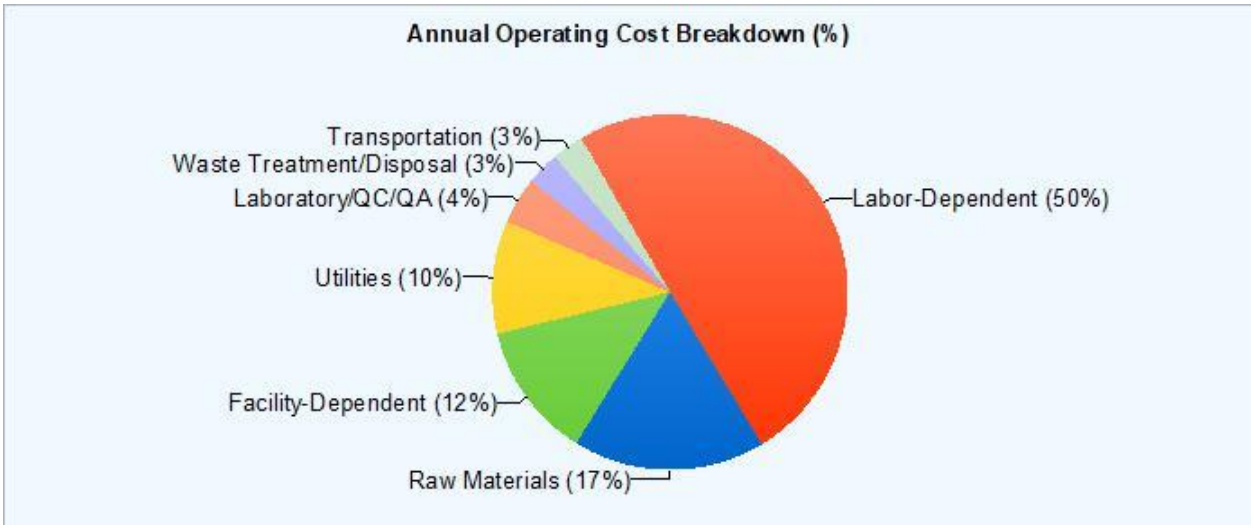

Figure 14. Annual Operating Cost Breakdown for the EoL-PVP recycling flowsheet.

Multi-Parametric Analysis

The economic figures shown in Table 30 strongly depend on two parameters, namely recycling volume and recycling fee. While the first one can be easily guessed by any possible investor, the second one is more difficult to know because it depends on the specific agreements between recyclers, collecting consortia and third parties. At the same time, these two factors are not independent on each other, i.e., the minimum recycling fee that is required to attain economic feasibility or profit depends on the PV throughput. For this reason, the COM interface of SuperPro Designer was used to vary simultaneously the PV throughput in the range 3000-30000 MT/year and the recycling fee from 0.25 to 0.7 $/kg. Figure 15 displays the impact on the return on the investment (ROI). The process becomes profitable for PV throughputs above 20,000 MT/year and recycling fees of at least $0.4/kg.

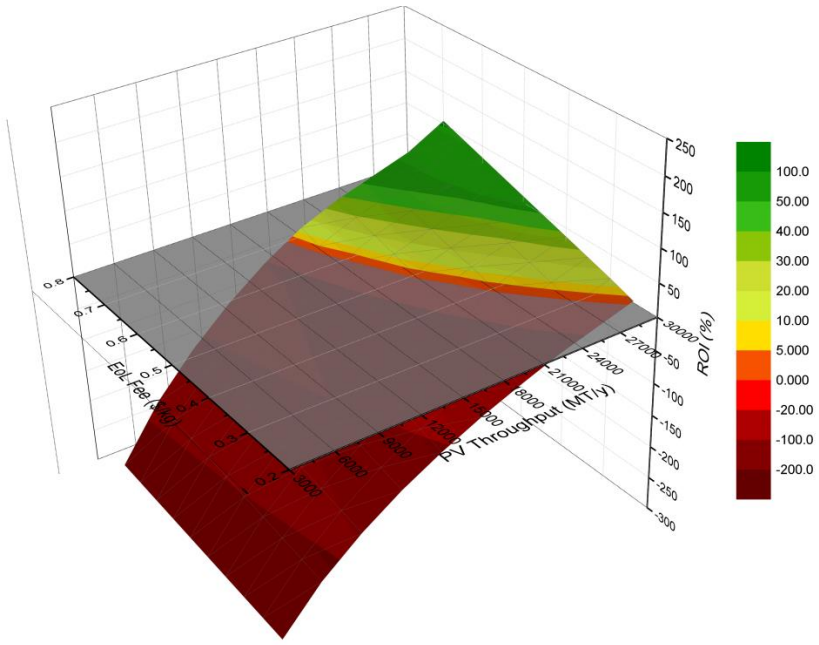

Figure 15. Results of the multi-parametric analysis in terms of ROI vs recycling fee and PV throughput.

1.5.4 Example #4 - Hydrometallurgical Recycling of Lithium-Ion Batteries

Lithium-ion batteries (LiBs) are high-capacity accumulators that find wide application in portable electronics and electric vehicles. The simplest unit within batteries, namely "single cell", is made of several components. The cathode is a lithiated nickel-manganese-cobalt oxide layered on an aluminium foil. The Ni:Mn:Co ratio in cathode materials varies from 1:1:1 to 8:1:1 The LiBs anodes consist of graphite coated on copper foils. Anode and cathode powders are bound to their current collectors (Cu foil, Al foil) by means of a binder made of polyvinylidene fluoride (PVDF). A porous separator acts as a permeable membrane to keep the two electrodes apart while allowing the transport of lithium. Separators are typically made of fibers (cotton, nylon, polyesters, glass), polymer films (polyethylene, polypropylene, polytetrafluoroethylene, polyvinyl chloride) or ceramics. The transport of lithium between electrodes is enabled by the presence of an electrolyte, which is a lithium salt such as lithium hexafluorophosphate ($LiPF_6$), perchlorate ($LiClO_4$), or tetrafluoroborate ($LiBF_4$) dissolved in organic carbonates (e.g., ethylene carbonate and diethyl carbonate). The casing is the protective shell surrounding the cell. It consists of iron and/or nickel-based materials and accounts for up to 15% of the cell weight. Cathode and anode account for about 35% and 25% of the LiB weight, respectively. Cell housing, electrolytes, binder, and separators account for the remaining 40%. The composition of LiBs is summarized in Table 31 [85].

Table 31. Composition of LiBs

Material	(%)
Casing	20-25
Cathode material	25-30
Anode material	14-19
Electrolyte	10-15
Cu foil	5-10
Al foil	5-8
Others	To balance

The volume of LiBs waste is proportional to their production. In general, the market of portable lithium-ion batteries has been increasing constantly in the last two decades due to massive deployment of laptops, mobile phones, and other portable devices. In 2008 in the USA and Europe, the consumption of batteries was estimated at 8 billion units per year, 2 billion units more than in Japan [109]. In 2015, the total amount of battery cathode material placed in the market was 140,000 metric tons (MT) [110]. Considering that this fraction accounts for about 25-30% of the total battery weight, the amount of Li-ion battery material theoretically placed on the market for the same year goes above 400,000 MT. A much greater increase in LIBs sales is expected in the next years due to the massive deployment of electric vehicles.

This example analyzes a physico-hydrometallurgical process for the recycling of portable lithium-ion batteries (LIBs). First batteries are treated by thermal and mechanical operations to free the electrode powder and separate the other valuable components. The generated electrode powder undergoes hydrometallurgical treatment for the extraction and separation of all valuable metals therein contained via leaching, precipitation, and solvent extraction. Manganese, cobalt, and lithium are recovered from their aqueous solutions by precipitation-crystallization as sulfates and carbonate, respectively. Nickel is recovered as carbonate by precipitation. A simplified version of the flowsheet is shown in Figure 16. The detailed flowsheet and the actual SuperPro Designer computer file of this example is available as part of the evaluation edition of SuperPro Designer which can be downloaded from www.intelligen.com.

The process runs in a mixed continuous-batch mode. The physical operations and the crystallization units run in continuous mode while the chemical operations (leaching, precipitation, solvent extraction) run in batch. The plant processes around 11,000-12,000 MT/year of Li-ion battery material, corresponding to 4,266 kg of battery material per batch. This example analyzes two cases (A and B). Case B employees extra equipment operating in staggered mode to reduce the cycle time of the process and increasing the throughput of the plant.

Figure 16. Recycling of Lithium-Ion Batteries

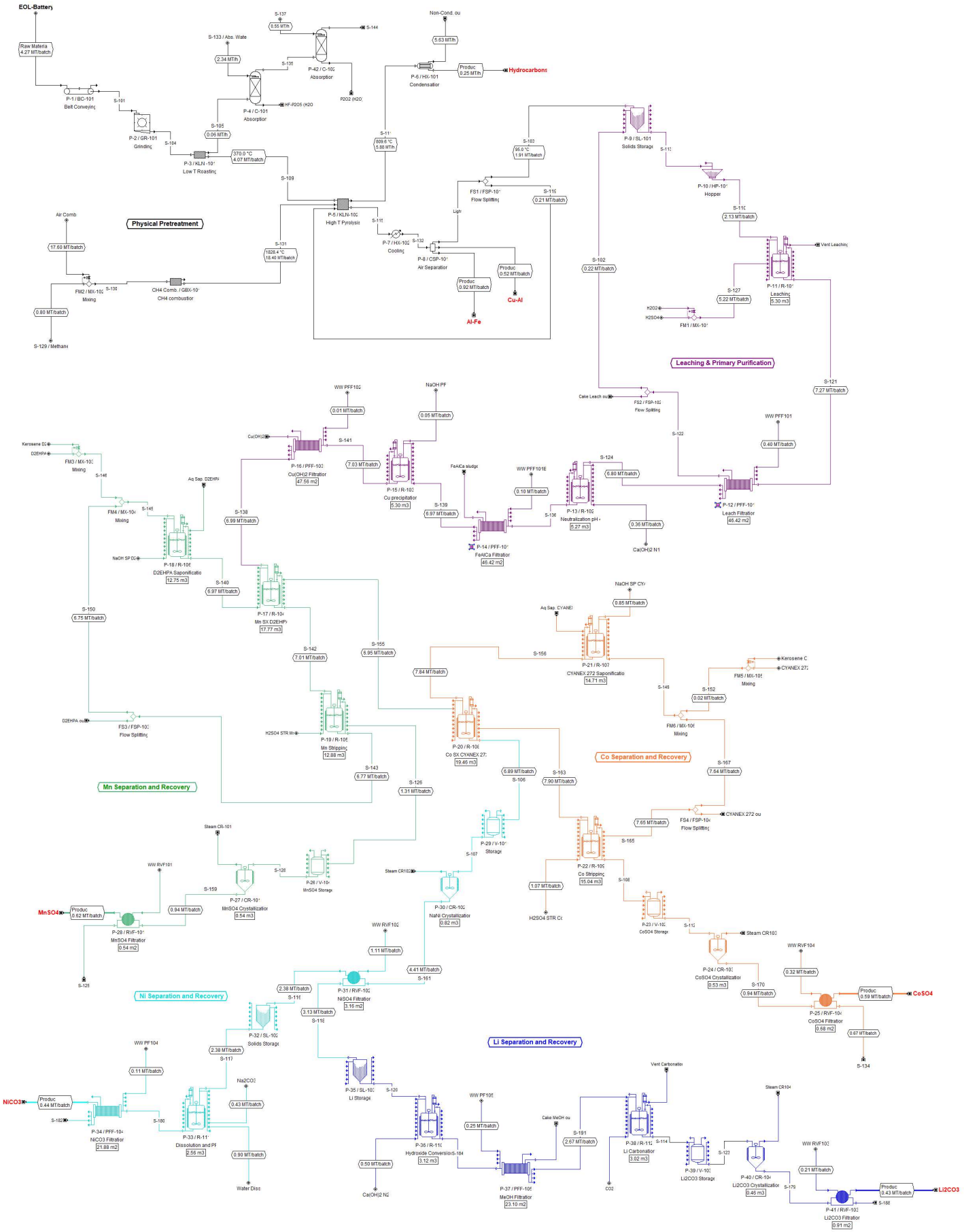

Process description

End-of-life lithium-ion batteries go through grinding (P-2/GR-101) and preliminary low-temperature roasting at 230 °C (P-3/KLN-101). The grinding operation breaks the battery casing, thus enabling the thermal decomposition of the battery electrolyte ($LiPF_6$) and the volatilization of the resulting products that are condensed and absorbed in water (P-4/C-101). The reaction taking place during low-temperature roasting is shown in Table 32.

Table 32. Reaction taking place during low-temperature roasting (procedure P-3).

Reaction Stoichiometry	Yield	Heat
2LiPF6 + 5H2O → 10HF + 2LiF + P2O5	100%	944 kJ/kg_{LiPF6}

Following the low-temperature roasting, the materials undergo thermal treatment at 750°C (P-5/KLN-102). This operation results in the pyrolysis of the plastics along with the carbothermic reduction of the cathode materials [111]. The reactions considered are listed in Table 33.

Table 33. Reactions taking place during high-temperature roasting (procedure P-5).

Reaction Stoichiometry	Yield	Heat
$4LiCoO_2 + 3C \rightarrow 4Co + 2Li_2O + 3CO_2$	97%	-4614 kJ/kg_{LiCoO2}
$4LiNiO_2 + 3C \rightarrow 4Ni + 2Li_2O + 3CO_2$	97%	-5678 kJ/kg_{LiNiO2}
$2.4LiMn_2O_4 + C \rightarrow 1.6Mn_3O_4 + 1.2Li_2O + CO_2$	97%	-5509 $kJ/kg_{LiMn2O4}$
$C_{414}H_{864} \rightarrow 6C_{19}H_{38} + 6C_{18}H_{38} + 6C_{17}H_{36} + C_{15}H_{32}$	100%	-2610 $kJ/kg_{C414H864}$

The volatile hydrocarbons produced by pyrolysis are condensed and recovered (P-6/HX-101), whereas the non-volatile material is cooled down (P-7/HX-102) prior to a pneumatic separation (P-8/CSP-101). This separation splits the non-volatile components into three streams: a heavy fraction (housing-casing materials), a medium fraction (current collector foils), and a light fraction (electrode powder and some impurities). The first two fractions are recovered as they are (they could be further processed) while the electrode powder is subjected to leaching (P-11/R-101) by sulfuric acid (H_2SO_4) and hydrogen peroxide (H_2O_2). During leaching, cobalt, nickel, manganese, and lithium are dissolved along with other metals considered as impurities (copper, aluminum, iron) [112]. The leaching requires 2 hours though the overall leaching procedure takes 3 hours to account for the transfer of reagents into the vessel and the transfer of products out of the vessel. The reactions taking place in the leaching procedure are listed in Table 34.

Table 34. Reactions taking place in leaching (procedure P-11).

Reaction Stoichiometry	Yield	Heat
$2LiCoO_2 + 3H_2SO_4(aq) + 3H_2O_2 \rightarrow 2CoSO_4(aq) + Li_2SO_4(aq) + 2O_2 + 6H_2O$	98%	-7788 kJ/kg_{LiCoO2}
$2LiNiO_2 + 3H_2SO_4(aq) + 3H_2O_2 \rightarrow 2NiSO_4(aq) + Li_2SO_4(aq) + 2O_2 + 6H_2O$	98%	-8578 kJ/kg_{LiNiO2}
$2LiMn_2O_4 + 5H_2SO_4(aq) + 3H_2O_2 \rightarrow 4MnSO_4(aq) + Li_2SO_4(aq) + 3O_2 + 8H_2O$	98%	-6590 $kJ/kg_{LiMn2O4}$
$Mn_3O_4 + 3H_2SO_4(aq) + H_2O2 \rightarrow 3MnSO_4(aq) + O_2 + 4H_2O$	98%	-819 kJ/kg_{Mn3O4}
$Co + H_2O_2 + H_2SO_4(aq) \rightarrow CoSO_4(aq) + H_2O$	98%	-7372 kJ/kg_{Co}
$Ni + H_2O_2 + H_2SO_4(aq) \rightarrow NiSO_4(aq) + H_2O$	98%	-7215 kJ/kg_{Ni}
$Li_2O + H_2SO_4(aq) \rightarrow Li_2SO_4(aq) + H_2O$	100%	-8198 kJ/kg_{Li2O}
$2LiF + H_2SO_4(aq) \rightarrow Li_2SO_4 + 2HF(aq)$	100%	175 kJ/kg_{LiF}
$2Fe + 3H_2SO_4(aq) + 3H_2O_2 \rightarrow Fe_2(SO_4)_3(aq) + 6H_2O$	100%	-11172 kJ/kg_{Fe}
$2Al + 3H_2SO_4(aq) + 3H_2O_2 \rightarrow Al_2(SO_4)_3(aq) + 6H_2O$	100%	-41027 kJ/kg_{Al}
$Cu + H_2SO_4(aq) + H_2O_2 \rightarrow CuSO_4(aq) + 2H_2O$	100%	-5015 kJ/kg_{Cu}

Following leaching, the solution is neutralized to pH 5 with $Ca(OH)_2$ to precipitate and remove iron, aluminum, and copper [113] upon consuming the residual H_2SO_4 with precipitation of $CaSO_4$. The neutralization reactions are listed in Table 35.

Table 35. Reactions taking place in neutralization-precipitation (P-13/R-102).

Reaction Stoichiometry	Yield	Heat
$H_2SO_4(aq) + Ca(OH)_2 \rightarrow CaSO_4 + 2H_2O$	100%	-1125 kJ/kg_{H2SO4}
$Fe_2(SO_4)_3(aq) + Ca(OH)_2 \rightarrow 2FeOOH + 3CaSO_4 + 2H_2O$	100%	-526 $kJ/kg_{Fe2(SO4)3}$
$Al_2(SO_4)_3(aq) + Ca(OH)_2 \rightarrow Al_2O_3 + 3CaSO_4 + 3H_2O$	100%	-251 $kJ/kg_{Al2(SO4)3}$

The resulting solids are removed using a plate & frame filter (P-14/PFF-101). Next, the dissolved copper is precipitated as $Cu(OH)_2$ by increasing further the pH to 6 with NaOH (P-15/R-103). The reactions assumed to occur in the precipitation of copper are listed in Table 36.

Table 36. Post-leaching neutralization reactions (P-15/R-103).

Reaction Stoichiometry	Yield	Heat
$NaOH \rightarrow NaOH(aq)$	100%	-1098 kJ/kg_{NaOH}
$CuSO_4(aq) + 2NaOH(aq) \rightarrow Cu(OH)_2 + Na_2SO_4(aq)$	98%	-350 kJ/kg_{CuSO4}

After precipitation, the precipitate is separated from the solution which is rich in cobalt, nickel, manganese, and lithium using a Plate & Frame filter (P-16/PFF-103). To split these elements into four

different streams, two solvent extraction circuits, using organophosphorus compounds D2EHPA and CYANEX 272, are performed sequentially [51]. The separation of manganese is performed using D2EHPA in kerosene (P-17) upon 75% saponification with NaOH (P-18). Small amounts of cobalt and nickel are also extracted in the process.

The extracted metals are later brought back into the aqueous phase by stripping with H_2SO_4 50% (P-19). The stripped solution contains a high concentration of manganese and low concentrations of nickel and cobalt impurities in acidic medium. Manganese sulfate monohydrate ($MnSO_4 \cdot H_2O$) is recovered from this solution with a yield of 95% *via* crystallization (70% water evaporation) and separated from the mother liquor using a rotary vacuum filter (P-28/RVF-101). The raffinate from the solvent extraction of manganese enters the second solvent extraction circuit, where CYANEX 272 in kerosene is used to extract the residual cobalt preferentially over nickel [109].

The extraction with CYANEX 272 also includes the saponification of the extractant (P-21/R-107), extraction itself (P-20/R-108), and stripping (P-22/R-109). The cobalt-rich stripped solution is sent to a crystallization unit (P-24/CR-103) where 95% of cobalt is crystallized as cobalt sulfate heptahydrate (CoSO4 · 7H2O) and separated using a Rotary Vacuum filter (P-25/RVF-104) upon evaporating 70% of the total water. The raffinate solution from solvent extraction contains nickel and lithium as dissolved sulfates along with the neutralization sulfate by-products (Na_2SO_4) accumulated through the previous operations. This stream undergoes evaporation-crystallization (P-30/CR-102) for the separation of nickel sulfate heptahydrate ($NiSO_4 \cdot 7H_2O$) and anhydrous sodium sulfate (Na_2SO_4) from Li_2SO_4, which remains in solution. The purity of the final nickel product is increased by re-dissolving the sulfate crystals in hot water and precipitating nickel as nickel carbonate ($NiCO_3$) through the addition of Na_2CO_3 (P-33/R-111). The re-dissolution and precipitation are performed in the same vessel, given the batch nature of the hydrometallurgical operations. The reactions considered in this step are listed in Table 37.

Table 37. Dissolution of sulfates and precipitation of $NiCO_3$ (P-33/R-111).

Reaction Stoichiometry	Yield	Heat
$Na_2SO_4 \rightarrow Na_2SO_4(aq)$	Up to 450 g/L Na_2SO_4	-13 kJ/kg_{a2SO4}
$NiSO_4 \cdot 7H_2O \rightarrow NiSO_4(aq) + 7H_2O$	100%	93 kJ/$kg_{NiSO4 \cdot 7H2O}$
$NiSO_4(aq) + Na_2CO_3 \rightarrow NiCO_3 + Na_2SO_4(aq)$	100%	-38 kJ/kg_{NiSO4}

The filtrate from nickel sulfate filtration (P-31/RVF-102) contains around 23% Li_2SO_4 along with nickel and cobalt impurities. This stream (S-118) is subjected to neutralization, carbonation, and crystallization. In the neutralization step (P-36/R-110), $Ca(OH)_2$ is added to precipitate the metal

impurities as $Ni(OH)_2$, $Co(OH)_2$, and $CaSO_4$ while keeping lithium in solution as lithium hydroxide (LiOH). The reactions taking place in the neutralization procedure are listed in Table 38.

Table 38. Conversion of lithium, cobalt, and nickel sulfates to hydroxides (P-36/R-110).

Reaction Stoichiometry	Yield	Heat
$L_{i2}SO_4(aq) + Ca(OH)_2 \rightarrow 2LiOH(aq) + CaSO_4$	100%	15 kJ/kg_{Na2SO4}
$CoSO_4(aq) + Ca(OH)_2 \rightarrow Co(OH)_2 + CaSO_4$	100%	-1295 kJ/kg_{oSO4}
$NiSO_4(aq) + Ca(OH)_2 \rightarrow Ni(OH)_2 + CaSO_4$	100%	-1368 kJ/kg_{NiSO4}
$MnSO_4(aq) + Ca(OH)_2 \rightarrow Mn(OH)_2 + CaSO_4$	100%	-185 kJ/kg_{MnSO4}

The separation of the insoluble hydroxides from the soluble LiOH is performed by filtration (P-37/PFF-105). After filtration, the lithium-rich filtrate (S-191) is subjected to carbonation to convert LiOH to Li_2CO_3. This is performed in a pressurized vessel (P-38/R-112) using carbon dioxide (CO_2) as carbonating agent. The liquid stream from carbonation is finally sent to a crystallization unit (P-40/CR-104) to evaporate 80% of the water and crystallize 90% of the dissolved lithium carbonate as anhydrous lithium carbonate (Li_2CO_3). The reaction that describes the carbonatation of LiOH is given in Table 39.

Table 39. Carbonation of LiOH (P-38/R-112).

Reaction Stoichiometry	Yield	Heat
$2LiOH(aq) + CO_2 \rightarrow Li_2CO_3 + H_2O$	99%	-2267 kJ/kg_{LiOH}

Process scheduling

Overall, the hydrometallurgical process for recycling of batteries runs in batch mode except for the thermal processing steps (e.g., roasting, crystallization). This implies that each piece of equipment is occupied for a certain time (procedure duration) cyclically through subsequent batches. Figure 17 displays the Equipment Occupancy Chart (EOC) for eight consecutive batches (each color represents a different batch). The batch cycle time (i.e., the time from leaching to the generation of the final product) is 13 h. Clearly, the batch time includes only the unit procedures running in batch since; the ones running in continuous mode are occupied for the whole time. The re-dissolution of nickel sulfate and re-precipitation of nickel carbonate (procedure P-33 which utilizes reactor R-111) has the longest duration of 3.25 h and is the cycle time bottleneck of the overall process. Consequently, the minimum time between two consecutive batches is also 3.25 h. Such a minimum cycle time enables to conduct 2,433 batches of the same process throughout the annual operating time of 330 days. The same chart highlights (second line from top) that the same plate and frame filter (PFF-101) is used to handle the

post-leaching and post-precipitation filtrations. This is made possible by the short duration of those operations.

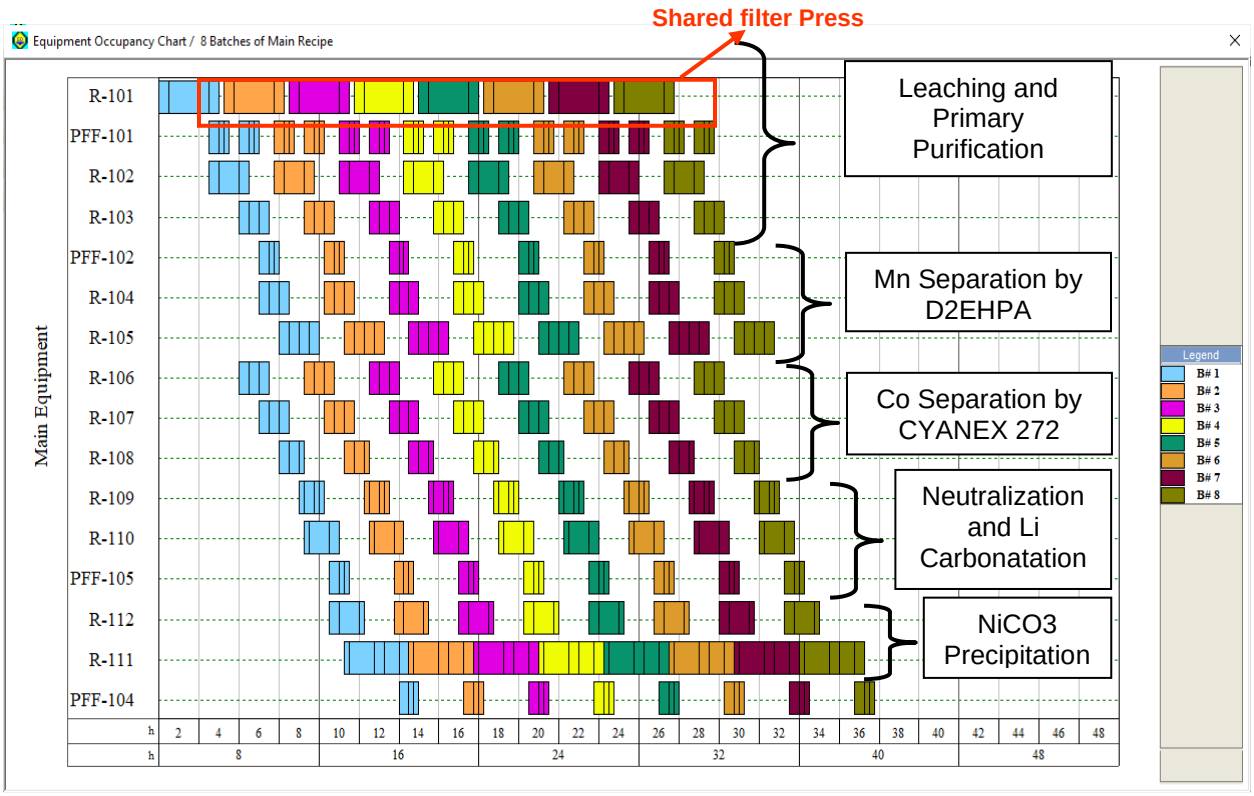

Figure 17. Equipment occupancy chart for 8 consecutive batches (Case A).

As mentioned above, the cycle time bottleneck sets the minimum cycle time of the process to 3.25 hours, which in turn limits the maximum number of batches to 2433 per year. Case B utilizes two extra reactors (STG01 > R-101 and STG01 > R-111) operating in staggered mode (alternating from batch to batch) and allocated to the procedures with the longest durations, those utilizing R-101 and R-111, respectively. Figure 18 displays the impact of the extra reactors on the cycle time of the overall process which is reduced from 3.25 hours to 2 hours which is the duration of the new cycle time bottleneck (P-13 utilizing reactor R-102). The reduced cycle time enables the plant to process 3,954 batches per year, an increase of 62%. Use of extra equipment operating in staggered mode is a common technique of increasing the production throughput of batch processes and can be readily analyze with SuperPro Designer.

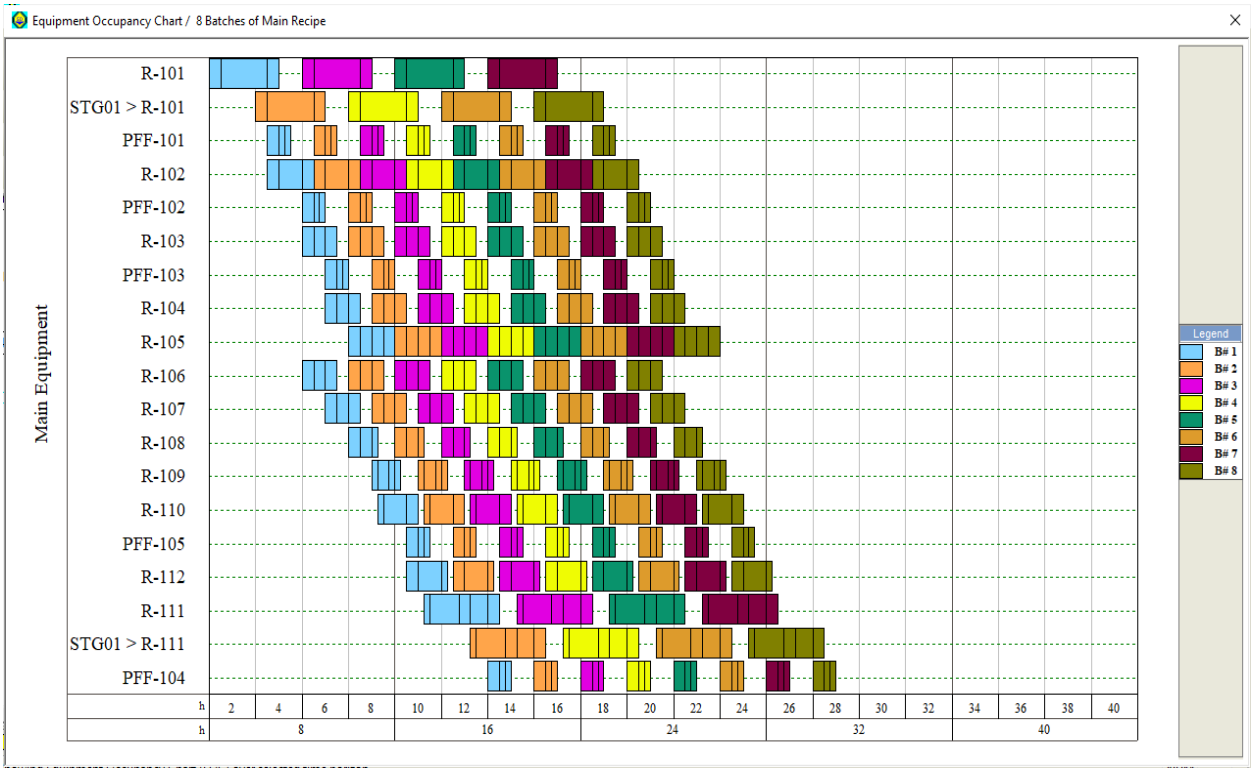

Figure 18. Equipment occupancy chart for 8 consecutive batches (Case B).

Material Requirements

The raw material requirements in MT/year and MT/batch for both Cases A and B are shown in Table 40. The table clearly indicates that a single batch involves the treatment of the same amount of battery material (4.27 MT), thus requiring the same amounts of raw materials, irrespective of the use of staggered and shared equipment. In contrast, the material requirements per year are different for the two process scenarios, as they depend on the total number of batches executed per year. As explained earlier, the extra equipment operating in staggered mode for Case B results in about 1500 additional batches per year, which increases the throughput of the process (EoL-LiBs throughput) from 10,380 MT to 16,869 MT of battery material per year. Table 40 indicates that H_2SO_4 50% is the largest raw material requirement despite the extensive recirculation upstream of the acidic liquid solutions. Water is the second most utilized material, followed by the caustic soda and lime used for neutralization-precipitation purposes. The consumption of the organic extractants D2EHPA and CYANEX 272 as well as their solvent kerosene is instead very low because their recirculation/reuse ratio within the process accounts for 99%.

Table 40. Material Requirements for the two cases

Material	Case A		Case B	
	MT/year	MT/batch	MT/year	MT/batch
Air	42,821	17.60	69,590	17.60
$Ca(OH)_2$	2,098	0.86	3,410	0.86
CO_2	778	0.32	1,265	0.32
CYANEX 272	18	0.01	30	0.01
D2EHPA	12	0.01	20	0.01
EOL-LiBs	10,380	4.27	16,869	4.27
H_2O_2	1,271	0.52	3,163	0.80
H_2SO_4 (50% w/w)	16,632	6.83	27,018	6.83
kerosene	30	0.01	49	0.01
Methane	1,946	0.80	422	0.11
Na_2CO_3	1,038	0.43	1,687	0.43
NaOH	130	0.05	211	0.05
NaOH (50% w/w)	4,670	1.92	7,588	1.92
Water	10,570	4.34	17,184	4.34
TOTAL	92,419	37.97	150,171	37.97

Cost and Cash Flow Analysis

The Executive Summary of the Economic Evaluation Report is shown in Table 41 for both cases. Clearly, the optimized process (Case B) produces better financial results. Despite the higher investment costs (about $5M) due to the extra reactors operating in staggered mode, the optimized process ensures higher revenues for around $21M/yr. This is due to the larger number of batches processed per year, allowing an increase in the battery recycling capacity by 6,500 MT/yr. In turn, the increased capacity produces an increase in the gross margin from about 44 to 53%, thereby resulting in a decrease in payback time from 4.1 to around 2.3 years. This highlights the benefits of batch process simulation tools, such as SuperPro Designer, that facilitate debottlenecking studies of integrated batch processes.

Table 41. Executive Summary for the two analyzed processes.

	Case A	Case B
Total Capital Investment	46,182,000 $	50,812,000 $
Capital Investment Charged to This Project	46,182,000 $	50,812,000 $
Operating Cost	19,114,000 $/yr	26,279,000 $/yr
Main Revenue	13,984,000 $/yr	22,723,000 $/yr
Other Revenues	20,062,076 $/yr	32,599,000 $/yr
Total Revenues	34,047,000 $/yr	55,323,000 $/yr
Cost Basis Batch Rate	4.27 MT UPRF	4.27 MT UPRF
Cost Basis Annual Rate	10,384 MT UPRF/yr	16,873 MT UPRF/yr
Unit Processing Cost	1,841 $/MT UPRF	1,558 $/MT UPRF
Net Unit Processing Cost	1,841 $/MT UPRF	1,558 $/MT UPRF
Unit Processing Revenue	3,279 $/MT UPRF	3,279 $/MT UPRF
Gross Margin	43.86 %	52.5 %
Return On Investment	24.25 %	42.9 %
Payback Time	4.12 years	2.33 years
IRR (After Taxes)	17.85 %	32.11 %
NPV (at 7.0% Interest)	37,335,000 $	109,225,000 $

UPRF = Total Flow of Stream 'EOL-Battery'

Figures 19 and 20 display the annual operating cost breakdown charts for Cases A and B, respectively**.** In both cases, the highest cost is represented by the raw materials, which accounts for 36% and 41% for Case A and B, respectively. The H_2SO_4 solution contributes 44% to the overall raw materials cost. This is mostly due to the large amounts of acid utilized for leaching and stripping, despite its relatively low unit price ($0.18/kg). The second highest cost (around 15%) among raw materials is associated with H_2O_2 used as a reducing agent in leaching, while the third one (19%) is associated with the natural gas burnt to heat up the thermal operations. It is important to remark that the end-of-life batteries were treated as a revenue source, instead of a raw material cost. It was assumed that the recycler does not pay to acquire the end-of-life batteries, but rather receives money ($0.5/kg) from the community to treat them.

The facility-dependent expenses are the second highest operating costs, accounting for 27% and 23% in Cases A and B, respectively. Depreciation of the fixed capital investment and maintenance of the facility are the main contributors to this cost. The decrease in facility-dependent cost observed in the optimized process is mostly due to the proportionally higher impact of the raw materials cost.

The low raw materials cost and the numerous batch procedures in the process, which intrinsically require many operators, result also in a proportionally high labor cost. Labor is in fact the third highest cost in both cases, accounting for 23% and 20%, respectively.

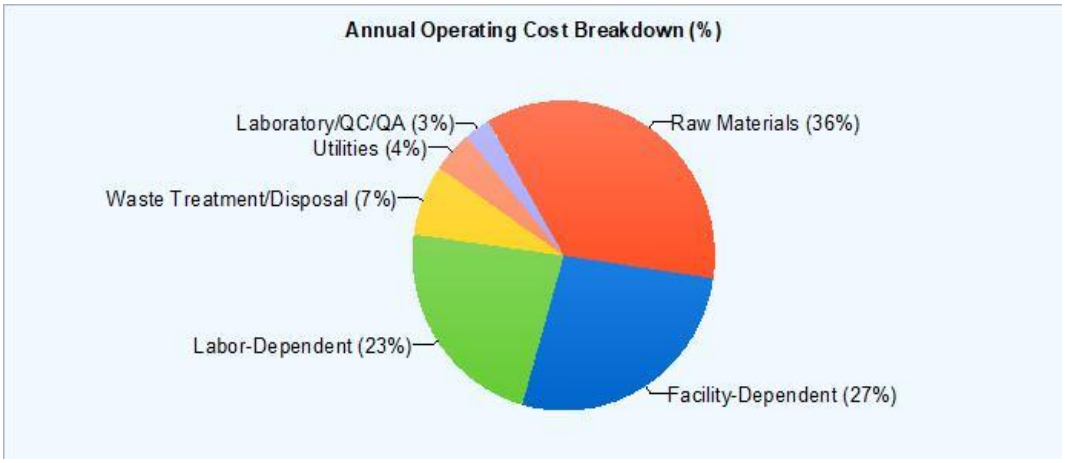

Figure 19. Annual Operating Cost Breakdown (Case A).

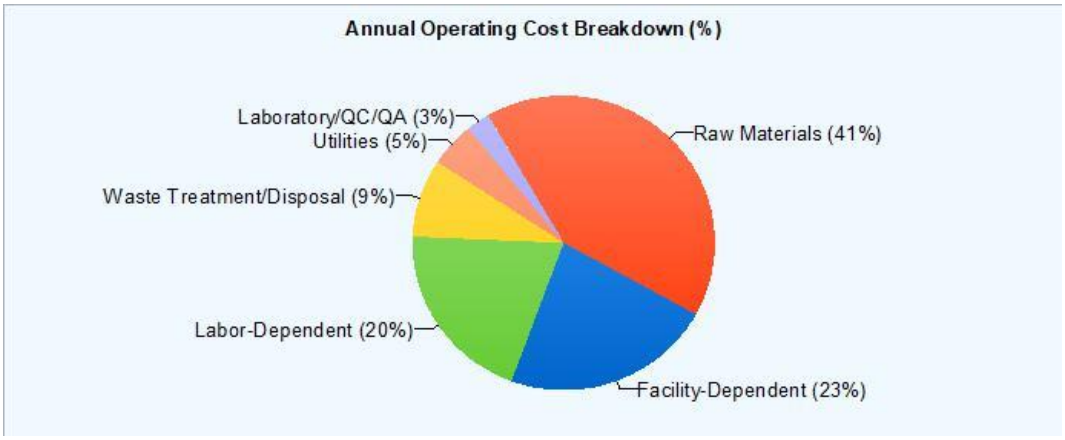

Figure 20. Annual Operating Cost Breakdown (Case B).

Table 42 displays the cash flow analysis for Case B generated by SuperPro Designer. Assuming a construction and start-up period of 33 months, the process starts generating revenues in the last 3 months of the third year of the investment. The cash flow becomes positive during the fourth year of the project. For a project lifetime of 15 years, the net present value (NPV) of the improved battery recycling project (Case B) is $128M for a discount interest rate of 7%. The internal rate of return (IRR) is 36.7% assuming total income taxes of 25%.

Table 42. Cash-flow analysis for the optimized recycling process (Case B). Prices are in 1000$.

Capital Investment	Sales Revenues	Operating Cost	Gross Profit	Depreciation	Taxable Income	Taxes	Net Profit	Net Cash Flow
- 14,004	0	0	0	0	0	0	0	- 14,004
- 18,672	0	0	0	0	0	0	0	- 18,672
- 15,801	13,831	14,916	- 1,085	2,898	0	0	1,813	- 13,988
0	55,323	26,279	29,044	2,898	29,044	7,261	24,681	24,681
0	55,323	26,279	29,044	2,898	29,044	7,261	24,681	24,681
0	55,323	26,279	29,044	2,898	29,044	7,261	24,681	24,681
0	55,323	26,279	29,044	2,898	29,044	7,261	24,681	24,681
0	55,323	26,279	29,044	2,898	29,044	7,261	24,681	24,681
0	55,323	26,279	29,044	2,898	29,044	7,261	24,681	24,681
0	55,323	26,279	29,044	2,898	29,044	7,261	24,681	24,681
0	55,323	26,279	29,044	2,898	29,044	7,261	24,681	24,681
0	55,323	23,381	31,942	0	31,942	7,985	23,956	23,956
0	55,323	23,381	31,942	0	31,942	7,985	23,956	23,956
4,131	55,323	23,381	31,942	0	31,942	7,985	23,956	28,088

IRR/NPV SUMMARY					
IRR Before Taxes	44.86%	Interest %	7.00	9.00	11.00
IRR After Taxes	36.74%	NPV	128,250.00	106,371.00	88,270.00

1.5.5 Example #5 - Manufacturing of NMC 811 Cathode Material for Lithium-Ion Batteries

Lithium-ion batteries (LiBs) are high-capacity accumulators that find wide application in portable electronics and electric vehicles. The cathode of LiBs is made from a lithium transition metal oxide layered on aluminum foil whereas the anode consists of porous carbon graphite layered on copper. During the charging process, lithium ions flow from the cathode to the anode through an electrolyte. During discharge, lithium ions flow back to the cathode, thereby ensuring power generation [114].

The key component of LiBs is the cathode material, which accounts for around 30% of the total weight of the battery. Early LiBs were based on pure lithium cobalt oxide ($LiCoO_2$) cathodes. Due to the low specific power and lifespan and to the high cost of Co, $LiCoO_2$ was later replaced by pure lithium manganese oxide ($LiMn_2O_4$). Exhibiting higher power and safety but less capacity and lifespan than $LiCoO_2$, $LiMn_2O_4$ has been gradually replaced by multi-metal oxides. The latest commercialized technology for battery cathode materials is based on a mixture of lithium cobalt-manganese-nickel

oxide, namely NMC [115]. In this material, appropriate modulation of the Ni:Mn:Co ratio provides the LiBs with a desirable balance of power, energy, capacity and lifespan. Early NMC materials utilized NMC with Ni:Mn:Co ratio of 1:1:1. The current tendency is to decrease the cobalt and manganese content at the advantage of nickel. Accordingly, nowadays NMC materials are produced at a ratio of 6:2:2 or 8:1:1 [85].

In 2015, the total amount of battery cathode material placed in the market was 140,000 metric tons (MT) [110]. This amount has been increasing steadily over the last years and is expected to increase up to 10 times following the switch to electric mobility. According to *Woodmac, UBS*, electric vehicles will represent 20% of the total automotive market by 2030 and the majority by 2035 [5]. Therefore, the production of LiBs, today around 750,000 MT/year, is expected to increase to 4,000,000 MT/year by 2025, which corresponds to about 1,200,000 MT/year of cathode material.

This example analyzes a process for the generation of LiB cathode material from primary and secondary raw materials. The main product of the process is a lithium-nickel-manganese-cobalt oxide with a Ni:Mn:Co ratio of 8:1:1, namely NMC 811 ($LiNi_{0.8}Mn_{0.1}Co_{0.1}O_2$). The raw materials used in the process include (i) older-generation NMC 111 cathode material scraps ($LiNi_{0.33}Mn_{0.33}Co_{0.33}O_2$), (ii) nickel metal, and (iii) a mixture of manganese oxides (MnO-Mn_3O_4-MnO_2). These three raw materials are processed simultaneously in three parallel hydrometallurgical lines comprising leaching and precipitation procedures. These procedures produce three intermediate streams containing the precursor materials for NMC 811. The hydrometallurgical treatment of NMC 111 scraps leads to an equimolar mixture of nickel, manganese, cobalt and lithium hydroxides ($Ni(OH)_2$, $Mn(OH)_2$, $Co(OH)_2$, $LiOH$). The nickel, which is required to achieve the proportion of 8:1:1 from the scraps that have a proportion of 1:1:1 is provided by leaching Ni metal and precipitating it as a hydroxide. Extra manganese is also required to compensate for the different leaching yields of the three raw materials and achieve the final 8:1:1 ratio. These three intermediate streams are stored in three different silos, from which they are pulled out at the 8:1:1 ratio and mixed by ball milling. The resulting material is then mixed with an equimolar amount of Li in the form of lithium carbonate (Li_2CO_3) and roasted under a controlled air atmosphere to generate the final NMC 811 material. Slightly over-stoichiometric amounts of Li may be used to improve the quality of the cathode properties; this is called over-lithiation. In addition to the NMC 811 product, the process generates crystalline sodium sulfate (a-Na_2SO_4) and a liquid stream containing more than 100 g/L of LiOH, which can also be considered as revenue sources of the process.

The production process runs in mixed batch-continuous mode. The three hydrometallurgical lines and the mixing of raw materials run in batch mode whereas the thermal operations (crystallization, roasting) run in continuous mode. Approximately 1.15 MT of NMC 811 are produced per hour, corresponding to 9,040 MT/year based on an annual operating time of 7,920 hours (330 days). Figure 21 displays the flowsheet of the process.

Figure 21. Manufacturing of NMC 811 Cathode Material for Li-Ion Batteries

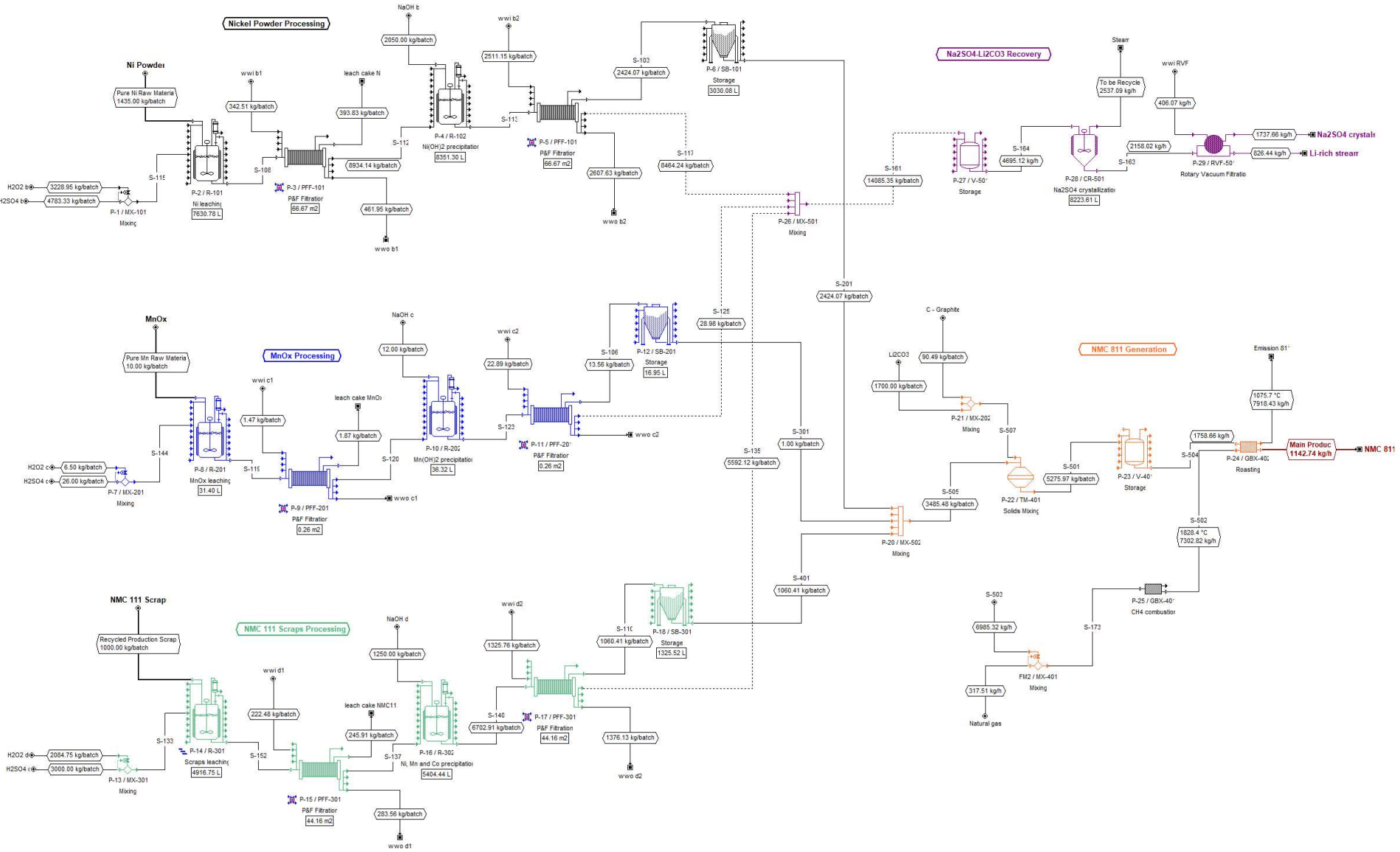

Process Description

In a first hydrometallurgical line, the nickel powder undergoes oxidizing-acidic leaching with a solution containing 30% H_2SO_4 and 10% H_2O_2 at 80°C (P-2/R-101). The leaching takes 2 h according to the stoichiometry of Table 43.

Table 43. Chemical reaction in leaching of the nickel metal powder (P-2/R-101).

Reaction Stoichiometry	Yield	Heat
$Ni + H_2O_2 + H_2SO_4(aq) \rightarrow NiSO_4(aq) + 2H_2O$	99%	-7215 kJ/kg_{Ni}

After leaching, the slurry is filtered in a filter press (P-3/PFF-101) to separate the leach liquor from the solid residue. Although the residual Ni from the leaching is very low (2-5%), the solid-liquid separation after the leaching is important to avoid having residual metallic Ni in the $Ni(OH)_2$ used as a precursor material for NMC 811. This step can be omitted if all Ni is dissolved during leaching. The filtrate containing around 550 g/L of $NiSO_4$ is then fed to another stirred vessel (P-4/R-102) where nickel is precipitated with NaOH as $Ni(OH)_2$. The chemical reactions involved in the precipitation of $Ni(OH)_2$ are listed in Table 44.

Table 44. Chemical reactions in neutralization-precipitation of nickel (P-4/R-102).

Reaction Stoichiometry	Yield	Heat
$NaOH \rightarrow NaOH(aq)$	100%	-1098 kJ/kg_{NaOH}
$H_2SO_4(aq) + 2NaOH(aq) \rightarrow Na_2SO_4(aq) + 2H_2O$	100%	-1144 kJ/kg_{H2SO4}
$NiSO_4(aq) + 2NaOH(aq) \rightarrow Ni(OH)_2 + Na_2SO_4(aq)$	99.99%	-198 kJ/kg_{NiSO4}

After the precipitation of $Ni(OH)_2$, another solid-liquid separation is conducted by filtration in a filter press (P-5/PFF-101). At the end of the filtration, the cake is washed with hot water (at 50°C) to remove the residual sodium sulfate (Na_2SO_4) formed in during neutralization and sent to a storage silo (P-6/SB-101). The filtrate, which is rich in Na_2SO_4 (S-117), is sent to the Na2SO4-Li Recovery section.

In a second and parallel hydrometallurgical line, the mixture of Mn oxides (25% MnO, 50% Mn_3O_4, 25% MnO_2), referred to as MnO_x, undergoes reducing-acidic leaching (P-8/R-201) at 80 °C with a solution containing 30% H_2SO_4 and 5% H_2O_2. Leaching takes place in 2 h according to the reaction of Table 45.

Table 45. Chemical reactions in leaching of MnO_x (P-8/R-201).

Reaction Stoichiometry	Yield	Heat
$MnO + H_2SO_4(aq) \rightarrow MnSO_4(aq) + H_2O$	99%	-1513 kJ/kg_{MnO}
$Mn_3O_4 + H_2O_2 + 3H_2SO_4(aq) \rightarrow 3MnSO_4(aq) + O_2 + 4H_2O$	97%	-819 kJ/kg_{Mn3O4}
$MnO_2 + H_2O_2 + H_2SO_4(aq) \rightarrow MnSO_4(aq) + O_2 + H_2O$	90%	-784 kJ/kg_{MnO2}

Following leaching, the slurry undergoes filtration in a filter press (P-9/PFF-201) to separate the leaching pregnant solution from the residue. As in the previous case, the solid-liquid separation after leaching is important to avoid having residual MnO_x in the $Mn(OH)_2$ used as precursor material for NMC 811. The filtrate, containing around 400 g/L of Mn(II) sulfate, is fed to another stirred vessel (P-10/R-202) where all dissolved Mn is precipitated as $Mn(OH)_2$ using NaOH as neutralizing agent. The chemical reactions involved in the precipitation of $Mn(OH)_2$ are listed in Table 46.

Table 46. Chemical reactions in neutralization-precipitation of Mn (P-10/R-202).

Reaction Stoichiometry	Yield	Heat
$NaOH \rightarrow NaOH(aq)$	100%	-1098 kJ/kg_{NaOH}
$H_2SO_4(aq) + 2NaOH(aq) \rightarrow Na_2SO_4(aq) + 2H_2O$	100 %	-1144 kJ/kg_{H2SO4}
$MnSO_4(aq) + 2NaOH(aq) \rightarrow Mn(OH)_2 + Na_2SO_4(aq)$	99.99%	-198 kJ/kg_{MnSO4}

Following the precipitation of $Mn(OH)_2$, another solid-liquid separation is conducted by filtration in a filter press (P-11/PFF-201). At the end of the filtration, the cake is washed with hot water (at 50°C) to remove the residual Na_2SO_4 and sent to a storage silo (P-12/SB-201), whereas the filtrate, rich in Na_2SO_4, is sent to the Na_2SO_4-Li Recovery section.

In a third and parallel hydrometallurgical line, the NMC 111 scraps ($LiNi_{0.33}Mn_{0.33}Co_{0.33}O_2$) is subjected to an acidic-reducing leaching (P-14/R-301) at 80 °C with a solution containing 30% H_2SO_4 and 10% H_2O_2. Leaching take place in a stirred vessel for 3.5 h according to the reactions of Table 47.

Table 47. Chemical reactions in leaching of NMC 111 scraps (P-14/R-301).

Reaction Stoichiometry	Yield	Heat
$6LiNi_{0.33}Mn_{0.33}Co_{0.33}O_2 + 9H2SO_4(aq) + 9H_2O_2 \rightarrow 2NiSO_4(aq) + 2MnSO_4(aq) + 2CoSO_4(aq) + 3Li_2SO_4(aq) + 6O_2 + 18H_2O$	98%	-8996 kJ/kg_{NMC111}

After leaching, the slurry undergoes filtration in a filter press (P-15/PFF-301) to separate the leach liquor from the residue. As in the previous cases, the solid-liquid separation after leaching is important to avoid having residues of NMC 111 in the precursor material for NMC 811. The filtrate containing $NiSO_4$, $MnSO_4$, $CoSO_4$ and Li_2SO_4, at about 100 g/L each, is then fed to another stirred vessel (P-16/R-302) along with NaOH to precipitate all nickel, manganese and cobalt as $Ni(OH)_2$, $Mn(OH)_2$, and $Co(OH)_2$, respectively. This process also converts all Li_2SO_4 into LiOH, which is soluble. The chemical reactions that take place in this procedure are listed in Table 48.

Table 48. Chemical reactions in neutralization-precipitation of NMC 111 scraps (P-16/R-302).

Reaction Stoichiometry	Yield	Heat
$NaOH \rightarrow NaOH(aq)$	100%	-1098 kJ/kg_{NaOH}
$H_2SO_4(aq) + 2NaOH(aq) \rightarrow Na_2SO_4 + 2H_2O$	100%	-1144 kJ/kg_{H2SO4}
$NiSO_4(aq) + 2NaOH(aq) \rightarrow Ni(OH)_2 + Na_2SO_4(aq)$	99.99%	-198 kJ/kg_{NiSO4}
$MnSO_4(aq) + 2NaOH(aq) \rightarrow Mn(OH)_2 + Na_2SO_4(aq)$	99.99%	-196 kJ/kg_{MnSO4}
$CoSO_4(aq) + 2NaOH(aq) \rightarrow Co(OH)_2 + Na_2SO_4(aq)$	99.99%	-1307 kJ/kg_{CoSO4}
$Li_2SO_4(aq) + 2NaOH(aq) \rightarrow 2LiOH(aq) + Na_2SO_4(aq)$	99.99%	-2 kJ/kg_{Li2SO4}

After precipitation, another solid-liquid separation is conducted in a filter press (P-17/PFF-301). At the end of the filtration, the cake is washed with hot water (at 50°C) to remove the residual Na_2SO_4 formed during the neutralization procedure. The mixture of metal hydroxides in the filter cake is sent to a storage silo (P-18/SB-301), whereas the filtrate containing Na_2SO_4 and (soluble) LiOH is sent to the Na_2SO_4-Li Recovery section.

For the generation of high-quality NMC 811, all transition metals must be present in the right molar ratio, i.e., 8:1:1. For this purpose, the three intermediate products are transferred from their respective storage silos to a mixing procedure (P-20/MX-502). The resulting mixture is then mixed with Li_2CO_3 and carbon graphite in a batch tumbler mixer (P-22/TM-401) simulating a ball mill. The concentration of Li_2CO_3 in the total Ni-Mn-Co-Li mixture (about 29% db – dry basis) can be slightly over-stoichiometric with regard to the transition metals. This is called over-lithiation and improves the quality and stability of the cathode material. The concentration of carbon graphite is instead set at 2% db. The resulting mixture is then fed to a roasting kiln operating at 700°C under controlled air atmosphere, which result in the generation and sintering of the cathode material NMC 811 and leads to the calcination of the residual metal hydroxides according to the reaction of Table 49.

Table 49. Chemical reaction in the preparation and sintering of NMC 811 (P-24/GBX-402).

Reaction Stoichiometry	Yield	Heat
$0.8Ni(OH)_2 + 0.1Mn(OH)_2 + 0.1Co(OH)_2 + 0.5Li_2CO_3 + 0.25O_2 \rightarrow LiNi_{0.8}Mn_{0.1}Co_{0.1}O_2 + 0.5CO_2 + H_2O$	100%	783 kJ/kg_{NMC811}
$Li_2CO3 \rightarrow Li_2O + CO_2$	100%	9198 kJ/kg_{Li2CO3}
$Ni(OH)_2 \rightarrow NiO + H_2O$	100%	45 $kJ/kg_{Ni(OH)2}$
$Mn(OH)_2 \rightarrow MnO + H_2O$	100%	281 $kJ/kg_{Mn(OH)2}$

The liquid streams emerging from the three hydrometallurgical lines are all rich in Na_2SO_4 (450-600 g/L) due to the neutralization-precipitation reactions. In addition, the solution generated in the

NMC 111 processing section also contains 50 g/L of LiOH. This lithium can be considered as a co-product upon concentration and removal of Na_2SO_4. Na_2SO_4 is removed by evaporative crystallization in a continuous crystallizer (P-28/CR-501) after mixing the liquid streams S-117, S-125, and S-135 with a flow-mixing procedure (P-26/MX-501). In the continuous crystallizer, 80% of the initial Na_2SO_4 is crystallized by evaporating 80% of water and cooling the mixture down to 5°C. The reaction describing the crystallization of Na_2SO_4 is shown in Table 50. The solid Na_2SO_4 crystals are then removed by rotary vacuum filtration (P-29/RVF-501), and the filtrate containing about 119 g/L of LiOH and 286 g/L of (soluble) Na_2SO_4 becomes a revenue source.

Table 50. Chemical reaction representing the crystallization of Na_2SO_4 (P-28/CR-501).

Reaction Stoichiometry	Yield	Heat
$Na_2SO_4(aq) \rightarrow Na_2SO_4$	90%	2034 kJ/kg_{Na2SO4}

Process Scheduling

Overall, this process runs in batch mode for a total annual time of 7,920 h (330 days). Although the overall process is set to batch mode, specific unit procedures within the flowsheet were individually set to continuous mode. All unit procedures within the hydrometallurgical lines as well as the mixture preparation (P-19/MX-402) and batch tumbler mixer (P-22/TM-401) procedures run in batch mode. In contrast, the unit procedures hosting thermal operations such as evaporation-crystallization (P-26/CR-501), roasting (P-24/GBX-402), and combustion (P-25/GBX-401) were set to continuous mode. Storage units (e.g., silos) running in continuous mode were added to the flowsheet whenever switching from batch to continuous procedures and *vice versa*. To avoid under sizing the equipment, the storage units were given a residence time two to three times higher than the occupancy of the next step in the flowsheet.

The process Gantt chart for a single batch is partially shown in Figure 22, while the Equipment Occupancy Chart for 8 consecutive batches of the process is displayed in Figure 23. The total recipe batch time, from leaching to mixing, is 9.5 h. Obviously, this batch time only accounts for the unit procedures running in batch mode as the ones running in continuous are occupied for the whole time. Although P-14/R-301 (NMC 11 leaching) is the unit procedure with the longest duration, the process bottleneck is the stirred vessel R-101, where Ni leaching is performed. That is the case because two reactor vessels (R-301 and R-301b) have been allocated to P-14 that operate in staggered mode and reduce its effective cycle time. Using two reactor vessels (R-301 and R-301b) in Stagger Mode to perform P-14 reduces the recipe cycle time from 4.5 h to 3 h, thereby increasing the number of batches from 1,758 to 2,637 per year.

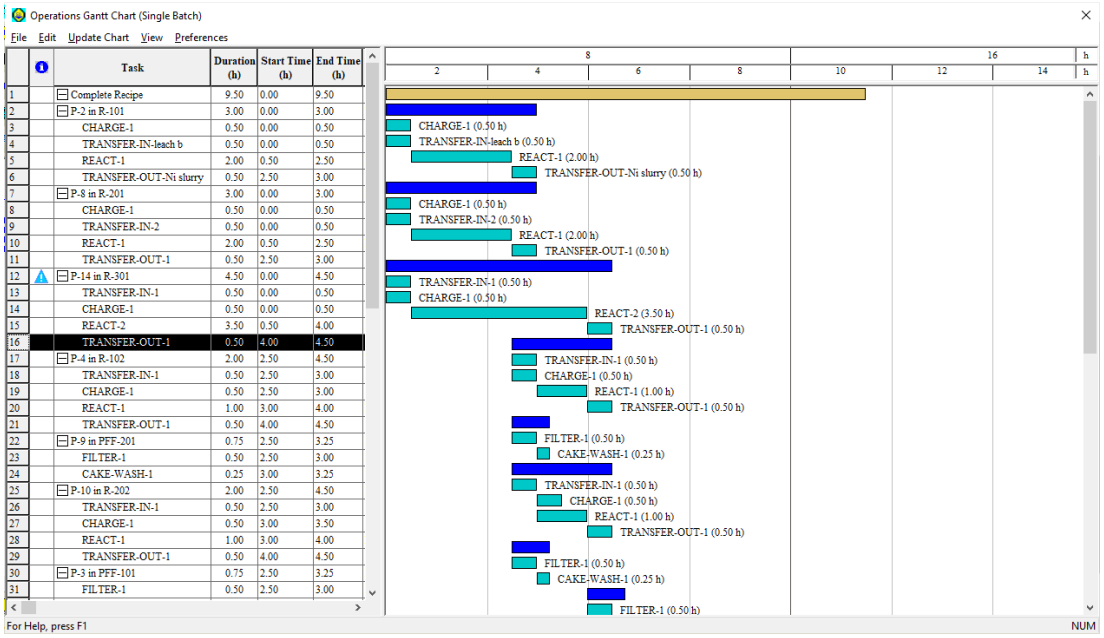

Figure 22. Operations Gantt chart of the Cathode Material Manufacturing process.

A second optimization strategy applied to the process is the sharing of equipment by multiple procedures. Although the flowsheet shows 6 different filter press icons across the three hydrometallurgical lines, in reality there is only 1 filter press per line, for a total of 3 filter presses as the post-leaching filtrations (P-3, P-9 and P-15) and post-precipitation filtrations (P-5, P-11 and P-17) are carried out in the same equipment unit (PFF-101, PFF-201 and PFF-301, respectively), without affecting the process throughput. Equipment sharing can only be done if there is no scheduling overlap between the procedures that share equipment. The sharing of equipment reduces the capital investment without negatively affecting the cycle time of the process.

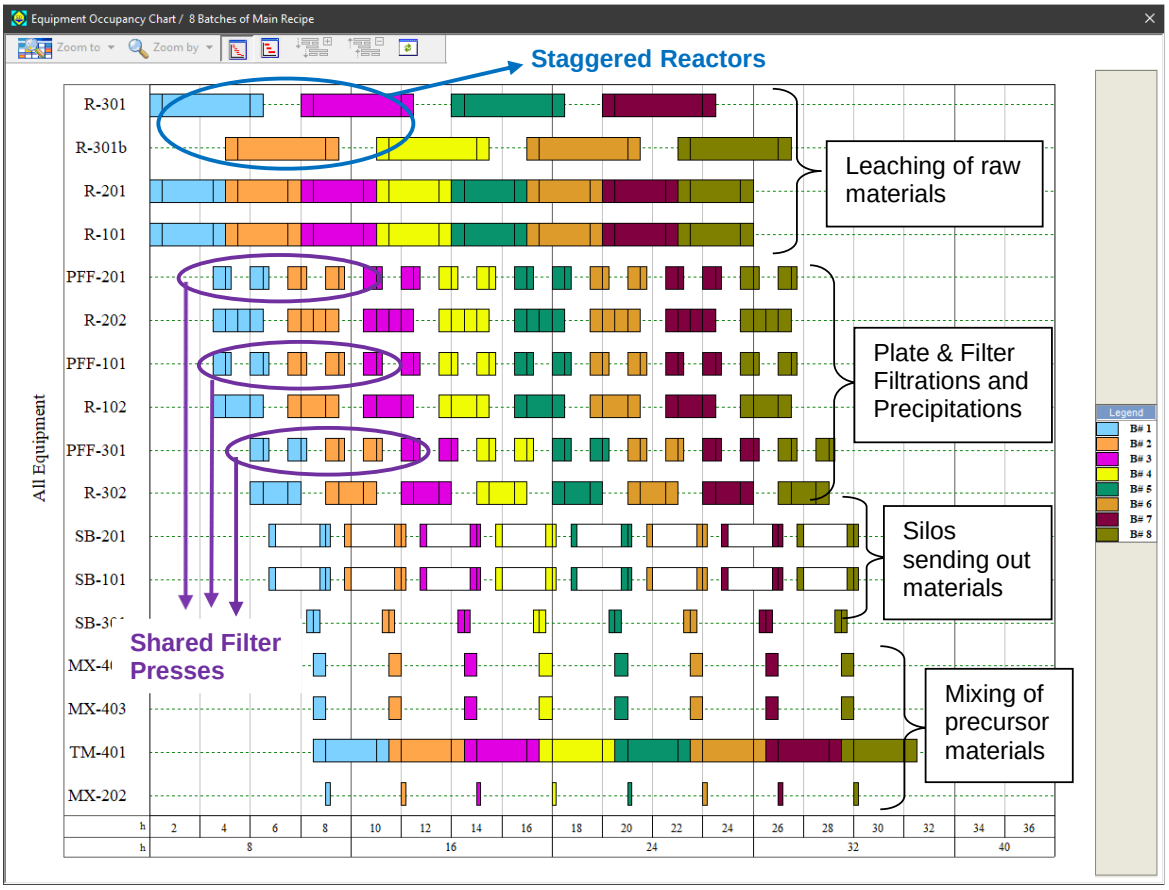

Figure 23. Equipment Occupancy Chart for 8 consecutive batches of the Cathode Material Manufacturing flowsheet.

Material Requirements

Table 51 shows the annual raw material requirements in kg for the Cathode Material Manufacturing process. A single batch enables the treatment of 1 MT of NMC 111 cathode scraps, corresponding to 2,637 MT/year. The required amount of Ni to achieve the 8:1:1 ratio comes from processing 1.43 MT of metallic Ni per batch, corresponding to 3,785 MT/year. Only 30 kg/batch of makeup MnO_x are required to achieve the 8:1:1 ratio. The process also requires 20,593 MT/year of H_2SO_4 50% and 14,029 MT/year of H_2O_2 25%, which together constitute 25% of the total input material flows. The NaOH used as neutralizing/precipitating agent is required at 3.31 MT/batch, corresponding to 8,734 MT/year.

Table 51. Material Requirements for the preparation of 9,040 MT/year NMC 811.

Bulk Material	Unit Cost ($)	Annual Amount		Annual Cost ($)	%
Air	0.00	55,260,884	kg	0	0.00
Carbon	3.00	238,622	kg	715,866	0.57
H2O2 (25%w/w)	0.20	14,029,353	kg	2,826,915	2.23
H2SO4 (50% w/w)	0.18	20,593,205	kg	3,624,404	2.86
Li2CO3	9.00	4,482,900	kg	40,346,100	31.88
LiNi0.33Mn0.33C	10.00	2,637,000	kg	26,370,000	20.84
Methane	0.35	2,511,858	kg	879,150	0.69
MnOx	3.50	26,370	kg	92,295	0.07
NaOH	0.50	8,733,744	kg	4,366,872	3.45
Ni	12.50	3,784,095	kg	47,301,188	37.38
Water	0.002	14,884,484	kg	29,769	0.02
TOTAL				126,552,559	100.00

Cost Analysis

Table 52 displays the Executive Summary table of the EER for the cathode material manufacturing flowsheet. As can be seen, the total capital investment to produce 9,047 MT/year of NMC 811 for Li-ion batteries is about $38M. The revenues per year are around $155 M against annual operating cost of $143M.

Figure 24 displays a breakdown of the annual operating cost. Raw materials account for 88% of the total operating expenses. As shown in Table 51, 37% of the raw material cost is associated with the pure Ni powder used as the main Ni source. The Li_2CO_3 and NMC 111 scraps account for about 32% and 21% of the total raw materials cost, corresponding to about 25% and 17% of the total operating costs, respectively. The large contribution of raw materials to the total operating costs is partially associated with the nature of this process; high-quality raw materials are processed through relatively simple operations to generate a high value-added product. More importantly, the NMC 111 scraps were considered as a raw material in this process. The purchase price of these scraps was estimated based on the content of Ni, Mn and Co, and the market value of these metals. If one considers the NMC 111 scraps as raw materials with *zero* cost (i.e., scraps available for recycling within the same company), it will cut down the total raw materials cost by 17%. The second highest operating cost (8%) is associated with labor expenses. This is mostly due to the batch nature of the process, which requires a great deal of resources for operation. The facility-dependent expenses account for only 2% of the overall

operating cost. Depreciation of the fixed capital investment and maintenance of the facility are the major contributors to these costs.

Table 52. Executive Summary for the battery material production process.

EXECUTIVE SUMMARY (2020 prices)	
Total Capital Investment	38,349,000 $
Capital Investment Charged to This Project	38,349,000 $
Operating Cost	143,742,000 $/year
Main Revenue	144,443,000 $/year
Other Revenues	12,999,972 $/year
Total Revenues	157,442,000 $/year
Cost Basis Annual Rate	9,040 MT UPRF/year
Unit Processing Cost	15,900 $/MT UPRF
Unit Processing Revenue	17,416 $/MT UPRF
Gross Margin	8.70 %
Return On Investment	26.79 %
Payback Time	3.73 years
IRR (After Taxes)	19.10 %
NPV (at 3.0% Interest)	37,795,000 $

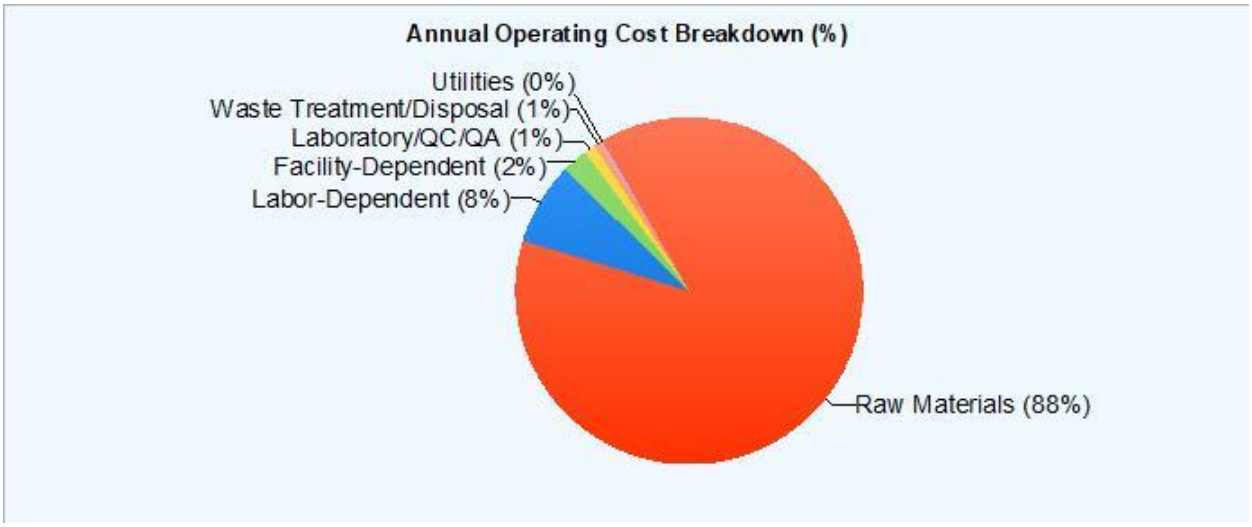

Figure 24. Annual Operating Cost Breakdown for the Cathode Material Manufacturing flowsheet.

Based on the preliminary evaluation of this project's economics, implementing a process to produce 9,040 MT of NMC 811 to be used as cathode material in LiBs is particularly appealing. Gross margins in the range of 13-14% and a return on investment of about 27% might ensure a payback time

in the range 3-3.5 years. Nevertheless, since the most significant contribution to the $143M operating costs originates from the raw materials, it is crucial to accurately determine the cost associated with the NMC 111 scraps used as a major source of metals.

Table 53 displays the cash flow analysis results. Assuming a construction and start-up period of 33 months, the process starts generating revenues in the last 3 months of the third year of the investment. The cash flow becomes positive during the fourth year of the project. For a project lifetime of 15 years, the net present value (NPV) of this project is $64M assuming an interest rate of 5%. The after-tax internal rate of return (IRR) is 24% assuming total income taxes of 25%.

Table 53. Cash-flow analysis for the NMC 811 manufacturing process. Prices are in 1000$.

Year	Capital Investment	Sales Revenues	Operating Cost	Gross Profit	Depreciation	Taxes	Net Profit	Net Cash Flow
1	- 6,910	0	0	0	0	0	0	- 6,910
2	- 9,214	0	0	0	0	0	0	- 9,214
3	- 19,529	39,361	46,569	- 7,208	1,583	0	- 5,625	- 25,155
4	0	157,442	143,535	13,907	1,583	3,477	12,014	12,014
5	0	157,442	143,535	13,907	1,583	3,477	12,014	12,014
6	0	157,442	143,535	13,907	1,583	3,477	12,014	12,014
7	0	157,442	143,535	13,907	1,583	3,477	12,014	12,014
8	0	157,442	143,535	13,907	1,583	3,477	12,014	12,014
9	0	157,442	143,535	13,907	1,583	3,477	12,014	12,014
10	0	157,442	143,535	13,907	1,583	3,477	12,014	12,014
11	0	157,442	143,535	13,907	1,583	3,477	12,014	12,014
12	0	157,442	143,535	13,907	1,583	3,477	12,014	12,014
13	0	157,442	141,951	15,491	0	3,873	11,618	11,618
14	0	157,442	141,951	15,491	0	3,873	11,618	11,618
15	13,771	157,442	141,951	15,491	0	3,873	11,618	25,389

IRR/NPV SUMMARY					
IRR Before Taxes	30.70 %	Interest %	5.00	7.00	9.00
IRR After Taxes	23.99 %	NPV	64,407.00	50,701.00	39,606.00

1.6 Summary

Process design is a complex task composed of process synthesis and process analysis steps. Process synthesis encompasses the selection and arrangement of unit processes and unit operations required to process raw materials and produce one or multiple products. Process analysis is the

evaluation and comparison of the effect of different process solutions and operating conditions on specific outputs. Both tasks require the integration of knowledge from many different scientific and engineering disciplines, and they are carried out at various levels of detail, depending on the process development stage they are performed. Both are greatly facilitated by the use of advanced process simulation tools, such as SuperPro Designer.

There are many important aspects to consider when designing hydrometallurgical processes. Some key points to remember are listed below:

- The sequencing of processing steps such as extraction, purification, and recovery of one or multiple metal values is based on experience and rules of thumb (heuristics). The selectivity towards the target values should be aimed from the leaching step. When this is not possible, the sequence of the purification operations plays the most crucial role in the profitable recovery of products. The first impurities to be removed are those present in larger quantities and/or the ones that can affect the efficiency and sustainability of successive operations. Ideally, the most difficult separations should be conducted later in the purification sequence while those requiring expensive equipment should be performed upon concentration.
- The recirculation of spent solutions is crucial to achieve economic feasibility in hydrometallurgical processes. The optimal recirculation ratio is a compromise between technical aspects (e.g., accumulation of impurities) and economic aspects (e.g., equipment size, waste/wastewater treatment costs).
- When dealing with processes characterized by high degrees of recirculation, choosing purification and recovery operations that do not cause significant changes in the solution properties (e.g., pH, temperature) is crucial. That limits the production of sludge and the consumption of raw materials (e.g., acids and bases) and utilities.
- Process simulators facilitate the analysis of integrated processes by performing material and energy balances, equipment sizing, economic evaluation, cycle time analysis, environmental impact assessment and other tasks.
- Profitability analysis consists of the calculation of gross margin, return on investment, payback time, net present value, internal rate of return and other measures.
- Process simulators facilitate sensitivity analysis for investigating the impact of changing input variables, such as product titer or production scale, on important process outputs. This activity can help to focus research and development resources on areas of the process that are likely to have the greatest economic impact.
- When some input parameters are expected to affect the economic feasibility but have variability in their values (e.g., the selling price of a product), a multi-parametric variability analysis can be performed by treating the unknown parameters as uncertain variables in the simulation. Variability

analysis will reveal the range of values of the uncertain parameters for which the process is economically feasible.

References

[1] D.A. Nelson, R.L. Kirkwood, J.M. Douglas, Conceptual design of chemical processes, in: Simul. Ser., American Institute of Chemical Engineers (AIChE), 1989: pp. 180–184.

[2] A.J. Williams, T.J. Williams, Conceptual Development and Capital Cost Estimating, AIChE Academy, AIChE, New York, NY, 2019.

[3] Autogenous and Semi-Autogenous Mills, in: Miner. Process. Des. Oper., Elsevier, 2016: pp. 263–285. doi:10.1016/b978-0-444-63589-1.00009-5.

[4] G. Towler, R. Sinnott, Chemical Engineering Design: Principles, Practice and Economics of Plant and Process Design, Elsevier BH, 2008.

[5] O.D. Neikov, Mechanical Crushing and Grinding, Handb. Non-Ferrous Met. Powders. (2019) 65–90. doi:10.1016/B978-0-08-100543-9.00002-6.

[6] B.A. Wills, Comminution in the minerals industry - An overview, Miner. Eng. 3 (1990) 3–5. doi:10.1016/0892-6875(90)90076-N.

[7] D. Bösch, Comminution-an Essential Component of Waste Treatment, (n.d.).

[8] G.R. Daborn, R. Derry, Cryogenic communition in scrap recycling, Resour. Conserv. Recycl. 1 (1988) 49–63. doi:10.1016/0921-3449(88)90007-9.

[9] S. Prasad, B.D. Pandey, Alternative processes for treatment of chalcopyrite - A review, Miner. Eng. 11 (1998) 763–781. doi:10.1016/s0892-6875(98)00061-2.

[10] Y. Zhang, Y. He, T. Zhang, X. Zhu, Y. Feng, G. Zhang, X. Bai, Application of Falcon centrifuge in the recycling of electrode materials from spent lithium ion batteries, J. Clean. Prod. 202 (2018) 736–747. doi:10.1016/j.jclepro.2018.08.133.

[11] U.U. Jadhav, H. Hocheng, A review of recovery of metals from industrial waste Industrial management and organisation, J. Achiev. Mater. Manuf. Eng. 54 (2012) 159–167.

[12] SGS Minerals Services, Lithium Extraction from Spodumene, SGS Mong. 2013. (2010). www.sgs.com/minerals (accessed December 11, 2019).

[13] S.K. Haldar, Mineral Processing, in: Miner. Explor., 2018: pp. 259–290. doi:10.1016/b978-0-12-814022-2.00013-7.

[14] R. Abbaschian, L. Abbaschian, R.E. Reed-Hill, Physical Metallurgy Principles, Fourth Edi, Cenage Learning, 2009.

[15] R. Yin, Metallurgical Process Engineering, 2011. doi:10.1007/978-3-642-13956-7.

[16] M. Derhy, Y. Taha, R. Hakkou, M. Benzaazoua, Review of the main factors affecting the flotation of phosphate ores, Minerals. 10 (2020) 1–22. doi:10.3390/min10121109.

[17] D.G. Wonyen, V. Kromah, B. Gibson, S. Nah, S.C. Chelgani, A review of flotation separation of Mg

carbonates (Dolomite and magnesite), Minerals. 8 (2018) 16–18. doi:10.3390/min8080354.
[18] N.P. Finkelstein, The activation of sulphide minerals for flotation: A review, Int. J. Miner. Process. 52 (1997) 81–120. doi:10.1016/s0301-7516(97)00067-7.
[19] S.K. Kawatra, Froth Flotation-Fundamental Principles, Res. Michigan Tech. Univ. (2002) 1–30.
[20] S. Mondal, A. Acharjee, U. Mandal, B. Saha, Froth flotation process and its application, Vietnam J. Chem. 59 (2021) 417–425. doi:10.1002/VJCH.202100010.
[21] S.R. Rao, Surface Chemistry of Froth Flotation, Surf. Chem. Froth Flotat. (2004). doi:10.1007/978-1-4757-4302-9.
[22] Y.R. Smith, J.R. Nagel, R.K. Rajamani, Eddy current separation for recovery of non-ferrous metallic particles: A comprehensive review, Miner. Eng. 133 (2019) 149–159. doi:10.1016/j.mineng.2018.12.025.
[23] A. Buekens, T.M. Letcher, The treatment of plastic in automobile shredder residue, Plast. Waste Recycl. (2020) 401–414. doi:10.1016/B978-0-12-817880-5.00015-3.
[24] M.E. Wadsworth, J.D. Miller, Hydrometallurgical Processes, in: Rate Process. Extr. Metall., 1979: pp. 133–244. doi:10.1007/978-1-4684-9117-3_4.
[25] T. Havlík, Experimental Methods of Investigating Hydrometallurgical Processes, in: Hydrometallurgy, 2008: pp. 309–340. doi:10.1533/9781845694616.309.
[26] M.L. Free, Hydrometallurgy - Fundamentals and Applications, John Wiley & Sons. Inc., Hoboken, New Jersey, 2013.
[27] T. Thenepalli, R. Chilakala, L. Habte, L.Q. Tuan, C.S. Kim, A brief note on the heap leaching technologies for the recovery of valuable metals, Sustainability. 11 (2019). doi:10.3390/su10023347.
[28] Y. KONISHI, S. ASAI, Bioleaching of Sulfide Mineral in Stirred Tank Reactors Operated in a Variety of Modes, Miner. Process. Extr. Metall. Rev. 19 (1998) 129–140. doi:10.1080/08827509608962435.
[29] D. Medina, C.G. Anderson, A Review of the Cyanidation Treatment of Copper-Gold Ores and Concentrates, Metals (Basel). 10 (2020) 897. doi:10.3390/met10070897.
[30] J.A. Gonzales, J. Dutrizac, Electrochemical coupling of metal extraction and electrowinning, in: Electrometall. 2001, 2001. https://inis.iaea.org/search/search.aspx?orig_q=RN:35087996 (accessed September 3, 2021).
[31] T. Havlik, Hydrometallurgy: Principles and application, 2008. doi:10.1533/9781845694616.
[32] B.I. Whittington, D. Muir, Mineral Processing and Extractive Metullargy Review Pressure Acid Leaching of Nickel Laterites: A Review Pressure Acid Leaching of Nickel Laterites: A Review, Press. Acid Leaching Nickel Laterit. A Rev. Miner. Process. Extr. Metullargy Rev. 21 (2000) 527–600. doi:10.1080/08827500008914177.
[33] T. Bagshaw, THE ALUMINIUM STORY BAUXITE TO ALUMINA: THE BAYER PROCESS An Introductory Text, 2017. https://nzic.org.nz/app/uploads/2018/09/Bauxite-to-Alumina-Book-2018.pdf (accessed July 14, 2020).

[34] B.A. Perlmutter, Types of Filtration Systems, in: Solid-Liquid Filtr., 2015: pp. 35–45. doi:10.1016/b978-0-12-803053-0.00003-1.

[35] I. Townsend, Automatic pressure filtration in mining and metallurgy, in: Miner. Eng., 2003: pp. 165–173. doi:10.1016/S0892-6875(02)00266-2.

[36] B.A. Perlmutter, Filtration Selection, Solid-Liquid Filtr. (2015) 57–77. doi:10.1016/b978-0-12-803053-0.00005-5.

[37] B.A. Perlmutter, Types of Filtration Systems, Solid-Liquid Filtr. (2015) 35–45. doi:10.1016/b978-0-12-803053-0.00003-1.

[38] B.A. Wills, J.A. Finch, Mineral Processing Technology, Eighth Edi, Elsevier, 2015. doi:10.1115/DSCC2013-3715.

[39] T. Sparks, Understanding filter presses and belt filters, Filtr. Sep. 49 (2012) 20–24. doi:10.1016/S0015-1882(12)70193-3.

[40] G.P. Demopoulos, Aqueous precipitation and crystallization for the production of particulate solids with desired properties, Hydrometallurgy. 96 (2008) 199–214. doi:10.1016/j.hydromet.2008.10.004.

[41] D. Qi, Chemical Separation Method, in: Hydrometall. Rare Earths, 2018: pp. 671–741. doi:10.1016/b978-0-12-813920-2.00007-6.

[42] M. Sethurajan, E.D. van Hullebusch, D. Fontana, A. Akcil, H. Deveci, B. Batinic, J.P. Leal, T.A. Gasche, M. Ali Kucuker, K. Kuchta, I.F.F. Neto, H.M.V.M. Soares, A. Chmielarz, Recent advances on hydrometallurgical recovery of critical and precious elements from end of life electronic wastes - a review, Crit. Rev. Environ. Sci. Technol. 49 (2019) 212–275. doi:10.1080/10643389.2018.1540760.

[43] J. McNeice, R. Kim, A. Ghahreman, Oxidative precipitation of cerium in acidic chloride solutions: part I – Fundamentals and thermodynamics, Hydrometallurgy. 184 (2019) 140–150. doi:10.1016/j.hydromet.2018.12.018.

[44] J. McNeice, R. Kim, A. Ghahreman, Oxidative precipitation of cerium in acidic chloride solutions: Part II – oxidation in a mixed REE system, Hydrometallurgy. 194 (2020). doi:10.1016/j.hydromet.2020.105331.

[45] D.S. Flett, Cobalt-Nickel Separation in Hydrometallurgy: a Review, Chem. Sustain. Dev. 12. 12 (2004) 81–91. doi:10.1515/ci.2010.32.1.36b.

[46] E. Gerold, S. Luidold, H. Antrekowitsch, Selective precipitation of metal oxalates from lithium ion battery leach solutions, Metals (Basel). 10 (2020) 1–15. doi:10.3390/met10111435.

[47] D.S. Flett, Solvent extraction in hydrometallurgy: The role of organophosphorus extractants, in: J. Organomet. Chem., 2005: pp. 2426–2438. doi:10.1016/j.jorganchem.2004.11.037.

[48] F. Xie, T.A. Zhang, D. Dreisinger, F. Doyle, A critical review on solvent extraction of rare earths from aqueous solutions, Miner. Eng. 56 (2014) 10–28. doi:10.1016/j.mineng.2013.10.021.

[49] G. Granata, A. Onoguchi, C. Tokoro, Preparation of copper nanoparticles for metal-metal bonding by aqueous reduction with d-glucose and PVP, Chem. Eng. Sci. 209 (2019) 115210.

doi:10.1016/j.ces.2019.115210.

[50] G. Granata, E. Moscardini, F. Pagnanelli, F. Trabucco, L. Toro, Product recovery from Li-ion battery wastes coming from an industrial pre-treatment plant: Lab scale tests and process simulations, J. Power Sources. 206 (2012) 393–401. doi:10.1016/j.jpowsour.2012.01.115.

[51] G. Granata, F. Pagnanelli, E. Moscardini, Z. Takacova, T. Havlik, L. Toro, Simultaneous recycling of nickel metal hydride, lithium ion and primary lithium batteries: Accomplishment of European Guidelines by optimizing mechanical pre-treatment and solvent extraction operations, J. Power Sources. 212 (2012) 205–211. doi:10.1016/j.jpowsour.2012.04.016.

[52] B.P. Littlejohn, Technical Review – Copper Solvent Extraction in Hydrometallurgy, (2007).

[53] K.C. Sole, M.B. Mooiman, E. Hardwick, Ion Exchange in Hydrometallurgical Processing: An Overview and Selected Applications, Sep. Purif. Rev. 47 (2018) 159–178. doi:10.1080/15422119.2017.1354304.

[54] M. Streat, Ion exchange processes in hydrometallurgy, Ion Exch. (2011) 1061–1072. doi:10.1515/9783110862430.1061.

[55] R. Rumbu, A Review on Copper Hydrometallurgy, J. South African Inst. Min. Metall. (1973) 158–173. https://books.google.com/books?id=iFV-DwAAQBAJ (accessed May 29, 2021).

[56] E. Abkhoshk, E. Jorjani, M.S. Al-Harahsheh, F. Rashchi, M. Naazeri, Review of the hydrometallurgical processing of non-sulfide zinc ores, Hydrometallurgy. 149 (2014) 153–167. doi:10.1016/j.hydromet.2014.08.001.

[57] F. Habashi, Handbook of extractive metallurgy II, 1997.

[58] E. Sayilgan, T. Kukrer, G. Civelekoglu, F. Ferella, A. Akcil, F. Veglio, M. Kitis, A review of technologies for the recovery of metals from spent alkaline and zinc-carbon batteries, Hydrometallurgy. 97 (2009) 158–166. doi:10.1016/j.hydromet.2009.02.008.

[59] M. Sethurajan, E.D. Van Hullebusch, D. Fontana, A. Akcil, H. Deveci, B. Batinic, J.P. Leal, T.A. Gasche, A. Kucuker, K. Kuchta, I.F.F. Neto, H.M.V.M. Soares, A. Chmielarz, J. Ao, P. Leal, Recent advances on hydrometallurgical recovery of critical and precious elements from end of life electronic wastes-a review Recent advances on hydrometallurgical recovery of critical and precious elements from end of life electronic wastes-a review, Crit. Rev. Environ. Sci. Technol. 49 (2019) 212–275. doi:10.1080/10643389.2018.1540760.

[60] E. Balomenos, D. Panias, I. Paspaliaris, Energy and exergy analysis of the primary aluminum production processes: A review on current and future sustainability, Miner. Process. Extr. Metall. Rev. 32 (2011) 69–89. doi:10.1080/08827508.2010.530721.

[61] O. V. Abramov, Materials Processing, 2019. doi:10.1201/9780203751954-15.

[62] Fundamental Aspects of Electrometallurgy, Fundam. Asp. Electrometall. (2002). doi:10.1007/B118178.

[63] C.R. Edwards, A.J. Oliver, Uranium Processing: A Review of Current Methods and Technology, JOM. 2 (2000). https://link.springer.com/content/pdf/10.1007%2Fs11837-000-0181-2.pdf (accessed May 30, 2021).

[64] EPA, Rare Earth Elements : A Review of Production , Processing , Recycling, and Associated Environmental Issues, United States Environ. Prot. Agency. (2012) 135. www.epa.gov/ord (accessed May 4, 2020).
[65] F. Habashi, Handbook of extractive metallurgy III, Wiley-VCH Verlag, 1997.
[66] D. Megaw, J. Moolman, P. Muzadi, T. Marcus, Copper sulphate crystallization plants at remote locations, J. South. African Inst. Min. Metall. 117 (2017) 779–784. doi:10.17159/2411-9717/2017/v117n8a8.
[67] C. Tyler, C.H. Winter, D.R. Boylan, Chemical Engineering Economics, 1960. doi:10.1080/00137916008965102.
[68] J. Paecey, X.J. Guo, E. Robles, Copper hydrometallurgy - current status, preliminary economics, future direction and positioning versus smelting, Trans. Nonferrous Met. Soc. China. 14 (2004) 560–568.
[69] M. Mokmeli, Pre feasibility study in hydrometallurgical treatment of low-grade chalcopyrite ores from Sarcheshmeh copper mine, (2019). doi:10.1016/j.hydromet.2019.105215.
[70] M.E. Schlesinger, M.J. King, K.C. Sole, W.G. Davenport, Hydrometallurgical Copper Extraction, 2011. doi:10.1016/b978-0-08-096789-9.10015-0.
[71] M.S. Peters, K.D. Timmerhaus, Plant Design and Economics for Chemical Engineers, Fourth edi, McGraw-Hill, Inc., 1991.
[72] B. Swain, Recovery and recycling of lithium: A review, Sep. Purif. Technol. 172 (2017) 388–403. doi:10.1016/j.seppur.2016.08.031.
[73] Y. Li, W. Lv, H. Huang, W. Yan, X. Li, P. Ning, H. Cao, Z. Sun, Recycling of spent lithium-ion batteries in view of green chemistry, Green Chem. 23 (2021) 6139–6171. doi:10.1039/d1gc01639c.
[74] B. Swain, Separation and purification of lithium by solvent extraction and supported liquid membrane, analysis of their mechanism: a review, J. Chem. Technol. Biotechnol. 91 (2016) 2549–2562. doi:10.1002/JCTB.4976.
[75] Z. Luo, J. Yang, H. Ma, M. Liu, X. Ma, Recovery of magnesium and potassium from biotite by sulfuric acid leaching and alkali precipitation with ammonia, Hydrometallurgy. 157 (2015) 188–193. doi:10.1016/j.hydromet.2015.08.018.
[76] C.R. Borra, J. Mermans, B. Blanpain, Y. Pontikes, K. Binnemans, T. Van Gerven, Selective recovery of rare earths from bauxite residue by combination of sulfation, roasting and leaching, Miner. Eng. 92 (2016) 151–159. doi:10.1016/j.mineng.2016.03.002.
[77] P.K. Choubey, M.S. Kim, R.R. Srivastava, J.C. Lee, J.Y. Lee, Advance review on the exploitation of the prominent energy-storage element: Lithium. Part I: From mineral and brine resources, Miner. Eng. 89 (2016) 119–137. doi:10.1016/j.mineng.2016.01.010.
[78] X. Dai, A. Simons, P. Breuer, A review of copper cyanide recovery technologies for the cyanidation of copper containing gold ores, Miner. Eng. 25 (2012) 1–13. doi:10.1016/j.mineng.2011.10.002.
[79] O.P. Karthikeyan, A. Rajasekar, R. Balasubramanian, Bio-Oxidation and Biocyanidation of Refractory Mineral Ores for Gold Extraction: A Review, Crit. Rev. Environ. Sci. Technol. 45 (2015)

1611–1643. doi:10.1080/10643389.2014.966423.
[80] K.A. Natarajan, Biotechnology in gold processing, Bull. Mater. Sci. 16 (1993) 501–508.
[81] J.C. Gentina, F. Acevedo, Copper bioleaching in Chile, Minerals. 6 (2016). doi:10.3390/min6010023.
[82] S. Yin, L. Wang, E. Kabwe, X. Chen, R. Yan, K. An, L. Zhang, A. Wu, Copper bioleaching in China: Review and prospect, Minerals. 8 (2018). doi:10.3390/min8020032.
[83] S. Panda, A. Akcil, N. Pradhan, H. Deveci, Current scenario of chalcopyrite bioleaching: A review on the recent advances to its heap-leach technology, Bioresour. Technol. 196 (2015) 694–706. doi:10.1016/j.biortech.2015.08.064.
[84] M.G. Aylmore, D.M. Muir, THIOSULFATE LEACHING OF GOLD-A REVIEW, 2001.
[85] T. Georgi-Maschler, B. Friedrich, R. Weyhe, H. Heegn, M. Rutz, Development of a recycling process for Li-ion batteries, J. Power Sources. 207 (2012) 173–182. doi:10.1016/j.jpowsour.2012.01.152.
[86] T.L. Williams, M.J. Gunn, A. Jaffer, P.I. Harvey, P.R. Tittes, The application of geoBiotics, LLC's GEOCOAT® technology to the bacterial oxidation of a refractory arsenopyrite gold concentrate, in: Hydrometall. 2008 Proc. 6th Int. Symp., 2008: pp. 474–483.
[87] J.A. Díaz, J. Serrano, E. Leiva, Bioleaching of arsenic-bearing copper ores, Minerals. 8 (2018) 1–19. doi:10.3390/min8050215.
[88] V.P. Evangelou, A.K. Seta, A. Holt, Potential role of bicarbonate during pyrite oxidation, Environ. Sci. Technol. 32 (1998) 2084–2091. doi:10.1021/es970829m.
[89] F. Acevedo, The use of reactors in biomining processes, 2000. http://www.ejb.org/content/vol3/issue3/full/4 (accessed October 13, 2020).
[90] T.A. Fowler, P.R. Holmes, F.K. Crundwell, Mechanism of pyrite dissolution in the presence of Thiobacillus ferrooxidans, Appl. Environ. Microbiol. 65 (1999) 2987–2993. doi:10.1128/aem.65.7.2987-2993.1999.
[91] H.M. Lizama, P.A. Zielinski, L.D. Kerby, C.C. Abraham, Comparison of biooxidation with carbon dioxide assimilation during bacterial growth on ferrous ion or elemental sulfur, Biotechnol. Bioeng. 77 (2002) 111–117. doi:10.1002/bit.10136.
[92] H. Aminian, C. Bazin, Solvent extraction equilibria in copper (II)-iron (III)-LIX984 system, Miner. Eng. 13 (2000) 667–672. doi:10.1016/S0892-6875(00)00049-2.
[93] A. Id, R. Processing, C. South, Solvent extraction of copper and zinc from bioleaching solutions with LIX984 and D2EHPA ®, J. Cent. South Univ. Technol. (English Ed. 12 (2005).
[94] H. Asghari, M.S. Safarzadeh, G. Asghari, D. Moradkham, The effect of impurities on the extraction of copper from sulfate medium using LIX®984N in kerosene, Russ. J. Non-Ferrous Met. 50 (2009) 89–96. doi:10.3103/S1067821209020035.
[95] N.B. Devi, B. Nayak, Liquid-liquid extraction and separation of copper(II) and nickel(II) using LIX ® 984N, J. South. African Inst. Min. Metall. 114 (2014) 937–943.
[96] E. Molleman, D. Dreisinger, The treatment of copper-gold ores by ammonium thiosulfate leaching,

Hydrometallurgy. 66 (2002) 1–21. doi:10.1016/S0304-386X(02)00080-4.
[97] B. Xu, K. Li, Q. Zhong, Q. Li, Y. Yang, T. Jiang, Study on the oxygen pressure alkaline leaching of gold with generated thiosulfate from sulfur oxidation, Hydrometallurgy. 177 (2018) 178–186. doi:10.1016/j.hydromet.2018.03.006.
[98] J.W. Choi, M.H. Song, J.K. Bediako, Y.S. Yun, Sequential recovery of gold and copper from bioleached wastewater using ion exchange resins, Environ. Pollut. 266 (2020). doi:10.1016/j.envpol.2020.115167.
[99] M.I. Jeffrey, D.M. Hewitt, X. Dai, S.D. Brunt, Ion exchange adsorption and elution for recovering gold thiosulfate from leach solutions, Hydrometallurgy. 100 (2009) 136–143. doi:10.1016/j.hydromet.2009.11.003.
[100] H. Zhang, D.B. Dreisinger, The recovery of gold from ammoniacal thiosulfate solutions containing copper using ion exchange resin columns, Hydrometallurgy. 72 (2004) 225–234. doi:10.1016/S0304-386X(03)00183-X.
[101] C. Abbruzzese, R. Massidda, F. Vegli, S. Ubaldini, Thiosulphate leaching for gold hydrometallurgy, 1995.
[102] J. Tao, S. Yu, Review on feasible recycling pathways and technologies of solar photovoltaic modules, Sol. Energy Mater. Sol. Cells. 141 (2015) 108–124. doi:10.1016/j.solmat.2015.05.005.
[103] IRENA, IEA-PVPS, End of Life Management. Solar Photovoltaic Panels, 2016.
[104] G. Sapra, V. Chaudhary, P. Kumar, P. Sharma, A. Saini, Materials Today : Proceedings Recovery of silica nanoparticles from waste PV modules, Mater. Today Proc. (2020) 6–11. doi:10.1016/j.matpr.2020.06.093.
[105] SPE, Global Market Outlook, 2018.
[106] European Parliament and The Council of European Union, DIRECTIVE 2012/19/EU OF THE EUROPEAN PARLIAMENT AND OF THE COUNCIL of 4 July 2012 on waste electrical and electronic equipment (WEEE) (recast) (Text with EEA relevance), 2012. https://eur-lex.europa.eu/LexUriServ/LexUriServ.do?uri=OJ:L:2012:197:0038:0071:en:PDF%0Ahttps://eur-lex.europa.eu/legal-content/EN/TXT/PDF/?uri=CELEX:32012L0019&from=EN (accessed September 1, 2021).
[107] J.R. Peeters, D. Altamirano, W. Dewulf, J.R. Duflou, Forecasting the composition of emerging waste streams with sensitivity analysis: A case study for photovoltaic (PV) panels in Flanders, Resour. Conserv. Recycl. 120 (2017) 14–26. doi:10.1016/j.resconrec.2017.01.001.
[108] A. Rubino, G. Granata, E. Moscardini, L. Baldassari, P. Altimari, L. Toro, F. Pagnanelli, Development and Techno-Economic Analysis of an Advanced Recycling Process for Photovoltaic Panels Enabling Polymer Separation and Recovery of Ag and Si, Energies. 13 (2020) 6690. doi:10.3390/en13246690.
[109] J. Xu, H.R. Thomas, R.W. Francis, K.R. Lum, J. Wang, B. Liang, A review of processes and technologies for the recycling of lithium-ion secondary batteries, J. Power Sources. 177 (2008) 512–527. doi:10.1016/j.jpowsour.2007.11.074.

[110] N. Lebedeva, F. Di Persio, L. Boon-Brett, Lithium ion battery value chain and related opportunities for Europe, Eur. Comm. Petten. (2016) 1–75. https://ec.europa.eu/jrc (accessed January 14, 2020).

[111] G. Lombardo, B. Ebin, M.R.J. St Foreman, B.M. Steenari, M. Petranikova, Chemical Transformations in Li-Ion Battery Electrode Materials by Carbothermic Reduction, ACS Sustain. Chem. Eng. 7 (2019) 13668–13679. doi:10.1021/acssuschemeng.8b06540.

[112] W. Lv, Z. Wang, H. Cao, Y. Sun, Y. Zhang, Z. Sun, A Critical Review and Analysis on the Recycling of Spent Lithium-Ion Batteries, ACS Sustain. Chem. Eng. 6 (2018) 1504–1521. doi:10.1021/acssuschemeng.7b03811.

[113] T. Abo Atia, G. Elia, R. Hahn, P. Altimari, F. Pagnanelli, Closed-loop hydrometallurgical treatment of end-of-life lithium ion batteries: Towards zero-waste process and metal recycling in advanced batteries, J. Energy Chem. 35 (2019) 220–227. doi:10.1016/j.jechem.2019.03.022.

[114] C. Li, X. Zhang, W. He, G. Xu, R. Sun, Cathode materials for rechargeable zinc-ion batteries: From synthesis to mechanism and applications, J. Power Sources. 449 (2020) 227596. doi:10.1016/j.jpowsour.2019.227596.

[115] R. Borah, F.R. Hughson, J. Johnston, T. Nann, On battery materials and methods, Mater. Today Adv. 6 (2020). doi:10.1016/j.mtadv.2019.100046.